Vol. 59 • No. 11

November 2016

Microwave Journal.com

Metamaterial Advancements

horizon house®

Founded in 1958

Don’t Settle for Average.

Demand Peak Performance.

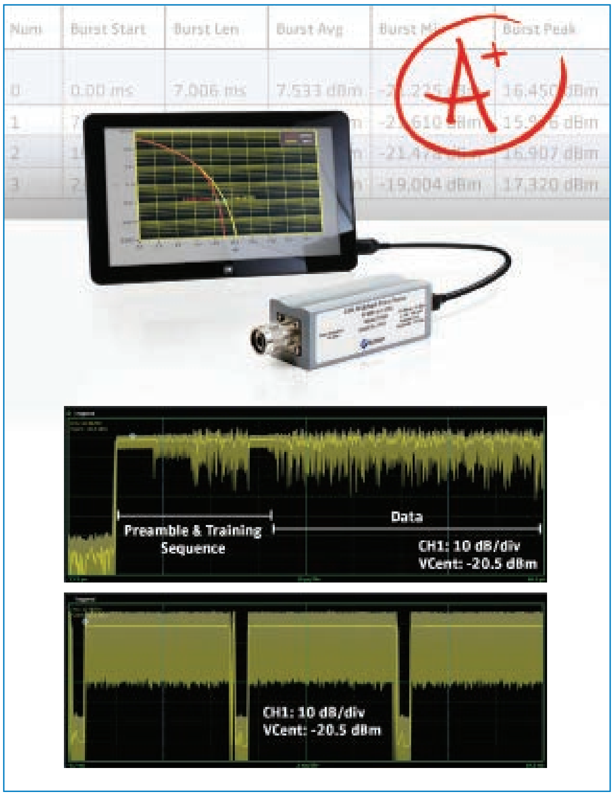

The 55 Series USB Peak Power Sensor

Real-Time Power Measurements for Complex Communications Signals

Others claim to have fast average measurements, but only the 55 Series measures continuous and burst average power faster than anyone in the industry. It adds wide-band peak and crest factor measurements, allowing you to see all aspects of your device’s performance. This USB Sensor delivers results 100 times faster than conventional meters and with its *Real-Time Power Processing*™ technology captures all glitches with 100ps resolution.

- 195 MHz Video Bandwidth
- 3 ns risetime
- 100,000 measurements/sec
- 100 MHz Sample Rate
- Multi-channel synchronized measurements

For more information visit us at **www.boonton.com**
or call +1 973-386-9696.

Wireless Telecom Group
Boonton Microlab Noisecom

Boonton


BETTER COMMUNICATION SOLUTIONS
Public Safety
Satcom, mmWave & Military
Aeronatutical/Space Transportation
AMER, EMEA, & D.A.S
MECA 5G Products & Equipment
MECA Electronics designs and manufactures an extensive line of RF/Microwave Equipment and Components with industry leading performance including D.A.S. Equipment, Low PIM Products, supports 5G & Millimeter-Wave, Power Dividers & Combiners, Directional & Hybrid Couplers, Fixed & Variable Attenuators, RF Terminations, Circulators/Isolators, DC Blocks & Bias Tees, Adapters & Jumpers. Models available in industry common connector styles: N, SMA, 2.92mm, TNC, BNC, 7/16, 4.1/9.5 & 4.3/10.0 DIN as well as QMA, Reverse Polarity SMA, TNC and various mounting solutions. Since 1961 MECA Electronics (Microwave Equipment & Components of America) has served the RF/Microwave industry with equipment and passive components covering Hz to 40 GHz. MECA is a privately held ISO9001:2008 Certified, global designer and manufacturer for the communications industry with products manufactured in the United States of America We stock products so that you do not need to.
Low PIM Attenuators
4.3/10.0
Low PIM Couplers
Low PIM Terminations
Millimeter-Wave
Tower Top & D.A.S Equipment
Power Divider/Combiner
Products in STOCK when you need it!
Buy
RF
RFPartsOnDemand.com
Online
Attenuators/Terminations
Directional Couplers
MIL-DTL-15370 Available
MECA Electronics, Inc.
Microwave Equipment & Components of America
The Professional's Choice for RF/Microwave Passive Components
459 E. Main St., Denville, NJ 07834
Tel: 973-625-0661 • Fax: 973-625-9277 • Sales@e-MECA.com
e-MECA.com
Since 1961
iBwave


MCL B 744
ADP-2-10
MCL A 745
ADP-1-10
MCL B 744
ADP-2-10
MCL B 744
ADP-2-10
MCL
GBA-12

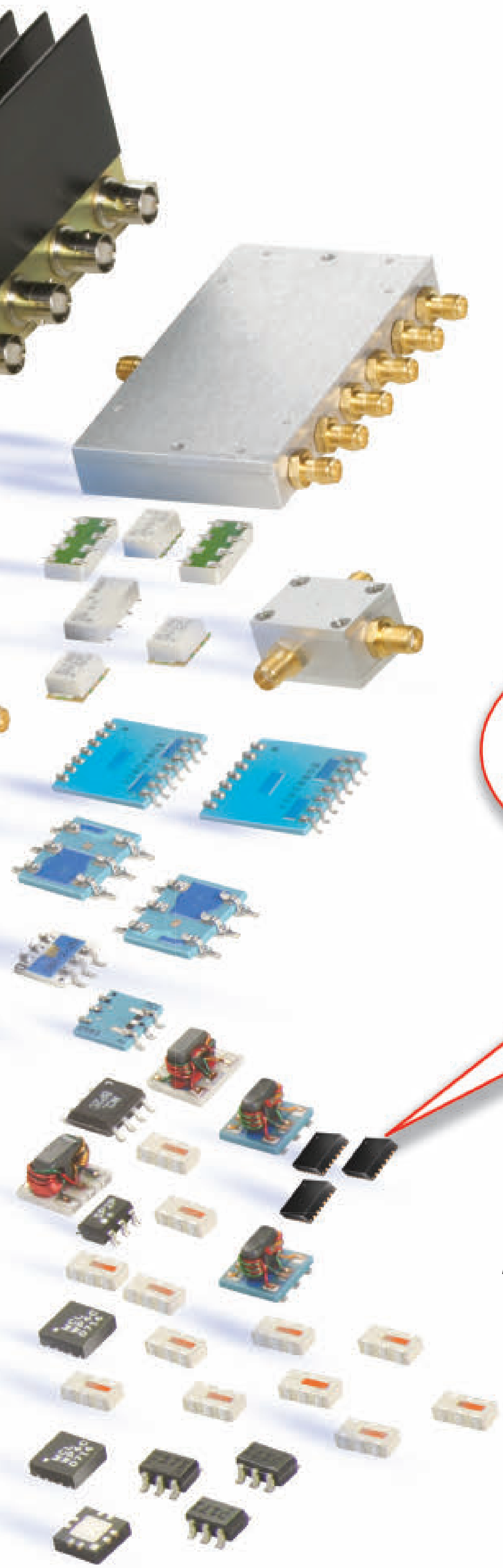

Communications & Power Industries

Beverly Microwave Division
150 Sohier Road • Beverly, MA 01915
Phone: +1 (978) 922-6000 • Email: bmdmarketing@cpii.com
www.cpii.com/bmd

Integrated Microwave Assemblies for Military Radar Applications

Upconverters And Digital Attenuators

Performance Advantages:

- L, S, C, X, Ku, Ka Bands
- High spurious rejection
- Adjustable Filter Bandwidth
- Gain Control
- RF Gating Capacity

Features:

- Designed to minimize spurious emissions while maintaining the transmitted waveform integrity
- Hermetic package
- Wide Operating temperature range

Receivers

Performance Advantages:

- L, S, C, X, Ku, Ka Bands
- Low Noise Figures
- Digital Gain Control
- Linearized RF Attenuation
- Very high Dynamic Range
- Fast Recovery Time
- Switched IF Filter

Features:

- Dual-conversion radar receivers
- High dynamic range to operate in a multiple system environment
- Hermetic package
- Wide Operating temperature range

Ask us about integrating your designs today.

• Solid State Power Amplifiers • Integrated Microwave Assemblies
• Receiver Protectors • Control Components • Transmitters • Amplifiers
• Modulators • Magnetrons • Crossed Field Amplifiers
• Ring Loop Traveling Wave Tubes • Power Couplers


mpG
K&L MICROWAVE
A DOVER COMPANY
TAKE THE RIGHT ROUTE
• 1 MHz to 27 GHz
• 2 to 20 Throw
• Switching Speed 50 to 500 nsec
• Power Handling 10 to 40 dBm
J2
J3
J4
J5
MFR-033F8 1P4T-6000/22000-0
K&L
S/N 66 D.C. 1625
TTL1
TTL2
PWR(-)
GND
PWR(+)
J1
Microwave Products Group
K&L MICROWAVE
BSC
POLE ZERO
Dow-Key Microwave
ENABLING COMMUNICATION AND SIGNAL CONTROL
www.klmicrowave.com • www.klfilterwizard.com • 410-749-2424 • sales@klmicrowave.com


New Wave in Noise
NOISEWAVE
NW3G-D
060911
NOISEWAVE
NW3G-D-12V
072703
NOISEWAVE
NoiseWave
your supplier of high performance, precise equipment for AWGN
NOISEWAVE
The new wave in NOISE
Ph. (973) 386-1119 • Fax (973) 386-1131 • info@noisewave.com • www.noisewave.com

Microwave Journal
November 2016
Vol. 59 • No. 11
Government and Military Electronics
mwjournal.com

CONTENTS

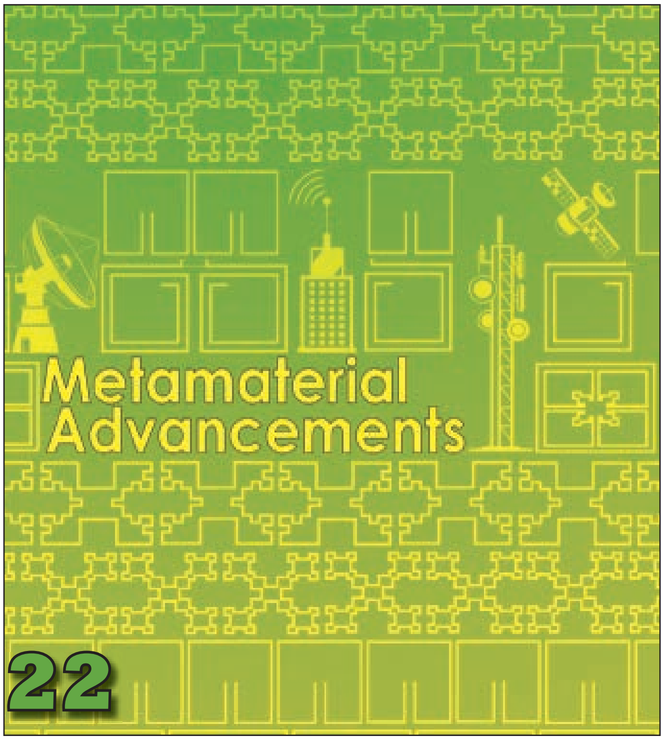

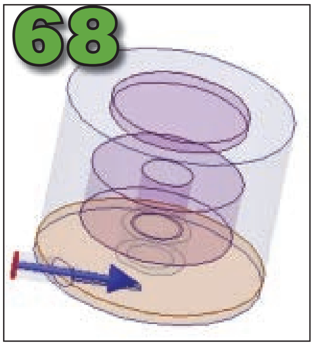

LOOK FOR BLOGS FROM:

- Keysight on Overcoming RF/Microwave Interference Challenges
- National Instruments, 5G Monthly Update
- Qorvo's Brent Dietz, Go Small or Go Home
- Rogers, PCB Design

microwavejournal.com/blogs

Cover Feature

Technical Feature

Application Note

AUGMENTED REALITY: HOW IT WORKS

STEP 1
Download the free Layar app from the iTunes (iOS) or Google Play (Android) store.

STEP 2
Launch the app to view enhanced content on any page with the layar logo.

STEP 3
Frame the entire page in the screen and tap to experience enhancements (tap screen again for full screen view).

Look for the Layar logo on participating pages.

AR pages may expire after 30 days.

59 YEARS OF PUBLISHING EXCELLENCE


ONE PLATFORM, ZERO BARRIERS
SIMPLY SMARTER
NI AWR DESIGN ENVIRONMENT
NI AWR Design Environment is one platform — integrating system, circuit, and electromagnetic analysis — for the design of today's advanced wireless products from base stations to cellphones to satellite communications. Its intuitive use model, proven simulation technologies, and open architecture supporting third-party solutions translates to zero barriers for your design success. Simply smarter design.
Learn more at ni.com/awr
AWR
NATIONAL INSTRUMENTS™
Microwave Office | Visual System Simulator™ | Analog Office | AXIEM | Analyst™

Microwave Journal CONTENTS

mwjournal.com

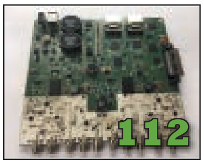

Product Features

Tech Briefs

Departments

Microwave Journal (USPS 396-250) (ISSN 0192-6225) is published monthly by Horizon House Publications Inc., 685 Canton St., Norwood, MA 02062. Periodicals postage paid at Norwood, MA 02062 and additional mailing offices.

POSTMASTER: Send address corrections to *Microwave Journal*, PO Box 1143, Skokie, IL 60076 or e-mail mwj@halldata.com. Subscription information: (847) 763-4943. This journal is issued without charge upon written request to qualified persons working in the RF & microwave industry. Other subscriptions are: domestic, $120.00 per year, two-year subscriptions, $185.00; foreign, $200.00 per year, two-year subscriptions, $370.00; back issues (if available) and single copies, $10.00 domestic and $20.00 foreign. Claims for missing issues must be filed within 90 days of date of issue for complimentary replacement.

STAFF

Publisher: Carl Sheffres
Editor: Patrick Hindle
Technical Editor: Gary Lerude
Managing Editor: Jennifer DiMarco
Associate Technical Editor: Cliff Drubin
Multimedia Staff Editor: Leslie Nikou
Multimedia Staff Editor: Barbara Walsh
Contributing Editor: Janine Love
Consulting Editor: Harlan Howe, Jr.
Consulting Editor: Frank Bashore
Consulting Editor: David Vye
Consulting Editor: Raymond Pengelly
Electronic Marketing Manager: Chris Stanfa
Digital Content Production Specialist: Lauren Tully
Audience Development Manager: Carol Spach
Traffic Manager: Edward Kiessling
Director of Production & Distribution: Robert Bass
Art Director: Janice Levenson
Graphic Designer: Sachiko Stiglitz

EUROPE

International Editor: Richard Mumford
Office Manager: Nina Plesu

CORPORATE STAFF

CEO: William M. Bazzy
President: Ivar Bazzy
Vice President: Jared Bazzy

EXECUTIVE EDITORIAL OFFICE
685 Canton Street, Norwood, MA 02062
Tel: (781) 769-9750
FAX: (781) 769-5037
e-mail: mwj@mwjournal.com

EUROPEAN EDITORIAL OFFICE
16 Sussex Street, London SW1V 4RW, England
Tel: Editorial: +44 207 596 8730 Sales: +44 207 596 8740
FAX: +44 207 596 8749

SUBSCRIPTION SERVICES
Send subscription inquiries and address changes to:
Tel: (847) 291-5216
e-mail: mwj@halldata.com

BPA WORLDWIDE

www.mwjournal.com

Printed in the USA

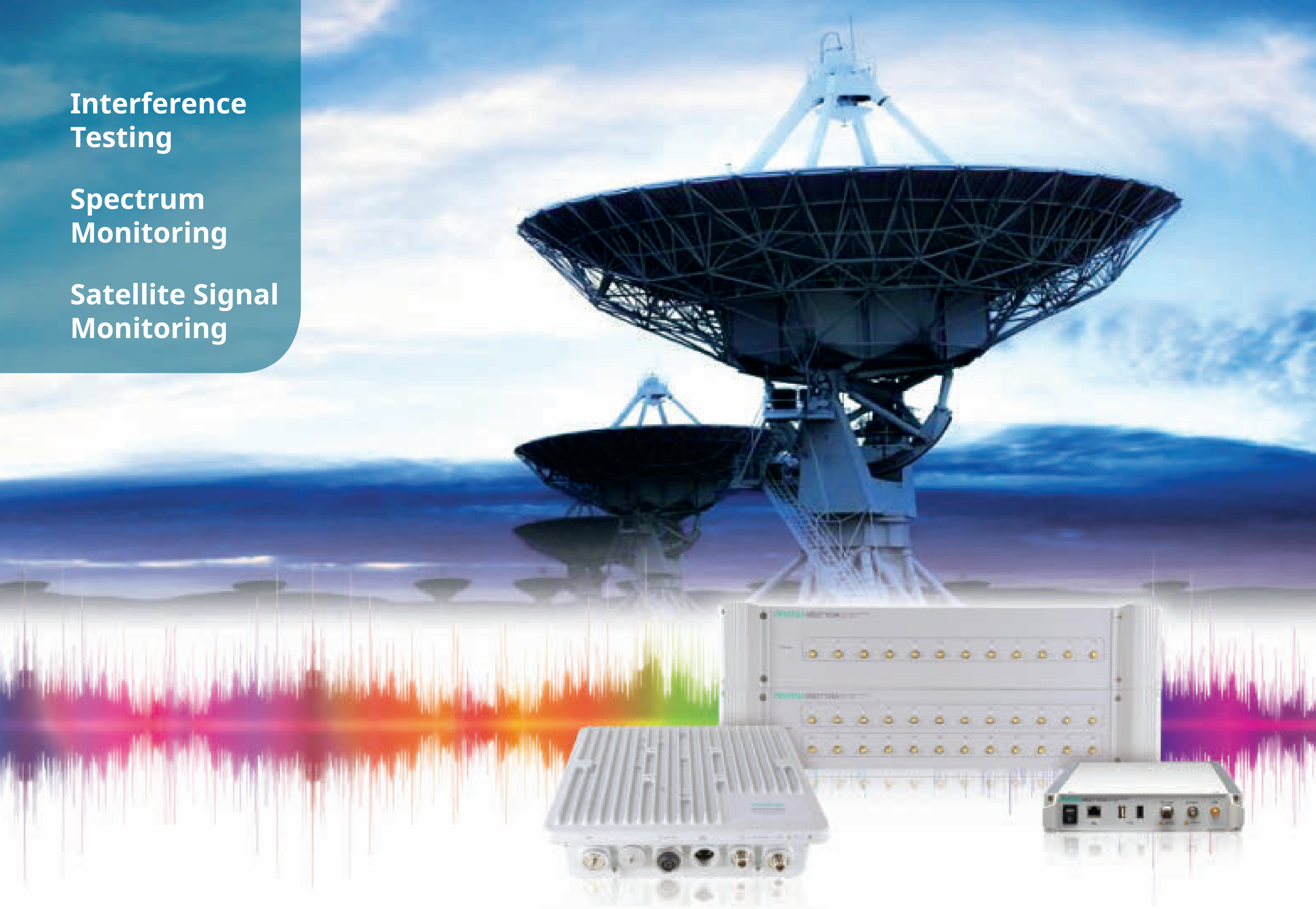
Interference Testing
Spectrum Monitoring
Satellite Signal Monitoring

Microwave Journal Online

Scan page using layar app

Visit us @ mwjournal.com

eLEARNING free webinars

Performing On-Wafer VNA Measurements from 70 kHz to 110 and 145 GHz
Sponsored by: Anritsu 11/1

Unlocking Wideband 5G & mmWave Insights to 110 GHz
Presented by: Keysight Technologies 11/2

Analyzing HF & LF RadHaz Scenarios with 3D EM Simulation
Presented by: CST 11/3

Tackling the Challenges of Next Generation ADAS Vehicle Architectures
Sponsored by: National Instruments 11/3

EMC Simulation for Space Applications with CST STUDIO SUITE
Presented by: CST 11/10

Passive Components
Sponsored by: Mini-Circuits 11/10

AntSyn
Sponsored by: National Instruments/AWR 11/16

Transformer Simulation
Presented by: CST 11/17

Ampleon Brings RF Power Innovations Towards Industrial Heating Market
Sponsored by: Ampleon 11/17

Antenna Analysis and Design with Characteristic Mode Analysis
Presented by: CST 11/22

Web Survey

What will be the first successful commercial application of AESAs?

Look for our multiple choice survey online at mwjournal.com

September Survey

Which Briton said, “The only laws of matter are those which our minds must fabricate, and the only laws of mind are fabricated for it by matter?”

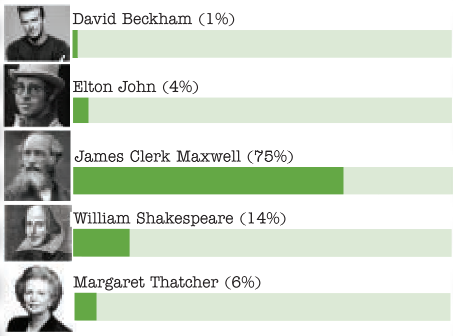

Executive Interviews

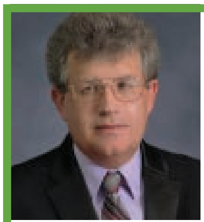

Dr. Alexander Chenakin, vice president, Advanced Technologies at **Micro Lambda Wireless Inc.**, discusses the company’s market strategy, new products and future industry development in oscillator technology.

Cees Links, general manager of **Qorvo’s** low power wireless business, maps the landscape of the Internet of Things: the applications, competing technologies and the claims Qorvo is staking.

WHITE PAPERS

Altair

Innovative Integration a molex company

NATIONAL INSTRUMENTS

Catch *Frequency Matters*, the industry update from *Microwave Journal*, www.microwavejournal.com/FrequencyMatters

COM

DECEMBER MARK YOUR CALENDAR

1

WEBINAR **Simulating Electromagnetic Shielding for Compact, High-Performance Mobile Devices**
Sponsored by: CST

1

WEBINAR **PAM4 Demands Accurate S-parameters**
Sponsored by: Anritsu envision : ensure

5

Call for Papers Deadline
IMS
http://ims2017.org

5-9

APMC 2016
IMaRC

New Delhi, India

The 2016 Asia Pacific Microwave Conference (APMC) will cover the entire scope of microwave engineering, including RF/microwave, antennas & propagation and EMC/EMI. Co-located with APMC, the 2016 International Microwave and RF Conference (IMaRC) will focus on topics considered non-standard in the area of microwaves such as biological effects and nanotechnology.

www.apmc2016.org
www.imarc-ieee.org

6

WEBINAR **MMIC**
Sponsored by: Mini-Circuits

8

WEBINAR **Antenna Simulation**
Sponsored by: COMSOL

8

WEBINAR **Accurate Simulations of Multistage Axial VIRCATORS Operating in S-Band Using CST PARTICLE STUDIO**
Sponsored by: CST

3-7

IEDM

San Francisco, Calif.

The 2016 International Electron Devices Meeting (IEDM) is a premier forum for reporting technological breakthroughs in the areas of semiconductor and electronic device technology, design, manufacturing, physics and modeling. **www.ieee-iedm.org**

15

WEBINAR **Radome Simulation**
Sponsored by: CST

20

WEBINAR **Coreless Packaging Technology for Compact, High-Performance Mobile Devices**
Sponsored by: CST

FOR DETAILS, VISIT MWJOURNAL.COM/EVENTS

ComingEvents

CAll FOR PAPERS

EDI CON CHINA 2017
November 28, 2016

IMS2017
December 5, 2016

WAMICON 2017
January 4, 2017

RFIC 2017
January 9, 2017

EuMW 2017
February 13, 2017

mwjournal.com

2016

DECEMBER

IEEE International Electron Devices Meeting (IEDM)
December 3–7, 2016 • San Francisco, Calif.
www.ieee-iedm.org

APMC 2016 and IMaRC 2016
December 5–9, 2016 • New Delhi, India
www.apmc2016.org, www.imarc-ieee.org

88th ARFTG Microwave Measurement Conference
December 6–9, 2016 • Austin, Texas
www.arftg.org

IEEE MTT-S Latin America Microwave Conference (LAMC 2016)
December 12–14, 2016 • Puerto Vallarta, Mexico
www.lamc-ieee.org

JANUARY

RWW2017
January 15–18, 2017 • Phoenix, Ariz.
www.radiowirelessweek.org

DesignCon 2017
January 31–Feb. 2, 2017 • Santa Clara, Calif.
www.designcon.com

FEBRUARY

Mobile World Congress 2017
February 27–March 2, 2017 • Barcelona, Spain
www.mobileworldcongress.com

MARCH

SATELLITE 2017
March 6–9, 2017 • Washington, DC
www.satshow.com

GOMACTech 2017
March 20–23, 2017 • Reno, Nev.
www.gomactech.net

Microwave & RF 2017
March 22–23, 2017 • Paris, France
www.microwave-rf.com

IWCE 2017
March 27-31, 2017 • Las Vegas, Nev.
www.iwceexpo.com

EMV
March 28–30, 2017 • Stuttgart, Germany
www.mesago.de/en/EMV/home.htm

APRIL

WAMICON 2017
April 24–27, 2017 • Cocoa Beach, Fla.
www.wamicon.org

EDI CON China 2017
April 25–27, 2017 • Shanghai, China
www.ediconchina.com

Expo Electronica
April 25–27, 2017 • Moscow, Russia
www.expoelectronica.ru

MAY

AUVSI's Xponential
May 8–11, 2017 • Dallas, Texas
www.xponential.org

CS ManTech 2017
May 22–25, 2017 • Indian Wells, Calif.
http://csmantech.org

Space Tech Expo USA 2017
May 23–25, 2017 • Pasadena, Calif.
www.spacetechexpo.com

JUNE

RFIC 2017
June 4–6, 2017 • Honolulu, Hawaii
http://rfic-ieee.org

IMS2017
June 4–7, 2017 • Honolulu, Hawaii
http://ims2017.org

EW Europe
June 6–8, 2017 • Olympia, London
www.eweurope.com

89th ARFTG Conference
June 9, 2017 • Honolulu, Hawaii
www.arftg.org

Sensors Expo & Conference
June 27–29, 2017 • San Jose, Calif.
www.sensorsexpo.com

COVER FEATURE
INVITED PAPER

Metamaterial Advances for Radar and Communications

Dr. Eli Brookner
Raytheon Co. (Retired), Lexington, Mass.

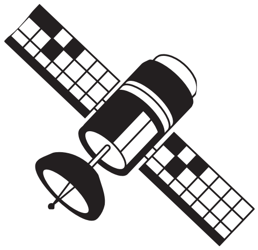

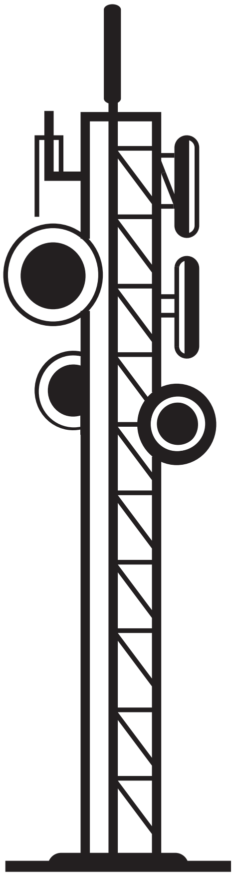

Metamaterial antennas have progressed considerably in the last few years. Kymeta demonstrated transmission to satellites and back using 20 and 30 GHz antennas about the size of a laptop, which use metamaterial resonators for phase shifting. Echodyne and Xerox PARC have developed metamaterial arrays for radar. The Army Research Laboratory funded the development of a metamaterial 250 to 505 MHz antenna with a λ/20 thickness. Complementing this, a conventional tightly coupled dipole antenna (TCDA) has been developed which provides a 20:1 bandwidth with a λ/40 thickness. Target cloaking has been demonstrated at microwaves using metamaterials. Stealthing, by absorption using a thin flexible and stretchable metamaterial sheet, has been shown to provide 6 dB absorption over an 8 to 10 GHz band, with greater absorption over a narrower range. Metamaterial has been used in cell phones to provide antennas that are 5× smaller (1/10th λ) having 700 MHz to 2.7 GHz bandwidth. It has also provided isolation equivalent to 1 m separation in antennas with 2.5 cm separation and is used for phased array wide angle impedance matching (WAIM).

Metamaterials are man-made materials in which an array of structures less than a wavelength in size are embedded (see ***Figure 1***).[1] These materials have properties not found in nature, such as a negative index of refraction. For one form of metamaterial the permittivity (ε) and permeability (μ) are both negative. When this happens the index of refraction $n = \sqrt{\mu\varepsilon}$ is negative, the negative sign being used for the square root.[2, 3] Actual materials have complex-valued ε and μ. The real parts of both ε and μ do not have to be negative to display negative refraction.[3]

A material with negative n is rarely found in nature. However, it can be produced by forming an array of metal split rings and rods (short parallel wires). The split ring resonators produce a permeability μ that is negative while the rods produce a permittivity ε that is negative. The dimensions of the metallic rings and rods must be smaller than a wavelength, but larger than an atomic dimension, to obtain a negative index of refraction. With metamaterial it is possible to achieve imaging beyond Abbe's diffraction limit which for modern optics is about $\lambda/2$. For regular materials, subwave-length imaging is hard to achieve because the evanescent waves containing the subwave-length information decay exponentially with distance, making them effectively nonexistent at the image plane.[4]

Purdue University has shown through simulation that metamaterial can provide imaging beyond the diffraction limit for visible light having a wavelength of 0.7 µm using two layers of anisotropic material.[4] The University of Illinois experimentally attained a $1/12^{th}$ λ resolution at 0.38 µm by using thin layers of silver, germanium and chromium.[5] The silver provided a negative permittivity which was sufficient for focusing beyond the diffraction limit, while the germanium enabled the silver film to be smooth. Using what is called a resonant metalens, Institut Langevin, ESPCI Paris Tech & CNRs achieved a resolution of $\lambda/80$ in the far field at microwave frequencies.[6] They believe that metalenses can be built at visible wavelengths using nanoparticles or nanowires as resonators. Applying imaging beyond the diffraction limit to integrated circuit lithography helps to advance Moore's Law.

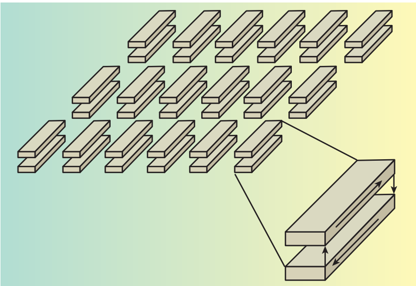

▲ *Fig. 1 A metamaterial is a synthetic material with properties based on the sub-wavelength repeated structure.*[1]

The definition of metamaterial has been extended to include material having any combination of positive and/or negative ε and μ. It includes electromagnetic band gap (EGB) material (also called photonic crystals).[2] For some in the RF community it includes frequency sensitive surfaces (FSS).[2] Included here, also, are fractal frequency selective surfaces.

ANTENNAS

Kymeta Array

Kymeta is developing a metamaterial antenna for internet communications via satellites.[7-11] They operate at 20 and 30 GHz and are about the size of a laptop computer. Their cost goal is about $1K for each antenna (see ***Figure 2***). For the internet communication links they would have something like 2 MB/s for the uplink and 20 MBs for the downlink. The RF radiated power is on the order of a few watts. Kymeta has a contract to supply these antennas for the O3b satellite system for which 12 satellites are already in circular equatorial orbit at a medium altitude of 8,062 km (see ***Figure 3***). Transmission from the ground to the satellites and back has been demonstrated. Kymeta originally received about $65 million in funding, mostly from Intellectual Ventures, about $10 million of which is from Bill Gates.

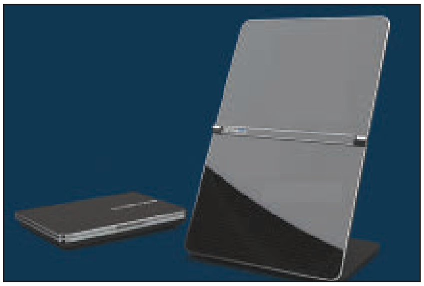

▲ *Fig. 2 Kymeta electronically steered metamaterial communications antenna.*[7, 8]

Fig. 3 O3b constellation.

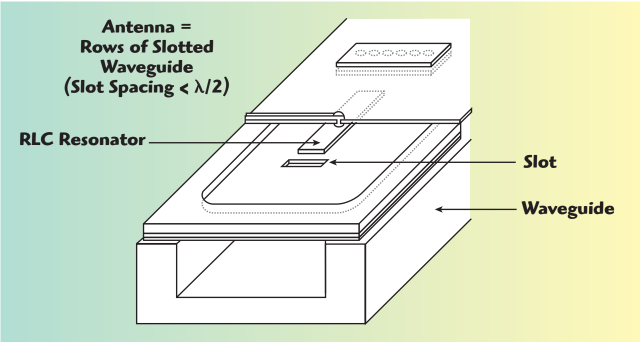

Fig. 4 Waveguide row showing slot and resonator locations.[11]

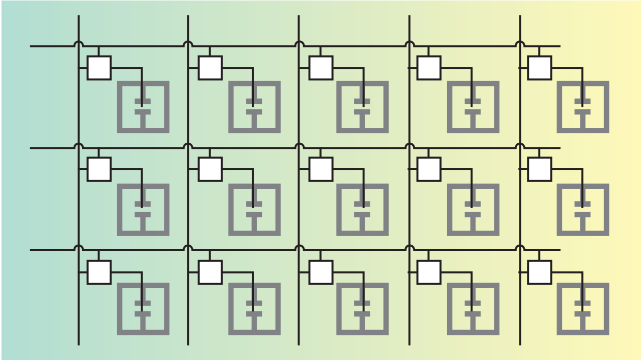

Fig. 5 Three waveguide rows of metamaterial resonators.[11]

Explanations of how the antenna might scan based on published material are now given for two architectures. For the first architecture, the array is formed from several rows or traveling wave feeds which could be a leaky waveguide over which a slotted metal cover is placed (see ***Figure 4***).[7,11]

Think of it as a slotted waveguide. The antenna consists of rows of these slotted waveguides which are end fed (see ***Figure 5***). Assume that it is desired to radiate in a specified direction. One then determines at which slots the signals have the desired phase shift to form a beam in that direction. Then only from these slots is the signal allowed to radiate. The signals from the other slots are blocked. The switch is a bandpass filter resonator placed over each slot that controls whether the signal is, or is not, radiated from the slot. When the resonator center frequency is at the frequency of the signal coming out of the slot, the signal passes through the resonator to radiate. If frequency of the resonator is shifted away from the signal frequency, the signal from that slot is blocked by the resonator and does not radiate. The resonators use liquid crystals whose dielectric constants can be controlled by bias voltages to shift their resonant frequencies.[7] The spacing between the slots is much less than the conventional ~λ/2 in order to have a large number of slots with the desired phase shift.

This leads to a thinned array wherein the thinning is pseudo-random and different for each different scanning angle. There are random phase and amplitude errors for the radiated signals because the signals at a slot will not always have the exact phase and amplitude needed for that slot position, and the resonator center frequency will not always be at the signal frequency. The thinning and errors lead to high antenna sidelobes.[12] Kymeta described a feedback technique for lowering the sidelobes.[9] In order to scan the beam in the direction perpendicular to the rows, the slots from row to row can be shifted


DELIVERY WITHIN THREE DAYS
SHOP OUR MILLIMETERWAVE STOCK ROOM
IN STOCK
Active Multipliers
IN STOCK
Faraday Isolators
IN STOCK
Harmonic Mixers
IN STOCK
Power Dividers
IN STOCK
Horn Antennas
IN STOCK
WG to Coax Adapters
IN STOCK
Omni-Directional Antennas
IN STOCK
Amplitude Detectors
IN STOCK
Directional Couplers
IN STOCK
Power Amplifiers
IN STOCK
Taper Transitions
VISIT US ONLINE FOR MORE
WWW.SAGEMILLIMETER.COM
MADE IN USA
www.sagemillimeter.com | 3043 Kashiwa Street, Torrance, CA 90505
T: 424-757-0168 | F: 424-757-0188 | sales@sagemillimeter.com
SAGE
Millimeter, Inc.

to achieve a phase shift from row to row. It is also possible for the signals that feed each row to have a different phase shift; but this does not appear to be their choice. The antenna has the ability to use frequency scanning in the row direction, as well.

Figure 6 shows an actual resonator,[7] a circuit consisting of an etched capacitor and inductor in parallel. The etched circuit is placed over a liquid crystal dielectric (previously described) which is placed on top of a ground plane. The liquid crystal's permittivity can be changed by applying a bias voltage between the etched RLC circuit and the ground plane. This bias voltage allows control of the resonator center frequency, placing it at the frequency of the signal when it is to be radiated and away from the signal frequency when it is to be blocked. The amplitude and phase shift of a generic resonator is shown in ***Figure 7***. A close-up of the antenna face with its closely spaced elements is shown in ***Figure 8***. Instead of a leaky waveguide with slotted cover one can use a microstrip, coplanar waveguide, parallel plate waveguide, dielectric slab or lossy waveguide.[11] Because there are no active components, the cost of building this antenna with many slots, or elements, is low.

The method of antenna scanning described above is not a hologram but a thinned array having pseudo-random thinning. Kymeta's website shows such a random thinning of the radiating elements. Strictly speaking this is not a metamaterial antenna[13]

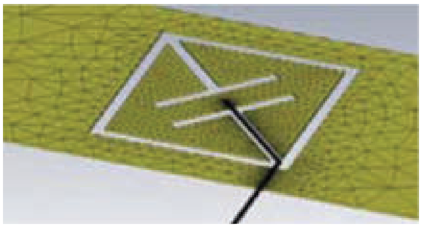

Fig. 6 Metamaterial RLC resonator.[7]

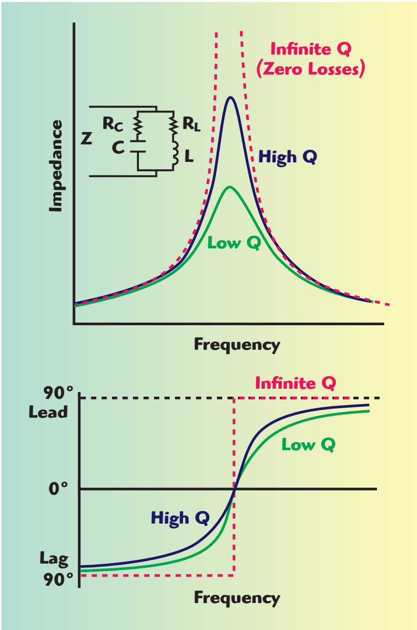

Fig. 7 Generic parallel RLC resonator filter.

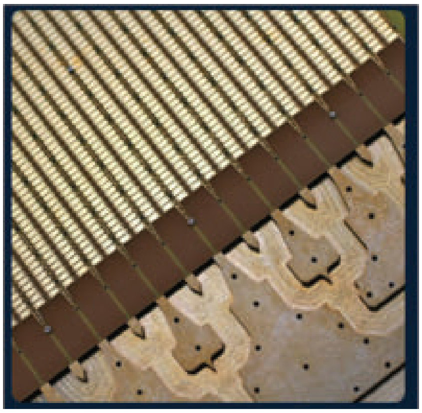

Fig. 8 Close-up of Kymeta antenna (from Kymeta website).

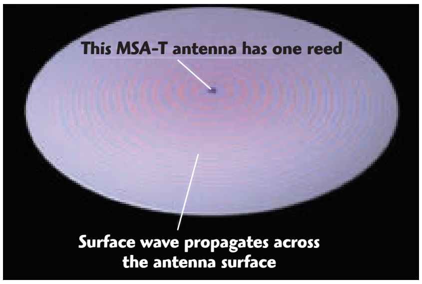

Fig. 9 Center fed circular array architecture (from Intellectual Ventures website, Copyright©Intellectual Ventures Management, LLC [IV]).

Fig. 10 Echodyne metamaterial array radars: MESA-D-DEV K-Band radar (a) and MESA-DAA K-Band radar (b).[15]

Has Amplifier Performance or Delivery Stalled Your Program?

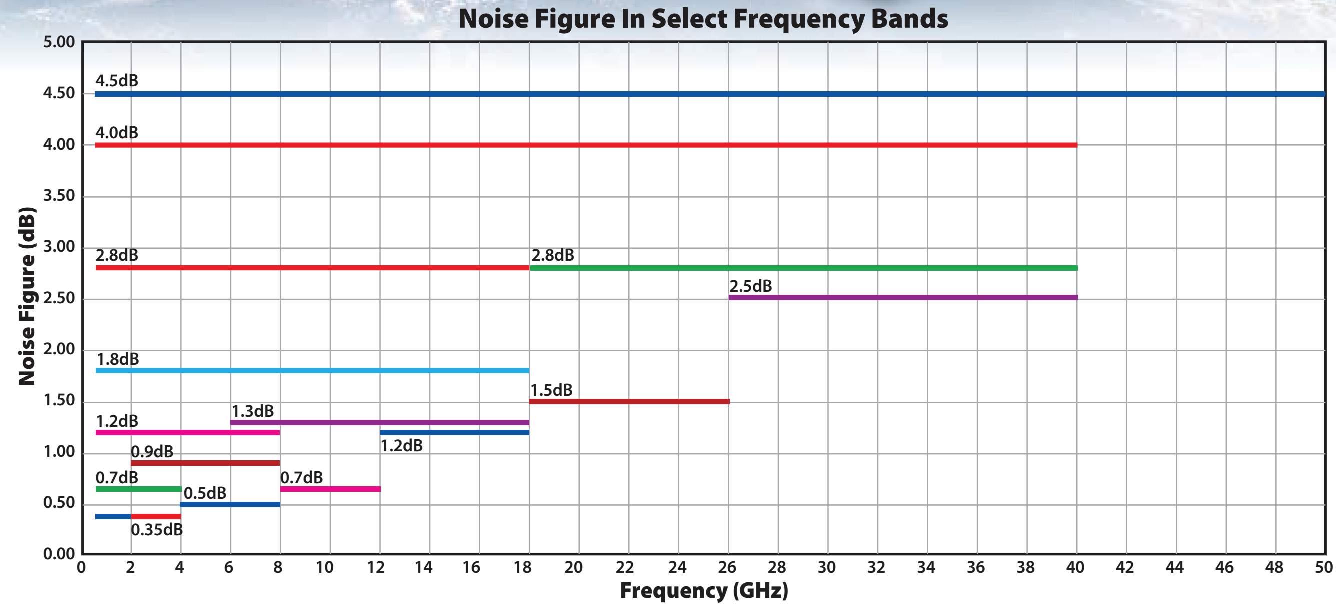

B&Z TECHNOLOGIES

Innovating to Excel

www.bnztech.com

TABLE 1
MESA-DEV K-BAND RADAR SPECIFICATIONS[17]

PARAMETER	VALUE
Field of View	±60° in azimuth ±40° in elevation
Beam Switching Speed	< 1 microsecond
Range	0 dBSm objects at > 500 m
Size	22 × 7.5 × 2.5 cm^3 including package
Weight	820 gm including package
Frequency	K-Band
Polarization	Horizontal
Calibration	None required
DC Power	Single DC power supply (+7 to +28 VDC)
Control Interface	USB Type C
Radar Modes	Short and Long Range FMCW

TABLE 2
MESA-DAA K-BAND RADAR TENTATIVE SPECIFICATIONS[17]

PARAMETER	VALUE
Application	Airborne detect and avoid (DAA) for small unmanned aircraft systems (UAS)
Range	> 3 km
Field of View (FOV)	±60° in azimuth ±40° in elevation Multiple units combined for greater FOV
Scanning Speed	1 Hz for FOV to 10 Hz for updating locations of previously detected objects

TABLE 3
MESA-X-EUV X-BAND PASSIVE ARRAY SPECIFICATIONS[17]

PARAMETER	VALUE
Field of View	±50° in azimuth ±45° in elevation
Beam Switching Speed	< 1 microsecond
Size	2.5 cm (1 in) thick excluding package
Weight	< 1.4 kg (3.1 lb)
Frequency	X-Band
Broadside Gain	19 dBi at 10.15 GHz
Polarization	Horizontal
Calibration	None required
DC Power	Single DC power supply (12 VDC)
Control Interface	Serial USB 2.0
RF In/Out	SMA coax port to user transceiver
Radar Modes	Pulsed and CW compatible

because it does not make use of the resonators being placed in an antenna material in an array configuration in order to change its permittivity and/or permeability. Instead it uses the properties of each resonator independently to act as an on-off switch. It is a clever and novel concept wherein one achieves phase shifting without the use of an active phase shifter and is a new type of electronically scanning array (ESA). The resonators were originally developed to create a metamaterial with a negative permittivity.[14]

A second architecture, shown on the Intellectual Ventures website, uses a circular metamaterial antenna instead of a rectangular antenna (see ***Figure 9***). In this configuration the antenna is center fed. Here one could use two circular disks with the bottom disc having the RF signal fed into to its center and with the top disc having the slots in a rectangular lattice with the resonator switches above them. Again, only slots which have the desired phase radiate; and, again, it is a pseudo-random thinned array. In this case it forms a hologram.[7,11] A potential competing technology to the Kymeta approach is to use a conventional AESA built using low cost extreme MMIC technology.[15, 16]

Echodyne Array

A second company, Echodyne, has developed metamaterial arrays for radar using these antennas (see ***Figure 10*** and ***Tables 1-3***).[17] Echodyne, like Kymeta, is funded by Intellectual Ventures and Bill Gates. Switching times needed for the intended radar applications, e.g., 1 µs, are much shorter than needed for communications.

Xerox PARC (see ***Figure 11***) is developing a car radar that uses a metamaterial array antenna.[18] It illuminates a wide angle on transmission and uses digital beam forming (DBF) to form many simultaneous beams and, in turn, an image of its surroundings. It has a 120° field of view and is intended for self-driving cars. Remember, Xerox PARC gave us the PC mouse as we know it as well as laser printing.

CONFORMAL ANTENNAS

Army Low Profile VHF

A metamaterial with negative ε produces what is called an artificial magnetic ground plane or a magnetic dielectric. Such a material would allow a dipole antenna (which ordinarily needs to be a ¼ wavelength above a metallic ground plane) to be flush with the artificial magnetic ground plane. This is possible because the electric field in the artificial magnetic ground plane can be

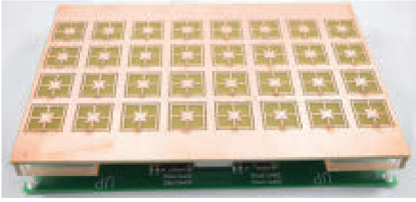

Fig. 11 Xerox PARC metamaterial array for car radar.[18]

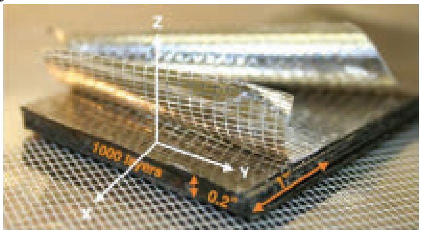

Fig. 12 Extremely low profile 250 to 505 MHz magnetic metamaterial antenna.[20]

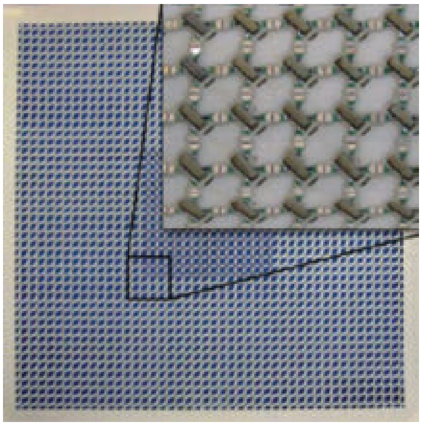

Fig. 13 Extremely low thickness wideband antenna array using tightly coupled dipole antennas.[24, 25]

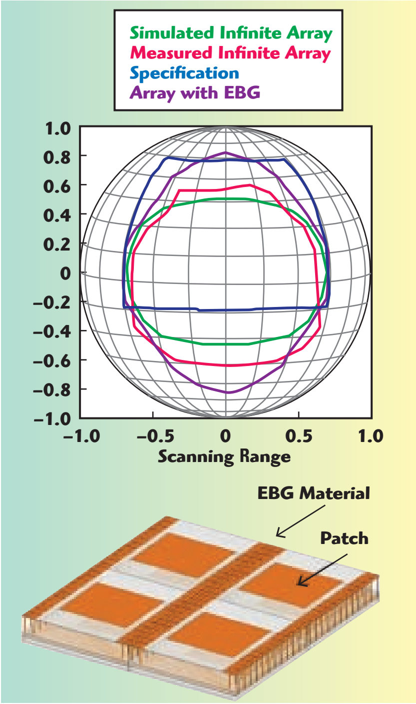

Fig. 14 Low cost, two-panel array with EBG enhancement for wide angle scan.[26]

equal and parallel to that in the dipole just above it. This is in contrast to a conducting ground plane where the electric field would be opposite in the ground plane and thus cancel out the electric field. The promise is that it would allow the construction of conformal dipole arrays. Such an antenna could replace the highly visible (by the enemy) feet-high whip antennas that are mounted vertically on the side of a HMMWV, leading to greater survivability.[19,20] The Army Research Laboratory has funded the development of a VHF/UHF metamaterial antenna (see ***Figure 12***).[20,21] Magnetic dielectrics having very wide bandwidths should be achievable in the band from 50 MHz to 20 GHz.[22]

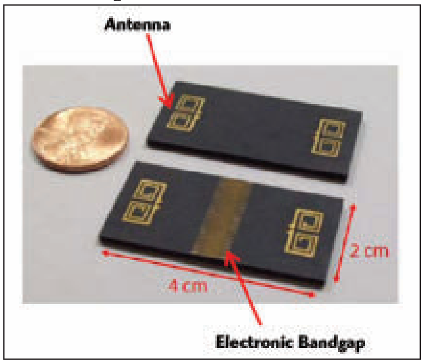

Fig. 15 EBG used to achieve isolation between and transmit and receive antennas[27] (courtesy of Professor K. Sarabandi, University of Michigan).

Very Wideband

Thales has demonstrated the placement of a conformal spiral antenna on a metamaterial with this antenna having a bandwidth from 2 to 8 GHz.[23] While discussing low profile wideband metamaterial antennas it is worth mentioning that a low thickness wideband antenna can be built without metamaterials using tightly coupled dipole antennas (see ***Figure 13***).[24,25]

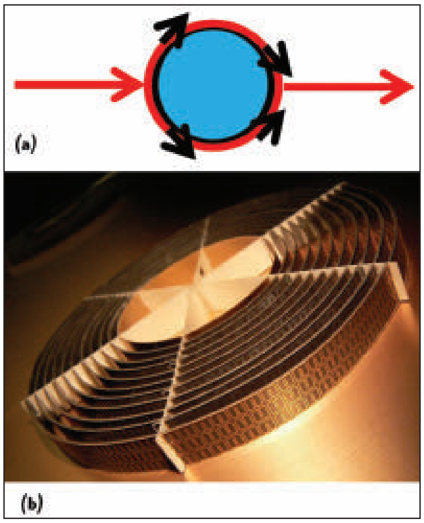

Fig. 16 Invisibility cloak concept (a) and Duke University microwave metamaterial cloaking device using metamaterial with split rings (b).[30]

ISOLATION AND WAIM

For their S-Band Digital Array Radar (DAR), Purdue University has used EBG material between patch radiating elements to reduce mutual coupling, resulting in a wider scan angle (see ***Figure 14***).[26] It serves to pro-

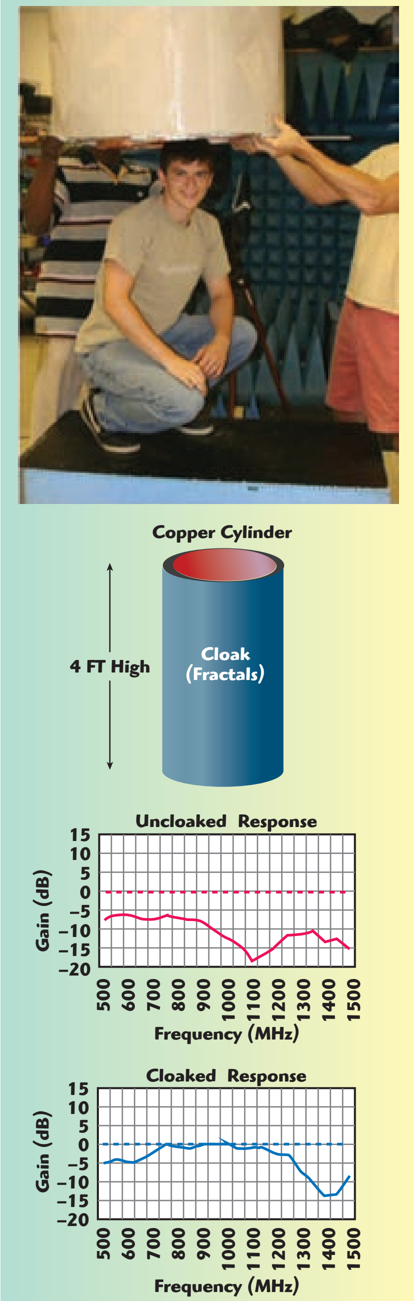

Fig. 17 Human invisibility cloak.[31, 32]

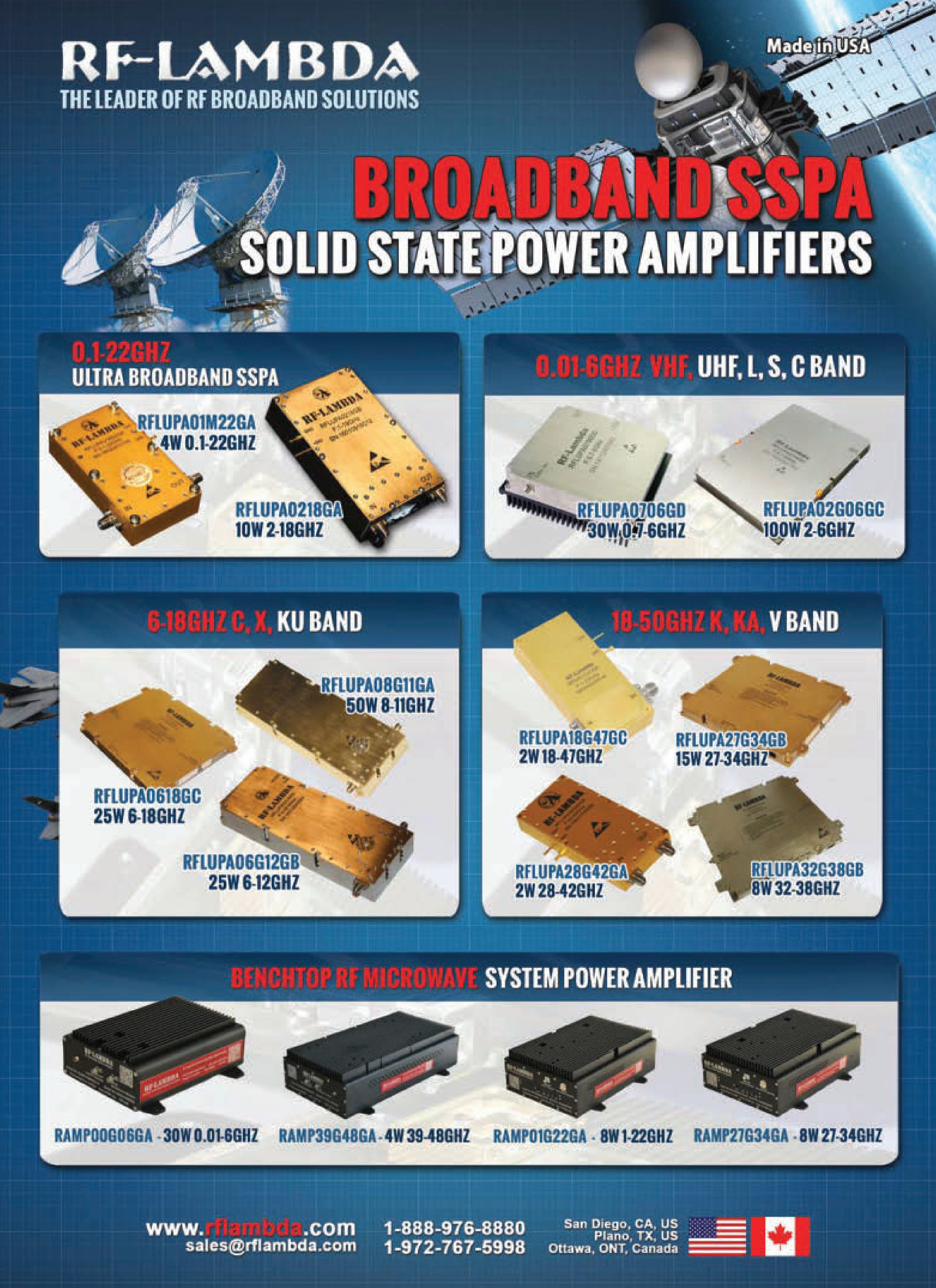
RF-LAMBDA
THE LEADER OF RF BROADBAND SOLUTIONS
Made in USA
BROADBAND SSPA
SOLID STATE POWER AMPLIFIERS
0.1-22GHZ
ULTRA BROADBAND SSPA
RFLUPA01M22GA
4W 0.1-22GHZ
RFLUPA0218GA
10W 2-18GHZ
0.01-6GHZ VHF, UHF, L, S, C BAND
RFLUPA0706GD
30W 0.7-6GHZ
RFLUPA02G06GC
100W 2-6GHZ
6-18GHZ C, X, KU BAND
RFLUPA08G11GA
50W 8-11GHZ
RFLUPA0618GC
25W 6-18GHZ
RFLUPA06G12GB
25W 6-12GHZ
18-50GHZ K, KA, V BAND
RFLUPA18G47GC
2W 18-47GHZ
RFLUPA27G34GB
15W 27-34GHZ
RFLUPA28G42GA
2W 28-42GHZ
RFLUPA32G38GB
8W 32-38GHZ
BENCHTOP RF MICROWAVE SYSTEM POWER AMPLIFIER
RAMP00G06GA - 30W 0.01-6GHZ
RAMP39G48GA - 4W 39-48GHZ
RAMP01G22GA - 8W 1-22GHZ
RAMP27G34GA - 8W 27-34GHZ
www.rflambda.com
sales@rflambda.com
1-888-976-8880
1-972-767-5998
San Diego, CA, US
Plano, TX, US
Ottawa, ONT, Canada

vide a wide angle impedance match (WAIM). In a program funded by the Army Research Lab, the University of Michigan used an EBG between the transmit and receive antennas separated by about 3 cm on a transponder operating at 2.72 GHz. They achieved 42 dB isolation, which is 24 dB above what would have been realized without the EBG (see ***Figure 15***). This is the isolation one would have realized, conventionally, for 1 m separation.[27]

COMMERCIAL WIRELESS

Metamaterial is used commercially in the wireless dual-band (2.4, 5 GHz) NDR3300 router.[28] Here eight antennas are placed on a RAYSPAN® metamaterial which allows the antennas to be smaller with better isolation. Metamaterial antennas are also used in our cell phones for the same purpose. They are 2D antennas less than 10 mm × 50 mm in area and paper thin.[29] Typically they are at least five times smaller than conventional antennas, i.e., 1/10th λ in size. Metamaterial antennas can be made broadband to support multiband operation such as 700 MHz to 2.7 GHz or GPS, Bluetooth, Wi-Fi and WiMax within one antenna array. It is claimed that they can be developed in a short time (two weeks to a month), are inexpensive to build, and provide low RF exposure to the user.[29]

CLOAKING AND STEALTHING

Target cloaking was first demonstrated at Duke University using metamaterials at microwaves. With cloaking, the electromagnetic wave transmitted by a radar goes around the target, making it invisible (see ***Figure 16a***). The Duke University microwave metamaterial cloaking device shown in ***Figure 16b*** uses concentric 1 cm wide rings. On each ring are etched split ring resonators that produce a negative index of refraction to

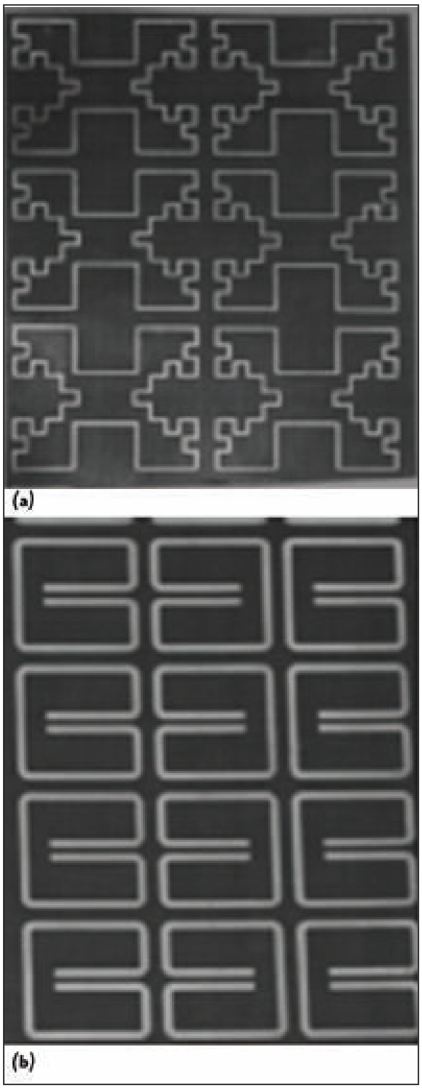

▲ *Fig. 18 Images of cloaking fractal (a) and split ring resonator (b) surfaces.*[31]

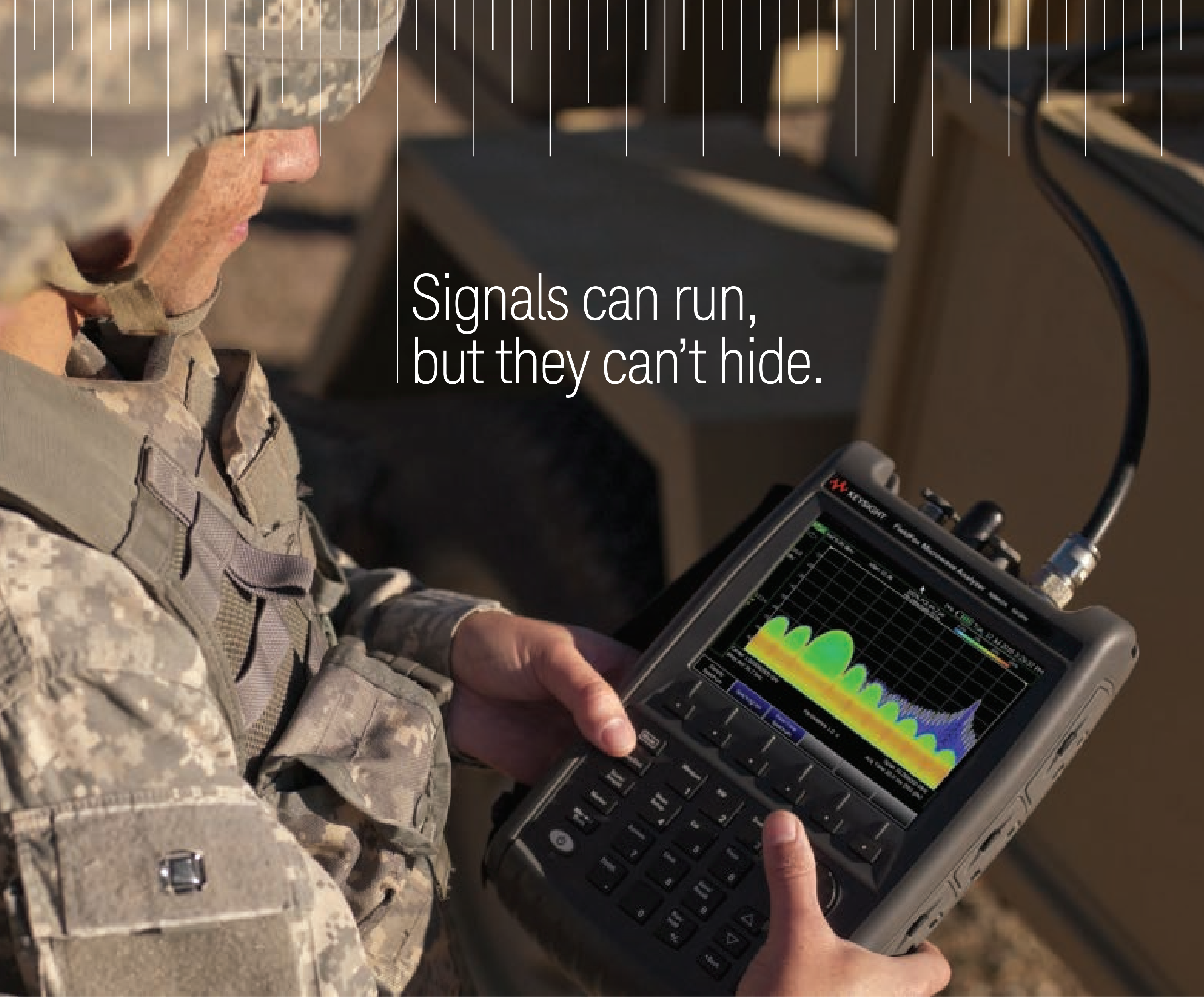
Signals can run,
but they can't hide.
KEYSIGHT

guide the microwave signal around a 5 cm center region that contains the object being stealthed. The outer diameter is 13 cm (~5 inches). Cloaking is achieved only over a narrow bandwidth.

Cloaking has more recently been demonstrated using fractals by Fractal Antenna Systems (see ***Figure 17***).[31,32] An engineer at the company was first placed in the path between a transmitter and receiver, blocking the signal such that it was reduced by 6 to 15 dB over the band from 750 to 1250 MHz. After being "cloaked" within a cylinder with a fractal coating around its surface and, again, placed in the path between the transmitter and receiver, the signal was no longer blocked. It was attenuated by only a fraction of a dB over the same 50 percent bandwidth. ***Figure 18*** shows both fractal and split ring resonator surfaces.

Another way to hide a target is for it to absorb the incident radar signal. Such stealthing has been demonstrated by simulation using a fractal frequency selective coating that is < 1 mm thick (see ***Figure 19***).[33] Absorption of 90 percent was achieved from 2 to 20 GHz and about 99 percent from about 10 to 15 GHz. Good absorption was achieved for all incident angles and polarizations. Iowa State University recently demonstrated stealthing with a stretchable, flexible metamaterial sheet consisting of silicon embedded with split ring resonators containing liquid metal alloy galinstan made

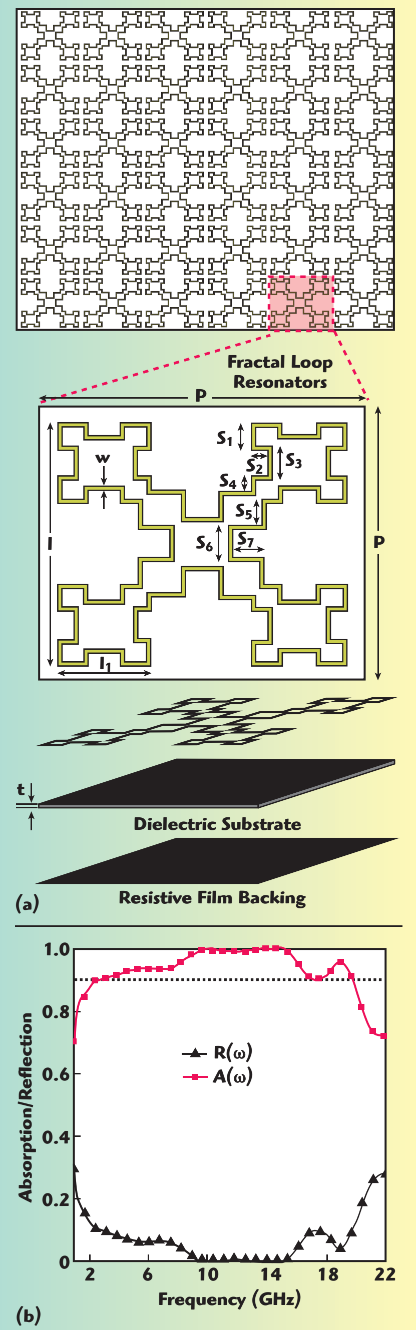

▲ *Fig. 19 Stealth by absorption: < 1 mm thick fractal metamaterial coating (a) and performance (b).*[33]

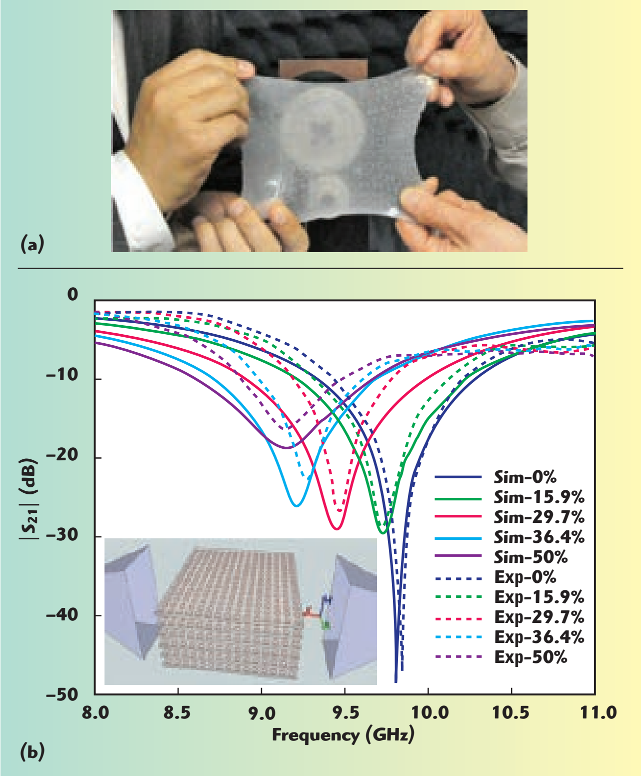

▲ *Fig. 20 Stretchable, flexible metamaterial absorber (a) and absorption for different meta-skin stretchings (b).*[33]

of gallium, indium and tin. It achieved a 6 dB target cross section reduction from 8 to 10 GHz with higher absorption over narrower bands (see ***Figure 20***).[34] It should be possible to apply this material conformally over the object to be "stealthed."

CONCLUSION

Metamaterials became an area of great interest as a result of a seminar paper by J. Pendry of the University of Cambridge.[35,36] There are now over a dozen books on the subject. One of these books (by Professor Munk),[37] questions whether one can actually produce material with a negative index of refraction. Dr. Munk claims that results obtained with what are called negative index of refraction materials can be achieved with non-negative index of refraction material. No matter what the explanation, it has been shown that it is possible, through the use of these materials, to achieve focusing beyond diffraction limit, cloaking and stealthing at microwave frequencies, conformal antennas at VHF/UHF, better isolation, electronic scanning arrays and reduced size antennas.■

References

1. S. Govind, "Realizing the Potential of Metamaterials," *Raytheon Technology Today Magazine*, Issue 1, 2012, pp. 24–27.
2. J.S. Derov, E.E. Crisman and A.J. Drehman, "Metamaterials and Their RF Properties," *Proceedings of the 2008 Antenna Applications Symposium*, Vol. 2, September 2008, pp. 176–189.
3. http://en.wikipedia.org/wiki/File:Negative refraction.ogg.
4. H. Liu and K.J. Webb, "NANOIMAGING: Bilayer Metamaterial Lens Breaks the Diffraction Limit," *Laser Focus World*, September 2009, pg. 35.
5. "Smooth Superlens Images at 1/12 Wave Resolution," *Laser Focus World*, March 2010.
6. G. Lerosey, "Resonant Metalens Resolves to Lambda/80," *Laser Focus World*, Vol. 46, No. 7, July 2010.
7. N. Kundtz, "Next Generation Communications for Next Generation Satellites," *Microwave Journal*, Vol. 57, No. 8, August 2014.
8. "MSA-T," *Intellectual Ventures*, www.intellectualventures.com/inventions-patents/our-inventions/msa-t.
9. M.C. Johnson, S.L. Brunton, J.N. Kutz and N.B. Kundtz, "Sidelobe Cancelling for Optimization of Reconfigurable Holographic Metamaterial Antenna," *IEEE Transactions on Antennas and Propagation*, Vol. 63, No. 4, April 2015, pp. 1881–1886.
10. J.B. Pendry, "Metamaterials," *International Radar Conference*, Keynote, October 2014.
11. A. Bily, J. Dallas, R.J. Hannigan, N. Kundtz, D.R. Nash and R.A. Stevenson, *US Patent No. 2014/0266946 A1*, September 18, 2014.
12. E. Brookner, "Practical Phased Array Antenna Systems," Section 2.1, Artech House, 1991.
13. S. Weiss (Army Research Lab) first alerted me to this.
14. D. Schurig, J.J. Mock and D.R. Smith, "Electric-Field-Coupled Resonators for Negative Permittivity Metamaterials," *Applied Physics Letters*, Vol. 88, No. 4, January 2006, pg. 041109.
15. E. Brookner, "Radar and Phased Array Breakthroughs," *Microwave Journal*, Vol. 58, No. 11, November 2015.
16. D.W. Corman, P. Moosbrugger and G.M. Rebeiz, "5G/Massive MIMO Channel, The Industry's Next Tipping Point," *Microwave Journal*, Vol. 57, No. 5, May 2014.
17. "MESA—Radars & Subsystems," http://echodyne.com/products/.
18. B. Casse, "Self-Driving Cars Need Better 'Digital Eyes' to Detect Pedestrians," *PARC blog*, October 2015, http://blogs.parc.com/2015/10/self-driving-cars-need-better-digital-eyes-to-detect-pedestrians/.
19. R. Shahidain, *Military Antennas*, 2009.
20. S.D. Keller et al., "Low Profile and Platform Specific Antennas," *Army Research Laboratory*, Adelphi, MD.

21. G. Mitchell and S. Weiss, *Army Research Laboratory*, Adelphi, MD; see also G. Mitchell and S. Weiss, "An Overview of ARL's Low Profile Antenna Work Utilizing Anisotropic Metaferrites," ARRAY-2016, October 2016.
22. J. S. Derov, private communication.
23. C. Renard and M. Soiron, "Wideband Multifunction Airborne Antennas," *International Radar Conference*, October 2009, pp. 1–3.
24. M. Sarcione, P. Hull, C. Whelan, D. Tonomura, T.V. Sikina, J. Wilson and R.E. Desrochers II, "Raytheon AESA Research: Past, Present and Future," *Raytheon Technology Today Magazine*, 2014, Issue 1, pp. 8–13.
25. J.A. Kasemodel, C.C. Chen and J.L. Volakis, "Broadband Planar Wide-Scan Array Employing Tightly Coupled Elements and Integrated Balun," *IEEE International Symposium on Phased Array Systems and Technology*, October 2010, pp. 467–472.
26. C. Fulton, Digital Array Radar, Ph.D. Thesis, Purdue University, 2010; see also C. Fulton and W. Chappell, "Low-Cost, Panelized Digital Array Radar Antennas," IEEE International Conference on Microwaves, *"Communications, Antennas and Electronic Systems,"* May 2008, pp. 1–10.
27. K. Sarabandi and Y.J. Song, "Subwavelength Radio Repeater System Utilizing Miniaturized Antennas and Meta-Material Channel Isolator," *IEEE Transactions on Antennas and Propagation*, Vol. 59, No. 7, July, 2011, pp. 2683–2690; also see Joseph Mait, Army Research Lab, Adelphi, MD.
28. T. Higgins, "What Do Metamaterials Really Do for Antennas?" *SmallNetBuilder*, January 2008, www.smallnetbuilder.com/content/view/30274/100/.
29. G. Poilasne, "RAYSPAN® Proprietary Metamaterial Antennas, A Proven SAR Reduction Solution," RAYSPAN, 2009, pp. 1–4. www.rayspan.com.
30. D. Schurig, J.J. Mock, B.J. Justice, S.A. Cummer, J.B. Pendry, A.F. Starr and D. R. Smith, "Metamaterial Electromagnetic Cloak at Microwave Frequencies," *Sciencexpress*, October 2006, pp. 1133628-1-4.
31. N. Cohen, "Fractals," Vol. 20, Nos. 3 & 4, pp. 227–232, World Scientific Publishing, 2012.
32. N. Cohen, "Wideband Omnidirectional Microwave Cloaking," *Microwave Journal*, Vol. 15, No. 1, January 2015.
33. F. Yue-Nong and G. Rong-Zhou, "An Ultrathin Wide-Band Planar Metamaterial Absorber Based on Fractal FSS and Resistive Film," *Chinese Physics B*, Vol. 22, No. 6, February 2013, pp. 067801-1-6.
34. S. Yang, P. Liu1, M. Yang, Q. Wang and J. Song, "From Flexible and Stretchable Meta-Atom to Metamaterial: A Wearable Microwave Meta-Skin with Tunable Frequency Selective and Cloaking Effects," *Scientific Reports*, Vol. 6, No. 21921, February 2016.
35. J.B. Pendry, "Negative Refraction Makes a Perfect Lens," *Physical Review Letters*, Vol. 85, No. 18, October 2000, pp. 3966–3969.
36. R.R. Marqués, F. Martín and M. Sorolla, "Metamaterials with Negative, Parameters: Theory, Design, and Microwave Applications," Wiley, 2008.
37. B.A. Munk, "Metamaterials: Critique and Alternatives," Wiley, 2009.

Dr. Eli Brookner *received his MEE and DrSc from Columbia University in 1955 and 1962, respectively; and he received his BEE from CCNY in 1953. From 1962 to 2014, as a principal engineering fellow with Raytheon Co., he was involved radar design for air traffic control, military and defence, space and navigation. These included ASDE-X, ASTOR RADARSAT II, AGBR, major space-based radar programs, NAVSPASUR, COBRA DANE, PAVE PAWS, MSR, COBRA JUDY Replacement, THAAD, SIVAM, SPY-3, Patriot, BMEWS, UEWR, SRP, Pathfinder, Upgrade for >70 ARSRs, AMDR, Space Fence and 3DELRR. Before Raytheon, he was with Columbia University Electronics Research Lab (now RRI), Nicolet and Rome Air Force Labs.*

Brookner received the IEEE 2006 Dennis J. Picard Medal for radar technology of application, the IEEE 2003 Warren White Award, the Journal of the Franklin Institute Premium Award for best paper (1966) and the IEEE Wheeler Prize for best applications paper (1998). He is a fellow of the IEEE, AIAA and MSS.

Brookner has nine patents and is the author of four books: "Tracking and Kalman Filtering Made Easy," 1998, Wiley; "Practical Phased Array Antenna Systems," 1991; "Aspects of Modern Radar," 1988; and "Radar Technology; 1977," Artech House. He has taught courses on radar, phased arrays and tracking worldwide (25 countries), with over 10,000 total attendees. He has authored over 230 papers, talks and correspondences (greater than 100 invited), contributed chapters to three books and has made many appearances as a banquet/keynote speaker. Six of his papers are reproduced in books of reprints (one in two books).

Cliff Drubin, Associate Technical Editor

New Chip Helps Communications and EW Radio Systems Adapt in Nanoseconds

To address the need for radio systems that can adapt to changing environments on the fly and be easily reconfigured once they're in the field, BAE engineers have developed the innovative MATRICS (Microwave Array Technology for Reconfigurable Integrated Circuits) chip. MATRICS helps address the future requirements of communications, electronic warfare and signal intelligence systems. The new, general-purpose chip enables engineers to develop customized radio systems without the need for application-specific chips that are expensive and time consuming to develop.

MATRICS was developed and matured with funding from the Defense Advanced Research Projects Agency (DARPA), as part of its Adaptive RF Technology (ART) program. The ART program aims to advance the hardware used in radios that can reconfigure themselves under a range of environmental and operating conditions.

Because MATRICS operates over a very wide spectrum of radio signals, systems based on this chip can benefit from reduced size, weight and power (SWaP) without the long development cycles and expensive engineering costs typically associated with customized chips. The reduced SWaP of the MATRICS chip makes it ideal for critical applications including unmanned aerial platforms and man-portable radios, where light weight and low power are at a premium. The MATRICS chip also lets engineers create rapid prototypes and working systems that can be fielded faster and that can accelerate the speed of delivery for new technology.

> "MATRICS is a radio frequency toolbox on a chip covering a broad range of radio waveforms..."

"MATRICS is a radio frequency toolbox on a chip," said Greg Flewelling, a senior principal engineer at BAE Systems. "It covers a broad range of radio waveforms so that many different types of systems can be designed around it, including ones that need wide spectrum awareness and adaptability to dynamic and challenging signal environments."

The speed of delivery from concept to the field is a critical component of the U.S. Department of Defense's Third Offset Strategy, which has created a demand for agile systems that can efficiently address changing conditions in real-time as new advanced technologies emerge. The DoD strategy also focuses on the need for accelerated development and the rapid fielding of new technology by modifying existing systems, concepts that are at the core of MATRICS' flexible design.

GaN Technology for AN/TPY-2 Radars

VIEW VIDEO

The U.S. Missile Defense Agency has awarded Raytheon Co. a contract modification to develop a transition to production process to incorporate gallium nitride (GaN) components into existing and future AN/TPY-2 radars. This initial effort will support the transition from gallium arsenide (GaAs) to GaN technology, which would further modernize the ballistic missile defense radar and drive down system obsolescence.

Currently fielded AN/TPY-2 radars use GaAs-based transmit/receive modules to emit high power radiation. Raytheon and MDA are pursuing a retrofit approach to leverage GaN elements.

> "GaN components have significant, proven advantages when compared to the previous generation GaAs technology."

"GaN components have significant, proven advantages when compared to the previous generation GaAs technology," said Raytheon's Dave Gulla, vice president of the Integrated Defense Systems Mission Systems and Sensors business area. "Through this effort, Raytheon will develop a clear modernization upgrade path for the AN/TPY-2 radar, enabling the system to better defend people and critical assets against ballistic missile threats at home and abroad."

The AN/TPY-2 is a transportable, X-Band radar that protects civilians and infrastructure in the U.S., deployed military personnel, and allied nations and security partners from the growing ballistic missile threat. According to recent Congressional testimony by the director of the U.S. Missile Defense Agency, the threat is growing as potential adversaries acquire a greater number of ballistic missiles, increase their range, incorporate countermeasures and make them more complex, survivable, reliable and accurate.

NGC Demos Counter-UAS Technologies

VIEW VIDEO

Northrop Grumman Corp. recently took part in the annual U.S. Department of Defense (DoD) Black Dart exercise for countering unmanned aerial systems (UAS).

Managed by the Joint Integrated Air and Missile Defense Organization, Black Dart is the DoD's largest live-fly, live-fire joint counter-UAS technology demonstration.

"The proliferation of UAS threats is a growing concern," said Chuck Johnson, director, integrated fires, Northrop Grumman Mission Systems. "In the highly complex threat scenarios we are seeing, the users need innovative and ag-

For More Information
Visit mwjournal.com for more defense news

ile capabilities such as beyond-line-of-sight detection and non-kinetic negation that can be rapidly integrated with fielded systems."

Northrop Grumman's Mobile Application for UAS Identification (MAUI) is a mobile acoustic sensor that operates on Android cell phones and uses the phone's microphone to detect Group 1 drones, defined as UAS' weighing less than 20 pounds, flying lower than 1,200 feet and flying slower than 100 knots. The MAUI software-based approach leverages commercial off-the-shelf mobile devices to provide beyond-line-of-sight detection and identification of UAS threats in high noise environments.

New Multi-Role Land Radar

Defense and security company Saab launched its land-based Giraffe 1X radar in the United States market. The new, compact radar system, which offers advanced capabilities against small targets and the capacity to address multiple threat types, will address the emerging requirements of the maneuver force.

The Sweden-based company also plans to transfer Giraffe 1X intellectual property to Saab Defense and Security USA, its U.S.-based subsidiary, with the intention of meeting U.S. market needs efficiently, effectively and securely.

Image Source: SAAB

The decision to transfer the technology was made to address U.S. security and information assurance requirements, facilitate U.S. sourcing of components, and, in the long term, create more U.S. jobs.

"We have already shown a unique ability to deliver our products into sensitive programs, such as the AN/SPS-77 on the U.S. Navy's Littoral Combat Ship Program," said Erik Smith, head of Saab Defense and Security USA. "But this move goes one step further. Transferring the intellectual property to a U.S. company and creating a U.S based development track for this system will tremendously benefit the U.S. warfighter and taxpayer, respectively, by accelerating capability to the field and reducing costs and risk."

Giraffe 1X offers short-range air defense, sense-and-warn capabilities, and counter-UAS (unmanned aerial systems) and counter-RAM (rocket, artillery and mortar) functions. It is mountable on vehicles, vessels and fixed installations, such as a building or a mast. Its compact, mobile design leverages commercial components in an open-architecture solution built on Saab's Giraffe family of radars.

Reactel, Incorporated
Reacting First to All Your Filter Needs.
REACTEL, INC.
Let our Engineers show you what we can do in tight spaces!
High Performance, Rugged Packaging, Small Size and Weight
Great things *can* come in small packages. Reactel filters are ideally suited for the demanding environments that unmanned vehicles encounter.
Many manufacturers rely on Reactel to provide units which are:
• High performance
• Lightweight
• Low profile
Contact a Reactel engineer with your filter or multiplexer requirements. We can create a unit which will be the perfect fit for your applications.
Reactel is happy to introduce our Filter RFQ App available for Apple and Android devices.
8031 Cessna Avenue • Gaithersburg, Maryland 20879 • Phone: (301) 519-3660 • Fax: (301) 519-2447
For general inquiries, please email reactel@reactel.com • Follow us on Twitter: @reacteljim
Go online to www.reactel.com to download your Reactel catalog today.
Intertek
@reacteljim

Leti and Taiwan Institute Partner on IoT and 5G Technologies

Leti, an institute of CEA Tech, and the Institute for Information Industry of Taiwan (III) have announced an agreement for mutual exploration of a wide range of information and communications technology (ICT) related to the Internet of Things (IoT) and 5G wireless connectivity.

The five-year collaboration will include, but is not limited to: joint development and implementation of IoT and 5G based smart ICT solutions for the EU and Taiwan, and scientific information exchanges. Also envisioned are cross-invitations to scientific events, joint implementation of international collaborative projects and partnerships, and work on experimental platforms and test beds that can be used to provide real-world validation of solutions.

"... an excellent opportunity to pilot and demonstrate innovative 5G and IoT-related solutions..."

Leti's background in IoT and 5G systems, including spectrum management, radio access technologies and protocols, as well as IoT open platforms for large-scale systems, will be a primary contribution, along with its technological roadmaps. In addition to its expertise in IoT systems, III will provide access to Taiwanese technology platforms, as well as industry-driven requirements and use cases.

"Our two organizations have very complementary skills and ecosystems, and it's a pleasure to launch our collaboration. Together we have an excellent opportunity to pilot and demonstrate innovative 5G and IoT-related solutions that will be useful for industries and individuals in Taiwan and the EU," said Leti CEO Marie Semeria at the official signing ceremony in Taipei.

"Taiwan is currently supporting and promoting IoT and smart city. The service and platform that are based on IoT technology will be the key factor for industrial development. III and Leti's collaboration will significantly enhance our ability to pursue our mission of promoting industrial applications, R&D technologies and IoT infrastructures," commented III executive vice president Pao-Chung Ho.

ETSI Next Generation Protocols Group Releases First Specification

The European Telecommunications Standards Institute (ETSI) Industry Specification Group on Next Generation Protocols (NGP ISG) announced the release of its first specifications, "GS NGP 001: Next Generation Protocols; Scenarios Definitions."

This document defines key scenarios to evolve the current Internet Protocol (IP) suite architecture and addresses the future technologies that will be embedded in next generation networks. The aim is to provide all stakeholders with harmonized requirements that will be suitable for multi-access communication including wireless, wired and cellular communications. IP protocols were defined in the 1970s but a ubiquitous internet requires a different approach today, with new security, addressing and mobility issues to take care of.

"...shape their protocol evolution for 5G systems and 21st century networking technology..."

"Current and future use cases include 4K videos on various devices, massive IoT, drone control or virtual reality to name but a few – use cases that have nothing to do with those of the '70s. Modernized network protocols architecture had to be triggered and this is why NGP ISG was created in January this year," said Andy Sutton, chairman of NGP ISG.

With this document, ETSI NGP hopes to influence the key communications standards bodies (e.g., 3GPP, ETSI, IEEE, IETF, ITU-T) to shape their protocol evolution for 5G systems and 21st century networking technology so as to address the issues identified and meet the recommendations provided. The document also compares and contrasts existing IP suite protocols with next generation networking and internetworking protocol architecture proposals.

Nanoscale Memristors Enhance Development of Neuroscience

In a new paper, researchers from the University of Southampton, UK, and members of the EU-funded Real neurons-nanoelectronics Architecture with Memristive Plasticity (RAMP) project have demonstrated how memristors could help aid the development of more precise and affordable neuroprosthetics and bioelectric medicines.

The research team developed a nanoscale Memristive Integrative Sensor (MIS) into which they fed a series of voltage-time samples, which replicated neuronal electrical activity. By acting like brain synapses, the metal-oxide MIS was reportedly able to encode and compress (up to 200 times) neuronal spiking activity recorded by multi-electrode arrays. Besides addressing the bandwidth constraints, the researchers claim that this approach is also very power-efficient in that the power needed per recording channel was up to 100 times less when compared to current best practices.

Lead author Isha Gupta, a postgraduate research student at Southampton University, commented, "Our work can significantly contribute towards further enhancing the understanding of neuroscience, developing neuroprosthetics and bio-electronic medicines by building tools essential for interpreting the big data in a more effective way."

For More Information Visit mwjournal.com for more international news

"...building tools essential for interpreting the big data in a more effective way."

"We are thrilled that we succeeded in demonstrating that these emerging nanoscale devices, despite being rather simple in architecture, possess ultra-rich dynamics that can be harnessed beyond the obvious memory applications to address the fundamental constraints in bandwidth and power that currently prohibit scaling neural interfaces beyond 1000 recording channels," said co-author Dr. Themis Prodromakis.

Beecham Research Backs UK's Open IoT Initiative

The Digital Catapult Open-LPWAN initiative — Things Connected — launched recently in London aims to help UK SMEs exploit the innovative features of Low Power Wide Area Network (LPWAN) technologies. With Beecham Research as the 'Knowledge Partner' the initiative will focus on jump-starting the UK LPWAN ecosystem by lowering barriers for technology access, innovation and application development.

"LPWANs offer a new low cost connectivity option to connect a large number of IoT devices over long distances in a power-efficient and cost-effective way, opening up enormous potential for a new wave of IoT applications," said Saverio Romeo, principal analyst at Beecham Research.

Things Connected will initially be focused on supporting London-based organisations and SMEs, with the network utilising 50 IoT gateways to establish a LPWAN covering Zone 1 across the capital. However, the ambition is to create a national innovation support programme around LPWAN test beds in different UK regions and provide UK SMEs, entrepreneurs and communities with the knowledge and skills to harness the technology. It will also bring together demand and supply side stakeholders to accelerate market growth and establish strong links to international LPWAN initiatives.

"...enormous potential for a new wave of IoT applications..."

Jeremy Silver, CEO, Digital Catapult, said, "We have reached a pivotal point in the deployment of the Internet of Things across the UK. We want to capture more of the digital dividend in the UK economy and to do so, it is fundamental that we accelerate the adoption of the IoT. By enabling the testing of IoT innovation, Digital Catapult Things Connected will enhance the quality of life for those across the capital and further empower London's impressive and innovative tech community."

Precision GNSS in Automotive a Reality by 2021

Low-cost, precision, global navigation satellite systems (GNSS) receivers will become a reality in the driverless cars, drones, and even smartphone markets by 2021. The automotive industry will be the main driver behind precision GNSS receiver adoption, in which centimeter-level accuracy is essential to complete driver safety systems with the redundancy necessary for autonomous vehicles.

"There are a variety of competing technologies currently under investigation by the automotive industry, but it will move to a hybridized approach, combining LIDAR, HD maps, sensor fusion, machine vision and precision GNSS," says Patrick Connolly, principal analyst at ABI Research. "As the receivers' average selling price drops below $50, we expect to see a more immediate market for location technology services, such as AR Heads Up Displays (HUD), in high-end vehicles. Vehicle-to-Vehicle, or V2V, communication might constitute another use case for high-precision GNSS."

> Competition ranges from crowdfunded start-ups to Internet giants, reflecting the scale of opportunity.

In addition to autonomous vehicles, there are opportunities for low-cost, precision GNSS receivers in autonomous unmanned vehicles (AUV), as well as commercial and consumer devices. Though the average selling prices of such GNSS receivers is $1,000 and higher, ABI Research finds the cost to be one of the most addressable inhibitors to market growth today.

"Precision GNSS achieves sub-meter accuracy through a variety of methods, including a network of reference stations," continues Connolly. "The biggest question mark today is not cost-related, but instead how to achieve reliable, worldwide satellite navigation coverage to support correction techniques, such as real time kinematic, or RTK; and precise point positioning, or PPP. This is an extremely expensive undertaking, with currently no guarantee of a return on investment."

Competition in the location technologies market ranges from crowdfunded start-ups to Internet giants, reflecting the scale of the opportunity. Traditional precision GNSS receiver vendors like Trimble and Novatel have the intellectual property, engineering experience, and ownership of correction networks.

In the consumer GNSS receiver market, u-Blox and Skytraq lead the way. Each developed low-cost single frequency PPP and RTK receivers, with a clear roadmap toward dual-frequency. Other consumer GNSS providers, like ST Microelectronics, Broadcom and Qualcomm, also appear active in this space.

Start-ups like North Surveying, NVS Technologies, REACH and Swift Navigation continue to disrupt the industry, bringing low-cost precision receivers to market. Their goal is to hit an ASP below $100 in the near future. And Radiosense is a startup that received a lot of attention for its previous work concerning precision GNSS on smartphones. It is now working on automotive solutions in a pilot in Austin, Texas. Locata has the potential to be the wildcard in the deck, working on a powerful synchronization and location technology that may find its way into consumer technologies by 2021.

"Most interesting in the location technology competitive landscape is the involvement of Internet giants Google and Alibaba," concludes Connolly. "Google recently announced it will make GPS pseudoranges available to developers, which, although extremely nascent, could open up the door for a lot of innovation. And in China, Alibaba is a major partner in the roll-out of Continuous Operating Reference Stations, or CORS, networks in the region."

Defense and Consumer Drone Makers Set Sights on Commercial sUAS Market

ABI Research forecasts the small unmanned aerial systems (sUAS) market will surpass $30 billion by 2025, producing a 32 percent CAGR. The commercial sector will surpass the defense market in 2017, and by 2025, it will account for more than 70 percent of all sUAS ecosystem revenues. This includes agriculture, industrial inspection, and professional videography applications.

"It is readily apparent why defense sector sUAS suppliers, such as AeroVironment, Aeryon Labs and Elbit Technologies, as well as consumer drone companies like 3D Robotics, DJI, Parrot, Yuneec and others, are aggressively targeting the commercial sector through acquisitions, internal development, partnerships, and investment," says Philip Solis, research director at ABI Research. "It is where the greatest long term growth opportunity lies. Many businesses within the commercial sector are willing to spend money on UAV-related services and applications to reduce costs and provide better service."

> Small unmanned aerial systems market to exceed $30 billion by 2025.

The commercial sector will exhibit the strongest growth over the forecast period, with applications for professional videography, as well as agriculture and industrial inspection, responsible for the bulk of the gains. Data, modeling, operator and other services, as well as industry specific application services, will be the primary growth drivers for the commercial sector.

The consumer sector will follow the commercial market, achieving second highest overall growth. The civil and prosumer sectors will likewise experience moderate growth,

For More Information Visit mwjournal.com for more commercial market news

while for the defense sector, growth will remain largely flat.

"The consumer sector is either low-end consumer products with limited appeal or high-end prosumer products that cost too much," concludes Solis. "But this will change. Parrot is already offering products with the functionality of prosumer products but at a mid-range consumer price. Companies like Qualcomm will further enable high-volume potential of the consumer market with their silicon and software. Intel is also focusing on the commercial market, bundling its application and dedicated processors, RealSense sensors, and software solutions from its series of machine learning-related acquisitions."

DAS Market Shifts to North American Enterprises as Growth Surges in Asia-Pacific

The North American enterprise market for buildings in the 100,000 to 500,000 square feet floor area range represents the majority of Distributed Antenna System (DAS) spending today. The segment will continue to gain share and account for 70 percent of the North American market in 2025. But it is the Asia-Pacific region that will experience the most rapid growth. A DAS is one way of distributing cellular coverage and capacity inside buildings when the existing macro network signals cannot penetrate the buildings.

"While the Asia-Pacific region today, accounts for a fraction of the total market, thanks to its large and rapidly growing 4G subscriber base, this region will experience the greatest DAS growth through 2025," says Nick Marshall, research director at ABI Research. "The region will experience four times the growth of North America and multiply its market revenue by seven. Given this trajectory, we anticipate the Asia-Pacific market to exceed the North American market sometime in 2022."

> Worldwide DAS market revenue to top $19 billion by 2025.

Through 2025, 4G will dominate DAS spending. ABI Research forecasts the first commercial 5G in-building systems will deploy sometime in 2021 in the Asia-Pacific and North America regions.

"North America will continue to be a maturing market for DAS," concludes Marshall. "As building structures that are greater than 500,000 square feet, such as high profile sports stadiums and airports, already have DAS systems, spend is now shifting to smaller buildings since subscribers demand 24/7 connectivity everywhere."


New from TMS
Are these ON Your Radar?
Hi-Power GaN X-Band SSPAs
TELEDYNE
GaN-based SSPAs are available in 350W, 550W, and 1KW models. Featuring 1GHz bandwidth, these SSPAs deliver extended bandwidth operation with de-rated output beyond 1GHz, and can be combined to achieve higher output power levels.
• Superior spurious emissions performance for radar applications
• Integrated bias control for GaN devices
• Modular architecture for flexible design and scalability
• Proprietary power-combining approach for greater efficiency
SSPA Modules - X-band, GaN SSPA modules in the 9-10GHz range span 25W to 350W of peak power, which can be used as driver amplifiers for higher power systems or on their own for lower power applications. These modules include their own bias control for GaN devices, but utilize external power supplies and control circuitry for configuration flexibility.
Unsurpassed RF Performance for 9-10 GHz Radar Applications from Teleydne Microwave Solutions (TMS)
TELEDYNE MICROWAVE SOLUTIONS
Everywhereyoulook™
800.832.6869
Microwave@Teledyne.com
TeledyneMicrowave.com
The Power of Consolidation
Cougar • Defence • Labtech • MEC • Microwave • Paradise Datacom

Around the **Circuit**

Barbara Walsh, Multimedia Staff Editor

MERGERS & ACQUISITIONS

Anritsu Corp., a pioneer in the implementation of next generation wireless technologies, announced it is acquiring **Azimuth Systems Inc.**, a provider of automated, real-world RF performance test solutions, for an undisclosed amount. Azimuth Systems will become a subsidiary of Anritsu. Anritsu, with the integration of Azimuth's intellectual property, product portfolio and installed base, expands its test solutions, leveraging the strengths of both companies in the growing IoT and 5G markets.

Computer Simulation Technology AG (CST) announces the acquisition of **Aurora Software and Testing SL** (AURORASAT), a technology provider of tools for the analysis, synthesis and design of passive microwave components. AURORASAT software products have been serving the RF and microwave industries for the last 10 years. FEST3D is a tool for the analysis and design of passive microwave components based on waveguide and coaxial cavity technology using advanced simulation algorithms for extremely low simulation times.

Nokia announced it has acquired **Eta Devices**, a U.S. start-up focused on improving the efficiency of power amplifiers (PA) used in cellular base stations, 802.11ac access points and handsets. Eta Devices was formed in 2010 to commercialize a patented asymmetric multilevel outphasing (AMO) technology, developed at MIT by engineering professors Joel Dawson and David Perreault, co-founders of the company. Termed ETAdvanced, the AMO approach improves PA efficiency by selecting the amplifier's supply voltage to best handle the RF signal level. Unlike envelope tracking, which provides continous dynamic adjustment of the amplifier supply voltage, Eta's approach seems to select from a discrete number of supply voltages and amplifiers.

Silicon Labs announced the acquisition of **Micrium**, a supplier of real-time operating system (RTOS) software for the Internet of Things (IoT). This strategic acquisition helps simplify IoT design for all developers by combining a leading, commercial-grade embedded RTOS with Silicon Labs' IoT expertise and solutions. Micrium's RTOS and software tools will continue to be available to all silicon partners worldwide, giving customers a wide range of options, even when using non-Silicon Labs hardware.

COLLABORATIONS

Modelithics Inc. and **IPDiA** have teamed to develop Modelithics models for IPDiA's high performance ultra broadband surface mount silicon capacitor. Modelithics and IPDiA worked closely as part of the Modelithics Vendor Partner (MVP) Program to characterize the 10 nF low profile (100 µm) capacitor (UBSC 935 152 492 510). Modelithics has developed two equivalent circuit model versions, one that features validation to 67 GHz, based on testing done in microstrip format offering substrate and pad scalability, and another that is validated to 110 GHz, using test data obtained with a coplanar waveguide fixture on quartz thin film.

Leti, an institute of CEA Tech, and the **Institute for Information Industry of Taiwan** (III), a non-profit non-governmental technology development organization, announced an agreement for mutual exploration of a wide range of information and communications technology (ICT) related to the Internet of Things (IoT) and 5G wireless connectivity. The five-year collaboration will include, but is not limited to joint development and implementation of IoT and 5G-based Smart ICT solutions for the EU and Taiwan, and scientific information exchanges. Also envisioned are cross-invitations to scientific events, joint implementation of international collaborative projects and partnerships, and work on experimental platforms and test beds that can be used to provide real-world validation of solutions.

ARC Technologies of Amesbury Mass., announced a new family of dielectric controlled polymeric materials for injection molding, thermoforming and composite applications. The material includes formulations with a wide variety of electrical properties. PP6000 is a low dielectric, low-loss thermoplastic compound with good resistance to moisture and most chemicals. It is ideal for applications at 24 GHz and 77 GHz, including radomes for automotive radar, and can be used as an impedance-matching material or as a dielectric spacer. **Maryland Thermoform Corp.** of Baltimore Md. is a high-performance thermoforming facility that has teamed with ARC Technologies to bring thermoformed versions of these opportunities to market.

Federated Wireless announced it has added **Airspan Networks** to its Spectrum Access System (SAS) and Environmental Sensing Capability (ESC) platform, CINQ XP. Airspan is a provider of LTE small cells and small cell backhaul solutions. They have been using the 3.5 GHz band all around the world and are now positioned to become a leader in shared spectrum Radio Access Networks (RAN), a crucial element of 5G. Together they plan to undertake a trial integration of Airspan's products with CINQ XP in an effort to demonstrate interoperability between the two in the Citizens Broadband Radio Service (CBRS) 3.5 GHz band.

Orbital ATK Inc. and **Stratolaunch Systems** announced a multi-year production-based partnership that will offer significant cost advantages to air-launch customers. Stratolaunch Systems, in cooperation with Vulcan Aerospace, is responsible for realizing Paul G. Allen's vision for space. Under this partnership, Orbital ATK will initially provide multiple Pegasus XL air-launch vehicles

For More Information For up-to-date news briefs, visit mwjournal.com

for use with the Stratolaunch aircraft to provide customers with unparalleled flexibility to launch small satellites weighing up to 1,000 pounds into low Earth orbit. Pegasus has carried out 42 space launch missions, successfully placing more than 80 satellites into orbit for scientific, commercial, defense and international customers.

NEW STARTS

Airbus Defence and Space is continuing to future-proof its site at Friedrichshafen, Germany, with the construction of a new Integrated Technology Centre (ITC). At the heart of the four-story centre with a basement and a footprint of around 4,200 m² will be a large central clean room for the development and construction of satellites. The building, with dimensions of around 70 m × 60 m and a height of over 20 m, will be an expansion of the existing Hall 6 — the current satellite integration facility.

Pexco LLC, a North American specialty plastics developer and manufacturer, marked Manufacturing Day by opening the Extrusion and Engineering Center of Excellence (ECOE) at its Philadelphia-area facility. This center offers engineering consultation and design services for companies that require custom-extruded products or components. The center is focused on the industrial market, including the lighting, filtration and traffic safety sectors, as well as customers in other fields that require specialized plastic extrusions or custom-engineered parts. To demonstrate its commitment to skilled American manufacturing and its Philadelphia operation, Pexco announced a multi-year investment in the Bucks County Technical High School in Fairless Hills, Penn.

European company **MicroEJ** drastically simplifies go-to-market development with software solutions that make working on devices easier and reduces both the risk and the time to market for each new product with fast iterations and prototypes. To meet growing demand in North America, the company announced formation of its U.S. subsidiary, headquartered in the Boston, Mass. area. By establishing operations in North America, MicroEJ gets closer to its customers and will be able to provide the best support for its solutions on the extensive portfolio of microcontrollers, embedded microprocessors and platforms the company supports.

ACHIEVEMENTS

The inaugural **EDI CON USA** conference and exhibition took place on September 20-22, 2016 at the Hynes Convention Center in Boston, Mass. Nearly 1500 attendees took advantage of the opportunity to meet one-on-one with more than 140 exhibitors from the RF, microwave and high-speed digital industries. In addition, the event offered 15 free training sessions on the show floor as well as 55 technical sessions, 24 workshops, 12 sponsored talks, 4 short courses and 2 panels for conference attendees. The conference boasted more than 100 speakers/instructors who are leaders in their industry, providing insights and suggestions on ways to address today's electronic design engineering challenges.

Around the **Circuit**

American Standard Circuits announced that the company has achieved its AS9100 Rev C Certification. AS9100 is the internationally recognized quality management system standard specific to the aerospace, aviation and defense industries. This standard is strongly supported and adhered to by major aerospace OEMs and is being required by vendors within the supply chain on an increasing basis. This certification strengthens ASC's competitive position and standardizes quality, reliability and safety processes across its aerospace programs. AS9100 is managed by the International Aerospace Quality Group (IAQG) and is based on the ISO 9001 quality management standard, with 80 additional requirements and 18 amplifications specific to aerospace business operations.

The Irish Times Innovation Awards proved a very successful event for **Arralis** this year, who won the IT and Telecommunications Award as well as the overall prize for Innovation of the Year for its 94 GHz radar chipset. Arralis' 94 GHz radar chipset has a wide range of applications including aiding unmanned landings by spacecraft, drone guidance systems, air defence systems, airport radar, driverless cars as well as internet and next generation 5G telecommunications. The awards ceremony which took place on October 5 at the Royal Hospital Kilmainham in Dublin, showcased Ireland's top innovative talent in the various sectors and had received applications from over 300 companies.

Cambridge Broadband Networks Ltd. (CBNL) has been awarded the prestigious Innovation Award by the Competitive Carriers Association (CCA), the leading association for competitive wireless providers and stakeholders across the US. CBNL received the award for its VectaStar® 28 and 39 GHz platform, which enables carriers to unlock the benefits of millimeter wave and realize an evolutionary path to 5G fixed wireless. By providing more efficient use of spectrum compared to legacy technology, carriers can utilize VectaStar to leverage the vast capacity of millimeter wave and transform backhaul and fixed wireless performance.

QinetiQ has been awarded 21 Subpart-J accreditation under Australia's new Defence Aviation Safety Regulations (DASR) beginning 30 September 2016. The scope and breadth of the approval from Australia's Defence Aviation Safety Authority is unique to QinetiQ as the provider of structural integrity services to the Australian Department of Defence. The DASR brings Australia into alignment with the European Military Airworthiness Requirements, providing a common baseline with more than 30 other countries. This commonality and the flexibility and efficiencies that DASR offers will benefit and enhance Australian military aviation safety into the future.

Future Engineers, along with **NASA** and the **American Society of Mechanical Engineers** (ASME) Foundation, announced the two winners from Future Engineers' "Think Outside the Box Challenge," a national design challenge issued to K–12 students to celebrate the launch of

the Bigelow Expandable Activity Module (BEAM), the first expandable habitat deployed on the space station. One national winner from each age division was selected from a total of 122 submitted designs from 26 states. The winner from the Teen Group (ages 13–19) was "The Expanding Pod," designed by Thomas Salverson of Gretna, Nebraska. The winner of the Junior Group (ages 5–12) was "Space Anchor," designed by Emily Takara of Cupertino, Calif. These students will receive a grand-prize trip to Las Vegas, Nev., for a tour of Bigelow Aerospace.

CONTRACTS

The **U.S. Army Corps of Engineers, Engineering and Support Center**, Huntsville (CEHNC) awarded **Science Applications International Corp.** the High Performance Computing Modernization Program (HPCMP) Integrated Technical Services (HITS) task order to provide program management and technical support necessary to advance the services, capabilities, infrastructure, and technologies in the HPCMP supercomputing centers. The single-award, hybrid firm-fixed-priced, cost-reimbursable, cost-plus-incentive-fee task order has a one-year base period of performance, four one-year options, and a total contract value of $575 million, if all options are exercised. Work will be performed at centers in Hawaii, Maryland, Mississippi, and Ohio.

The **U.S. Navy** awarded **Lockheed Martin** an initial $148.9 million contract for full rate production of Surface Electronic Warfare Improvement Program (SEWIP) Block 2 systems with four additional option years to upgrade the fleet's electronic warfare capabilities so warfighters can respond to evolving threats. Under this full-rate production contract, Lockheed Martin will provide additional systems to upgrade the AN/SLQ-32 systems on U.S. aircraft carriers, cruisers, destroyers and other warships with key capabilities to determine if the electronic sensors of potential foes are tracking the ship.

VSE Corp. was recently awarded an Equipment Related Services (ERS) task order under the **TACOM Strategic Services Solutions (TS3)** contract to support supply chain management for the reset of family of medium tactical vehicles at Red River Army Depot (RRAD). This task order consists of a base year with two one-year options for a potential value of up to $63 million. Under this task order VSE will provide supply chain management services to the Medium Tactical Vehicle Product Support Integration Directorates FMTV Reset program.

The **U.S. Army** awarded **BAE Systems** a $13.5 million order to begin producing the new Family of Weapon Sights-Individual (FWS-I) thermal weapon sight for soldiers. Under the low rate initial production award, the company will deliver more than 100 weapon sight systems as part of a previously announced five-year contract for the Army's Enhanced Night Vision Goggle III and Family of Weapon Sight-Individual (ENVG III/FWS-I) program. The BAE Systems-developed FWS-I solution integrates the company's first-to-market 12-mircon technology, which helps

make its offering smaller and lighter while providing superior image quality.

The **U.S. Army** has placed an initial order of approximately $10 million for **Harris Corp.'s** Falcon III® AN/VRC-118 Mid-tier Networking Vehicular Radio (MNVR) after receiving a Milestone C decision and authorization for a limited rate production of the radios. The two-channel Harris MNVR solution is based on the company's combat-proven Falcon III® tactical wideband networking technology and uses the Wideband Networking Waveform (WNW) and Soldier Radio Waveform (SRW). It enables warfighters to share voice, data and video and also operates as a node in a mobile network — so information can be transmitted from one MNVR system to another until it reaches its destination.

PAR Government Systems Corp., a wholly-owned subsidiary of PAR Technology Corp., announced the awarding of a $7.2 million research and development contract with the **U.S. Air Force Research Laboratory** (AFRL) and the **Defense Advanced Research Projects Agency** (DARPA). Under this four-year contract, PAR Government will be leveraging its expertise in image and video processing, cloud computing, data analytics, and digital media forensics. The contract work will be performed by PAR Government's Intelligence, Surveillance and Reconnaissance (ISR) Solutions Sector.

PEOPLE

▲ *Mark Wallace*

Keysight Technologies Inc. announced that **Mark Wallace** will succeed Guy Séné as head of Keysight's global sales organization effective Nov. 1, 2016. Séné will remain as an advisor through the end of the company's first fiscal quarter, Jan. 31, 2017, when he will retire. Wallace, who is currently vice president and general manager of the Americas Field Operations for Keysight, previously held a variety of leadership positions across sales, marketing and channel management for Hewlett-Packard, Agilent and Keysight. Séné has been senior vice president, worldwide sales at Keysight since August 2014. He joined Hewlett-Packard in 1976, and also worked at Agilent Technologies from 1999 to 2014.

RFMW Ltd. announced that **Kevin LaRue** has joined their organization as Worldwide Director of Coaxial Components. LaRue has served in senior management positions at well known RF industry OEMs such as Molex/Koch Industries, Rosenberger, Radiall, M/A-COM, Amphenol, Matrix Science/AMP and Hughes Aircraft Co., Connecting Devices Division. LaRue's role will include the responsibility of managing and growing all facets of RFMW's Interconnect products globally, including supplier relations, business development with customers and product line development. With a successful track record, LaRue's experience strengthens and confirms RFMW's specialization strategy and brings a fresh approach to coaxial component sales and marketing.

SWITCH-N-SAVE by CEL

NEW! RF Switches

SWAP THEM WITH OTHER SUPPLIER SWITCHES FOR BIG SAVINGS

LOWER COST SOLUTIONS

Cost Savings for New and Existing Customers

HIGHER RF PERFORMANCE

Better RF Performance than other RF Switches

HIGH JAPANESE QUALITY

Manufactured in Japan with High Quality, Packaging and Testing

CEL Part Numbers	Switch Type	MAX Freq. (GHz)	Insertion Loss (dB)		Isolation (dB)		P0.1dB (dBm)		Package Type
			2.5 GHz	6.0 GHz	2.5 GHz	6.0 GHz	2.5 GHz	6.0 GHz	
CG2179M2	SPDT	3.0	0.45	N/A	26	N/A	+30	N/A	(1.25 x 2.0 x 0.9)
CG2214M6	SPDT	3.0	0.35	N/A	25	N/A	+30	N/A	(1.1 x 1.5 x 0.55)
CG2163X3	SPDT	6.0	0.40	0.50	40	31	+29	+28	(1.5 x 1.5 x 0.37)
CG2185X2	SPDT	6.0	0.35	0.40	28	26	+29	+29	(1.0 x 1.0 x 0.37)
CG2176X3	Absorptive SPDT	6.0	0.45	0.55	30	22	+35	+37	(1.5 x 1.5 x 0.37)
CG2415M6	SPDT	6.0	0.35	0.45	32	26	+31	+31	(1.1 x 1.5 x 0.55)
CG2430X1	SP3T	6.0	0.50	0.60	28	25	+28	+28	(1.5 x 1.5 x 0.37)

CEL

WWW.CEL.COM/SWITCHES

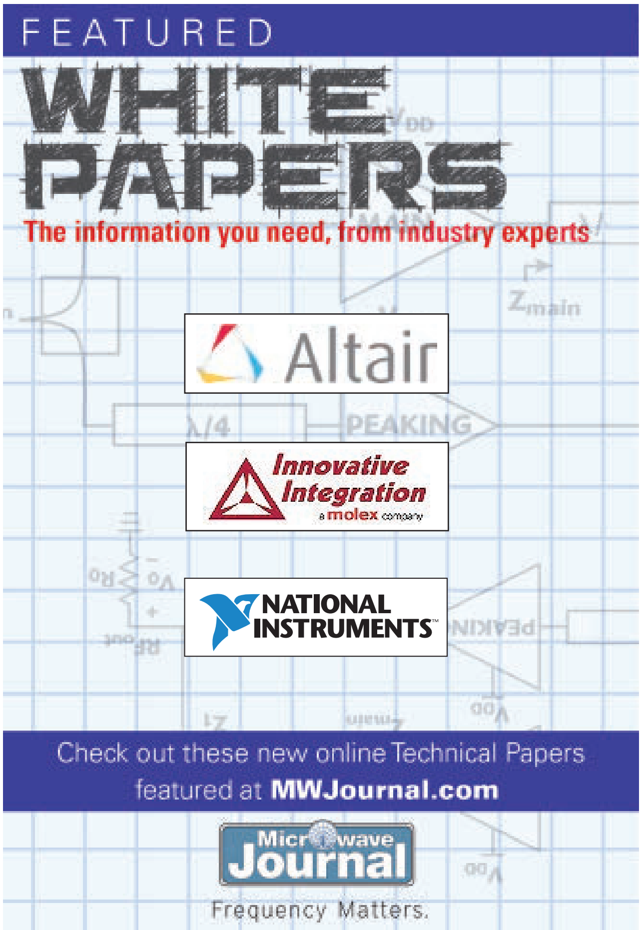

Around the **Circuit**

REP APPOINTMENTS

TechPlus Microwave Inc., a designer and manufacturer of RF/microwave filters, announced the appointment of **Munroe Communications** as their new representative. With over 30 years of experience in the RF/microwave community, Munroe Communications will provide sales solutions in aerospace, defense and R&D.

A master supply agreement between **e2v**, a global leader in the high reliability (hi-rel) semiconductor market, and **GaN Systems**, a manufacturer of gallium nitride power transistors, establishes e2v as the global supplier of GaN Systems' 100 V and 650 V hi-rel GaN transistor products and customer care for the A&D market. e2v will utilize its infrastructure and 30 years of experience in this area to support the hi-rel market with GaN's best-in-class and most reliable transistors and evaluation boards. e2v will offer state-of-the-art power management solutions that respond directly to the hi-rel market's growing SWaP (Size, Weight and Power) demands.

Antenna Systems Solutions S.L. (Celestia Technologies Group), a supplier of antenna measurement systems to the worldwide satellite, defense, wireless and government markets, announced that it has appointed **TranSemic Technology Ltd.** as its distributor in China and Hong Kong. The agreement includes distribution of electromagnetic metrology equipment, upgrades and spare parts. Under the agreement TranSemic will also become the primary provider of service and application support in the covered regions.

PLACES

Advanced Semiconductor Engineering Inc., a provider of semiconductor assembly and test services, held a groundbreaking ceremony at the site of its K24 building in the Nantze Export Processing Phase 2 Zone in Kaohsiung, Taiwan. The building is part of ASE's continued expansion plans for its research and development, and manufacturing campus in Taiwan. The 66,120 square meter K24 building will be the latest green building in ASE that incorporates green design in its construction with permeable pavement, stormwater management, earthquake proofing, energy efficient lighting and ergonomically constructed workspaces.

LOOK FOR BLOGS FROM:

Keysight on Overcoming RF/Microwave Interference Challenges

National Instruments, 5G Monthly Update

Qorvo's Brent Dietz, Go Small or Go Home

Rogers, PCB Design

microwavejournal.com/blogs

INVITED PAPER

Characterization and Modeling of High Q Dielectric Resonators

Edward C. Liang
MCV Microwave, San Diego, Calif.

This article addresses the practical issues using high Q dielectric resonator (DR) cavity designs for RF/microwave oscillators. DR materials and basic cavity structures are described, along with the characterization and measurement of cavity Q. The complex resonant modes and coupling structures are detailed, with special emphasis on the impact of coupling and tuning structures on various resonant modes. Electromagnetic (EM) simulation and the equivalent circuit of the resonator that can be incorporated into linear and nonlinear circuit simulations are discussed and demonstrated.

DR loaded cavities are important for RF/microwave filters and oscillators because of their high quality factor, Q and small size. They offer similar Q as the waveguide cavity in just an eighth to one twelfth the size. They provide excellent temperature stability when designed with a proper choice of dielectric material. However, the two common problems in dielectric resonator oscillator (DRO) design are degradation of the cavity Q from tuning and support structure and interference from higher order modes. Proper characterization of a DR loaded cavity can avoid these issues, allowing rapid prototyping with optimized DRO performance.

The widespread use of ceramic DRs to replace metallic resonant cavities in RF and microwave circuits started in the 1970s, with the first low loss, temperature stable barium tetratitanate ceramic materials.[1-4] Further development of high dielectric constant ceramics with adjustable temperature coefficients enabled microwave engineers to use these materials in oscillator and narrowband filter designs for radar detectors, cellular phone and public safety base stations, satellite receivers and satellite broadcasting (TVRO/DBS).[5-26]

DR CAVITY CHARACTERISTICS

The most direct way to reduce the cost of microwave circuits is to reduce their size. At a given frequency, the size of a DR is considerably smaller than that of an air resonant cavity, because the relative dielectric constant of the material is substantially larger than unity, which is the dielectric constant of air. Ideally, the size reduction equals the square root of the resonator's dielectric constant, ε_r. Even

TABLE 1
PROPERTIES OF COMMERCIALLY AVAILABLE DIELECTRIC MATERIALS

Series	ε_r	τ_f (ppm/°C)	Minimum Qf	f (GHz)
MDR-21	21 ± 1	5 ± 5	60,000	6.5
MDR-24	24 ± 1	1–3 ± 1	300,000	10
MDR-30	30 ± 1	0 ± 2	150,000	10
MDR-34	34 ± 1	2–3 ± 1	150,000	10
MDR-36	36 ± 2	0 ± 5	30,000	5
MDR-38	38 ± 1	0.7 ± 5	47,000	5
MDR-40	40 ± 1	3 ± 5	70,000	5
MDR-45	46 ± 1	-2–6 ± 0.5	43,000	6
MDR-47	47 ± 1	0 ± 10	46,000	6

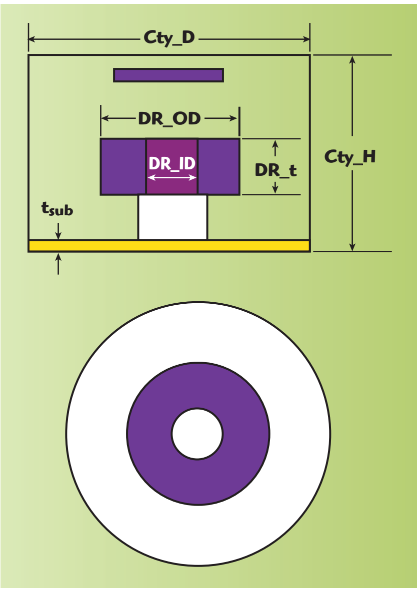

▲ *Fig. 1 Typical configuration of a dielectric loaded cavity.*

though the dielectric resonator and its metal enclosure need to be separated by substantial distance, one can reasonably achieve volume miniaturization of 1/8 to 1/12 comparing a dielectric resonator to an air cavity with the same Q. Examples of commercially available high Q dielectric materials are shown in ***Table 1***. In general, most dielectric materials can have their temperature coefficients adjusted, provided it does not affect the Q value. The product of dielectric Q and frequency (Qf) is pretty much a material constant in the usable frequency range.

A typical mechanical configuration of a DR loaded cavity is shown in ***Figure 1***. It is well known in practical high Q DR cavity design that the ratio of cavity height (Cty_H) to dielectric resonator thickness (DR_t) should be around 3 and that of cavity diameter (Cty_D) to dielectric diameter (DR_OD) should be greater than 1.5. Also, two other parameters that are not as well published can affect the design drastically: the ratio between the dielectric resonator outer diameter (DR_OD) and thickness (DR_t), denoted as the aspect ratio, and the ratio between the dielectric resonator inner diameter (DR_ID) and outer diameter (DR_OD).

The advantage of DR loaded cavities over rectangular waveguide and regular air cavities is depicted in ***Table 2***. Typically, the size of the air cavity is fairly large and may be impractical for many applications below 3 GHz. A DR with a dielectric constant of 45 and a Qf of 45,000 offers approximately 92 percent volume reduction while still maintaining very high Q. In the frequency range of 5 to 10

TABLE 2
CAVITY UNLOADED Q AND VOLUME VS. RESONATOR

	2 GHz	5 GHz	10 GHz
TE_{01} DR Cavity (ε_r = 30)	32,529 & 75 cm^3	16,500 & 5 cm^3	9,500 & 0.54 cm^3
TE_{01} DR Cavity (ε_r = 45)	15,412 & 43 cm^3	7,003 & 3.2 cm^3	3,764 & 0.33 cm^3
Rectangular Waveguide Cavity	18,361 & 595 cm^3	11281 & 36.1 cm^3	8,373 & 4.4 cm^3

GHz, a DR with a dielectric constant of 30 and a Qf of 150,000 achieves better cavity Q than the rectangular waveguide and 86 percent volume reduction. The advantage is obvious; however, DR loaded cavities present some challenges: spurious and quite complicated resonant modes.

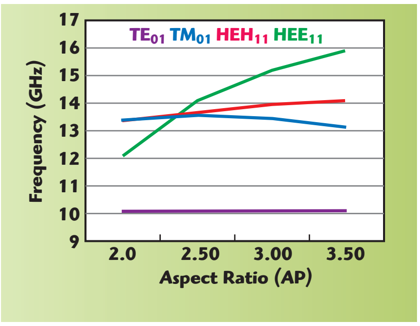

▲ *Fig. 2 Mode chart showing the four resonant modes of a DR cavity at 10 GHz (ε_r = 30 and Qf = 150,000).*

DR LOADED CAVITY MODES

The design of an RF/microwave oscillator using a DR loaded cavity must consider the cavity's resonant frequency, coupling to the source and load and high order spurious resonant modes. Although there are closed approximate solutions to calculate these parameters and EM numerical analysis can compute the results, a systematic study has not been published. The mode-matching technique in EM simulation has been used to calculate the resonant frequency, cavity Q and coupling in the cavity for a DR loaded cavity. The recent progress of commercially available 3D EM simulator techniques, increased computation speed and affordable large capacity memory enable engineers to perform DR cavity simulation and design in a reasonable time.

As an example, for a DR with ε_r =30, ***Figure 2*** shows the HFSS computations for the various modes at 10 GHz, as the aspect ratio (denoted as AP) varies from 2.0 to 3.5. This is known as a mode chart. The numerical values are summarized in ***Table 3***. Comparing the values in Table 3 and the unloaded Q of 15,000, the TE_{01} mode cavity retains around 60 to 70 percent of the Q (i.e., $1/\tan(\delta_{01})$) of the dielectric puck material. This is because the design employs the empirical rules that were noted earlier: 1) the ratio of the diameter of the metallic cavity to the outer diameter of the DR puck, denoted RR, is 1.5; and the ratio of the metallic cavity height to the thickness of the DR puck, denoted as HR, is 3. The Q of the TE_{01} mode cavity can be increased if larger RR and HR values are used, as shown in ***Table 4***. However, while Q can be increased, the spurious ratio, defined as the ratio of the first higher mode frequency to the fundamental TE_{01} mode frequency, will become smaller, meaning the higher mode is closer in frequency.

Table 5 shows the effects of an alumina (Al2O3) standoff and Rogers

TABLE 3

DR CAVITY RESONANT MODES AT 10 GHz
DR ε_r = 30 DR, Qf = 150,000

Aspect Ratio (AP)	2.0	2.5	3.0	3.5
TE_{01}	10.07	10.07	10.07	10.07
TM_{01}	13.40	13.59	13.49	13.16
HE_{11}	12.90	13.70	13.97	14.10
HE_{12}	13.40	14.10	15.21	15.93
Q (TE_{01})	9,322	9,557	9,508	9,190

TABLE 4

RAISING TE_{01} CAVITY Q BY INCREASING RR AND HR

AP	RR	HR	TE_{01}	Q (TE_{01})	First Spur	Spur Ratio
2.5	1.50	3.00	10.07	9,557	13.59	1.35
2.5	1.75	3.00	9.77	11,118	12.72	1.30
2.5	2.00	3.00	9.64	11,833	11.80	1.22
2.5	2.00	3.50	9.57	12,500	12.09	1.26
2.5	2.50	4.00	9.40	13,705	10.85	1.15

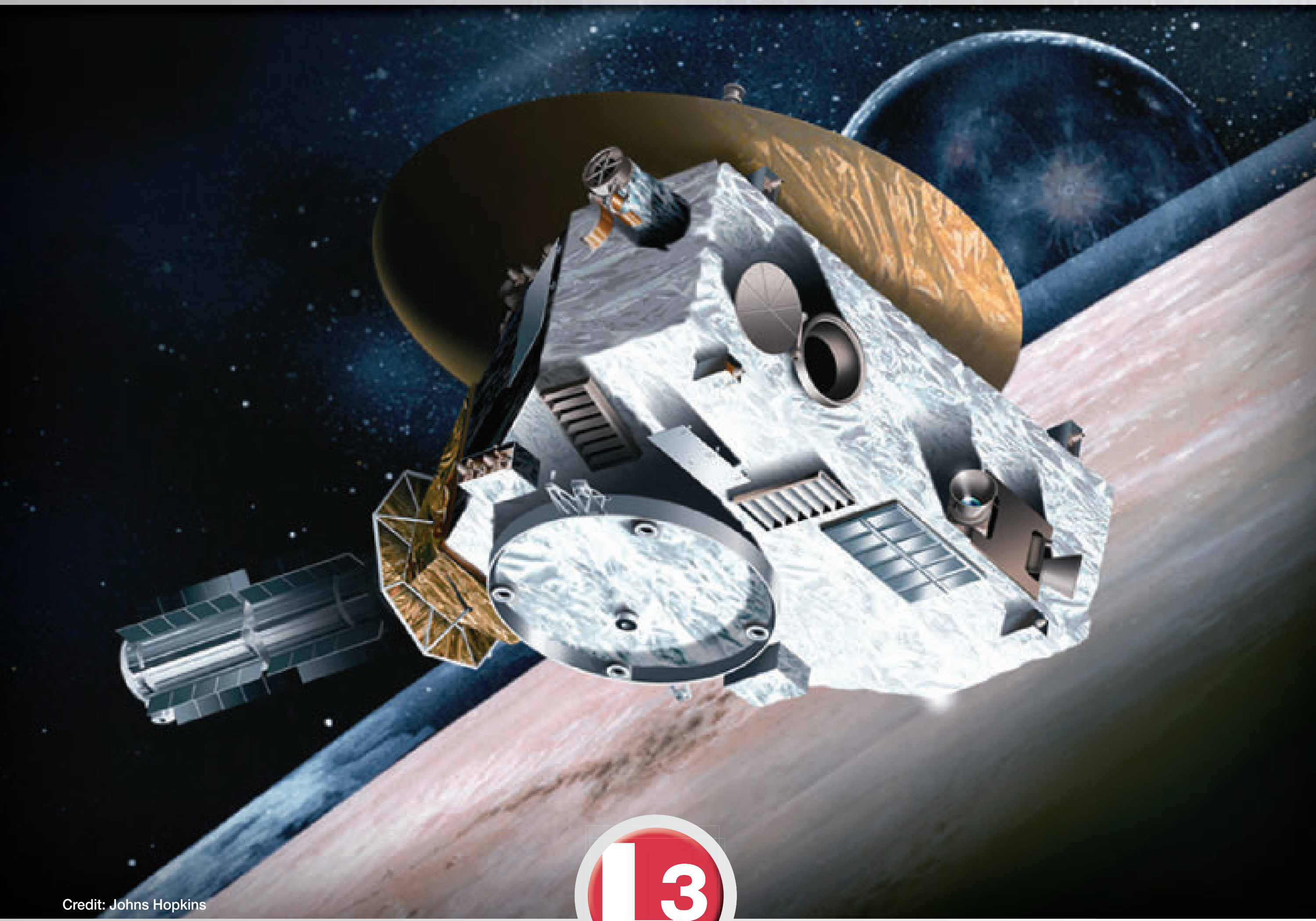

Credit: Johns Hopkins

RO3010 PCB, where RR = 1.5 and the ratio of the DR outside diameter to the insider diameter (DR_OD/DR_ID) is 2.5. All the design variations seem to be quite acceptable, namely with 5 percent degradation of cavity Q and maintaining a spurious ratio of at least 1.23. However, a significant degra-

TABLE 5
STANDOFF AND PCB EFFECTS (RR = 1.5, DR_OD/DR_ID = 2.5)

AP	HR	Standoff	PCB (mm)	TE_{01}	Q (TE_{01})	Spur Ratio
2.5	3.00	None	None	10.26	9,531	1.40
2.5	3.00	H	None	10.22	9,485	1.30
2.5	3.00	H	0.5	10.22	9,430	1.29
2.5	3.00	0.75H	0.5	10.25	9,155	1.29
2.5	2.75	0.75H	0.5	10.27	9,096	1.26
2.5	2.50	0.75H	0.5	10.31	8,899	1.25
2.5	3.00	H	1.0	10.22	8,998	1.23

TABLE 6
EFFECT OF FREQUENCY TUNING WITH 0.5 MM THICK TUNING DISK (AP = 2.5, RR = 1.5, HR = 3.0, DR_OD/DR_ID = 2.5, STANDOFF = H, PCB = 0.5 MM)

Disk Type	Normalized Disk Distance to Cover	TE_{10} (GHz)	Q (TE_{10})	Spur Ratio
Dielectric Disk	0.0	10.221	9,370	1.267
	0.2	10.206	9,259	1.268
	0.4	10.157	9,164	1.270
	0.6	10.051	9,099	1.273
Metal Disk	0.0	10.249	9,116	1.267
	0.1	10.275	8,854	1.185
	0.2	10.308	8,571	1.060
	0.3	10.365	8,152	0.942

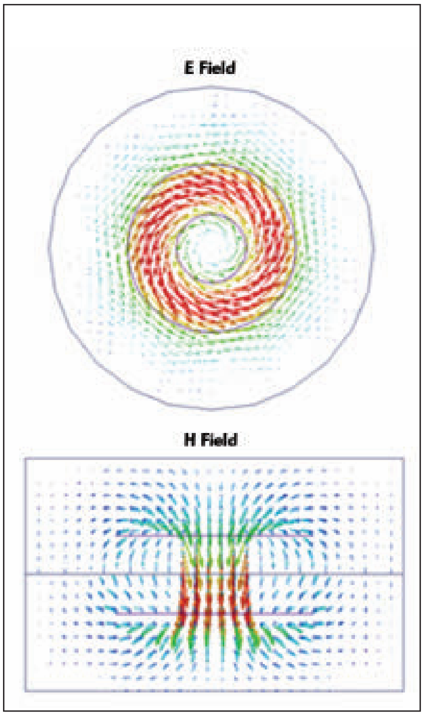

Fig. 3 Typical E and H fields of the TE_{01} mode resonator.

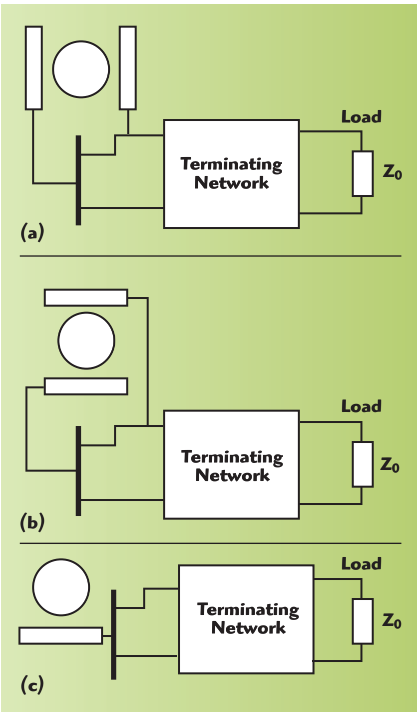

Fig. 4 DRO topologies: parallel feedback (a), parallel feedback (b), series feedback (c).

dation in Q occurs if the DR puck is placed too close to the PCB. Tuning can be achieved using either a metal or dielectric disc. ***Table 6*** compares the tuning as a function of the distance to the cover using a 0.5 mm tuning disk (the distance to the cover is normalized to the height of the DR). In general, for the same amount of frequency tuning, a metallic tuning disk can degrade the Q more than a dielectric tuning disk. The field distribution is important in designing the excitation and coupling of a resonant cavity. Typical E and H fields are shown in ***Figure 3***.

DRO TOPOLOGIES

Three topologies are used for DRO designs: one with the DRO in series feedback and two with the DRO in parallel feedback (see ***Figure 4***). The DR is either one-port or two-port coupled to the active device in the DRO. A 3D view of a one-port coupled DR cavity is shown in ***Figure 5***, where the arrow indicates the possible shifting of the excitation plane to that location.

Three examples of DRO designs are presented, each with a different length of the coupled microstrip line in the cavity. These represent the ratio of the loaded to unloaded Q (Q_L/Q_0) of 2/3, 1/2 and 1/3 and a coupling resistance of 0.5, 1.0 and 2.0 with respect to the equivalent series resonator of the DR cavity (R_0). ***Figure 6a*** shows the equivalent circuit of the one-port coupled DR cavity with an ideal transformer and phase shifter (using a section of transmission line) to match EM simulation and measured results. The coupling can be extracted from the ideal coupled resonator circuits in ***Figure 6b***. The coupling coefficient (β) can be obtained from the maximum return loss (RL_0), either from measurement (see ***Figure 6c***) or simulation, as follows:

$$RL_0 = -20\log\frac{|1-\beta|}{|1+\beta|} \quad (1)$$

$$\beta = \frac{1-\rho_O}{1+\rho_O} \text{ or } \frac{1+\rho_O}{1-\rho_O} \quad (2)$$

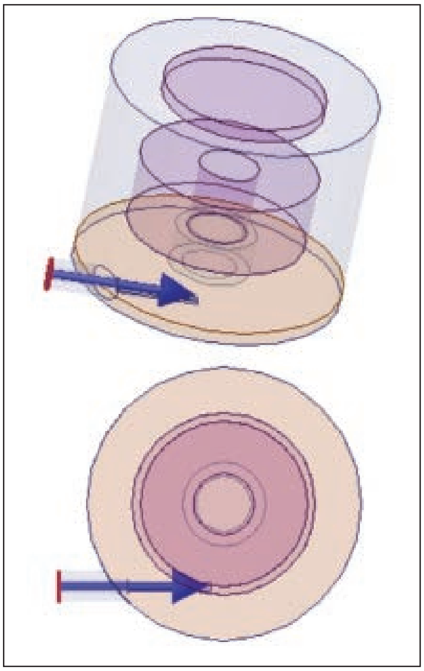

▲ *Fig. 5 One-port coupled DR cavity.*

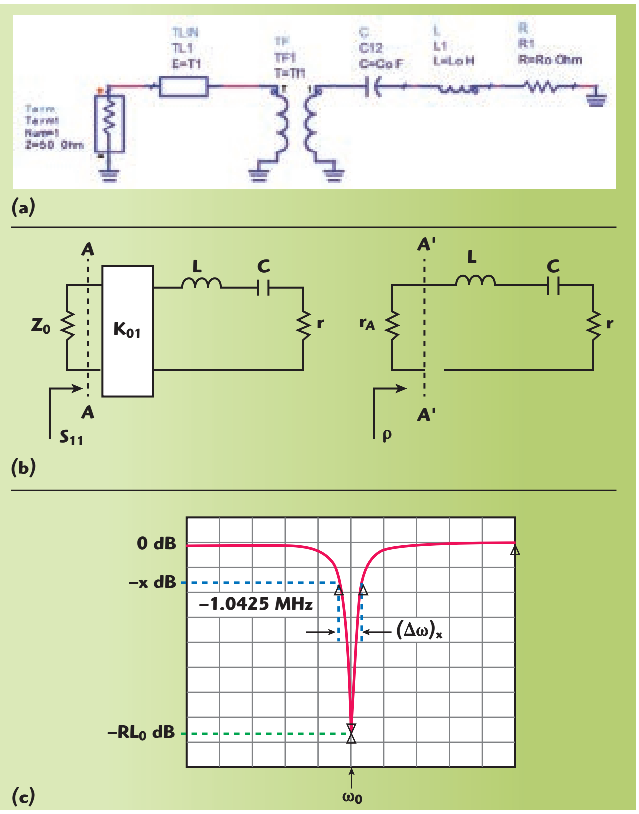

▲ *Fig. 6 Equivalent circuit of a one-port coupled DR cavity with ideal transformer and section of transmission line for shifting the phase (a) circuit for coupling and resonator Q_0 extraction (b) and return loss measurement used to calculate the coupling coefficient (β).*

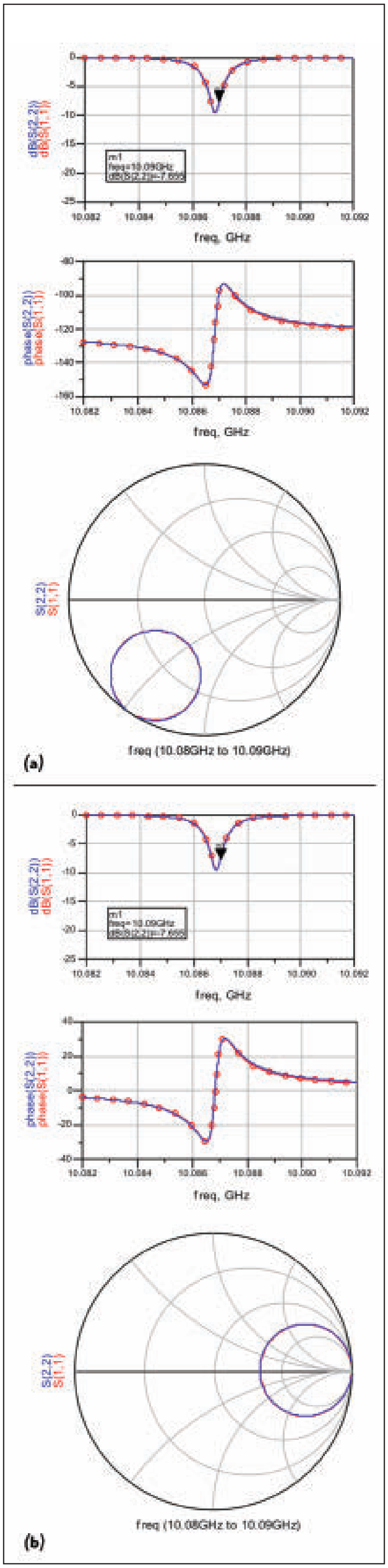

▲ *Fig. 7 HFSS simulation and equivalent circuit of the under-coupled design with the excitation at the coaxial input plane (a) and the reference shifted 5.1 mm into the cavity (b).*

The Smith chart can be used to determine the case of under-coupled ($\beta<1$) or over-coupled ($\beta>1$). The following equations are used to obtain the unloaded Q (Q_0):

$$Q_0 = Q_L(\chi,\beta)F(\chi,\beta),$$

where $F(\chi,\beta) =$

$$\sqrt{\frac{(1+\beta)^2|\rho|_\chi^2 - (1-\beta)^2}{1-|\rho|_\chi^2}} \qquad (3)$$

For the first design example, the under-coupled condition where the coupled resistance (R_A) equals $0.5R_0$, two sets of simulation results are shown: one without shifting the excited reference plane (see ***Figure 7a***), the other shifted to make it almost identical to the ideal equivalent circuit (see ***Figure 7b***). Similarly, ***Figure 8*** shows the critical-coupled condition, where R_A equals R_0; ***Fig-***

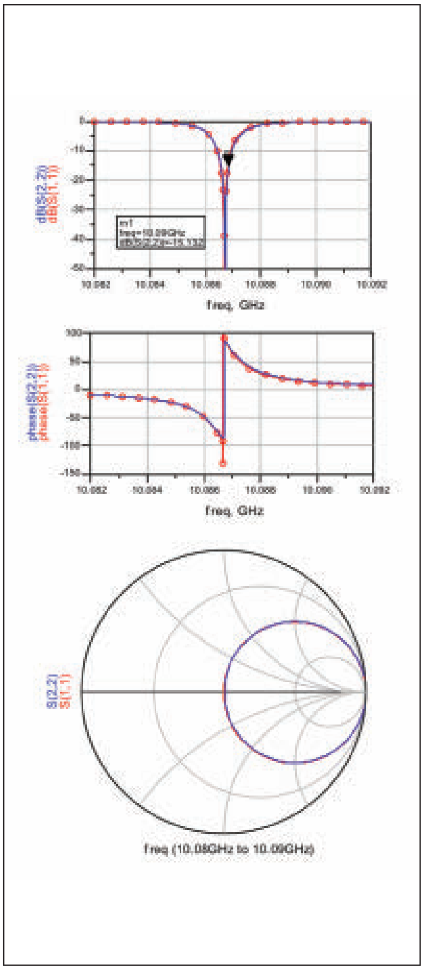

▲ *Fig. 8 HFSS simulation and equivalent circuit for the critical-coupled design, with the excitation reference shifted to emulate an ideal series resonator.*

ure 9 shows the over-coupled case, where R_A equals to $2R_0$.

A two-port coupled DR cavity has the two ports arranged either on the same side of the cavity or facing opposite directions (see ***Figure 10***). A coupled cavity should yield a Q_L/Q_0 ratio between 0.5 and 0.66 to optimiz the phase noise of the oscillator. The corresponding transmission loss of a coupled DR cavity should range from 6.5 to 9.5 dB, according to:

$$Q_0 = \frac{Q_L}{1 - 10^{-\frac{IL}{20}}} \quad (4)$$

Most relevant works regard the two topologies in Figure 10 to be electrically identical. However, the equivalent network of ***Figure 10c*** fits the EM simulation of ***Figure 10a*** fairly well, while ***Figure 10b*** only fits ***Figure 10d*** well. The difference is the phase of S_{21}. ***Figure 11*** substantiates the equivalent circuits for the two-port topologies, showing the HFSS simulations for the respective circuits.

CONCLUSION

This article addressed the issues of dielectric resonator loaded cavities in RF/microwave oscillator design, discussing DR characterization and modeling. The major characteristics of DR loaded cavities were analyzed, including cavity Q, resonant frequency, high order modes and coupling structures. Data obtained by 3D EM simulation should help designers achieve high Q in the cavity and avoid high order spurious modes that can interfere with the fundamental mode. Equivalent networks were presented that match the EM simulation results in the narrow band of the oscillator frequency. This research should help advance RF/microwave DRO design and development.■

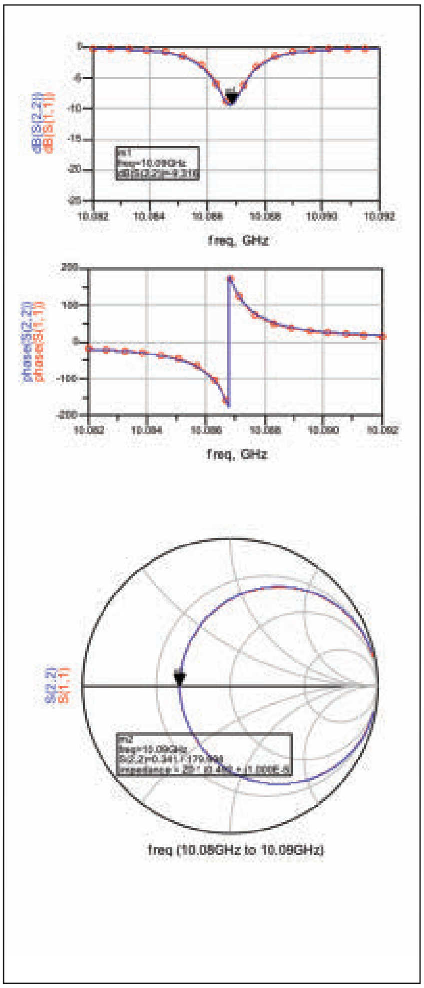

▲ *Fig. 9 HFSS simulation and equivalent circuit for the over-coupled design, with the excitation reference shifted to emulate an ideal series resonator.*

Compex

Capacitors, Resistors, and Thin Film Products

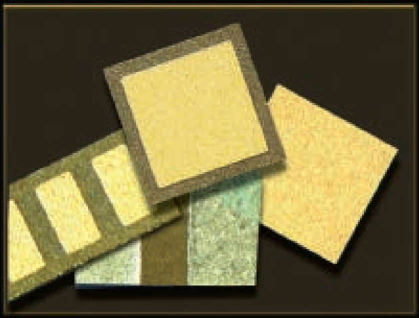

Single Layer Ceramic Capacitors

- Custom Diced To Your Value And Size
- Broadest Variety Available

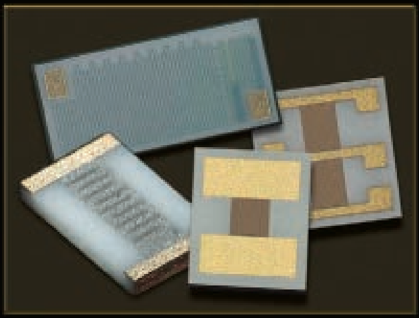

NEW

Thin Film Resistors

- Alumina, Aluminum Nitride, Quartz, Silicon And Beryllium Oxide
- Tolerances Down To 0.01%
- Top Side And Edge-Wrap Terminations

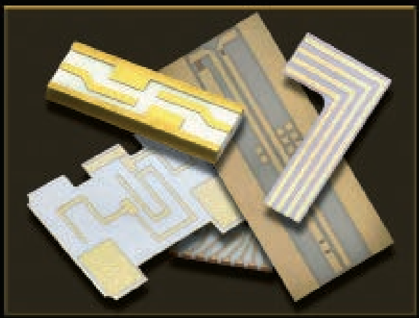

Thin Film Substrates and Submounts

- Lithography And Mask-less Options
- Thickness Accuracy To 5 Microns
- Integrated Resistors

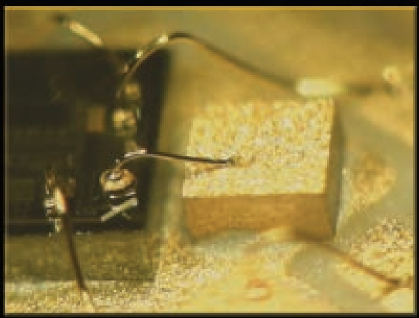

Mounting Shorts

- Instant Conductive Bonding Pads
- Height Matching Reduces Lead Length And Inductance

A Solar Powered Small Business
Established 1976

ISO 9001:2008, ISO 14001:2004, RoHS and REACH Compliant

439 Commerce Lane, West Berlin, NJ 08091 • 1515 Elmwood Avenue, Cranston, RI 02910
856 335 2277 • www.compexcorp.com • sales@compexcorp.com

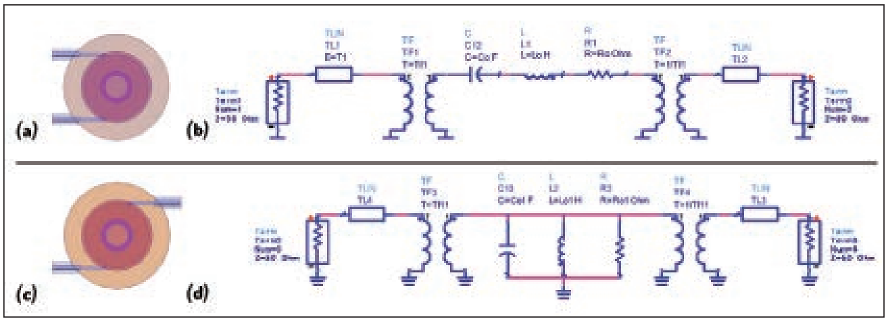

▲ *Fig. 10 Two-port DR cavity with both ports on the same side of the cavity (a) and equivalent network (b). Two-port cavity with the ports on opposite sides (c) and equivalent network (d).*

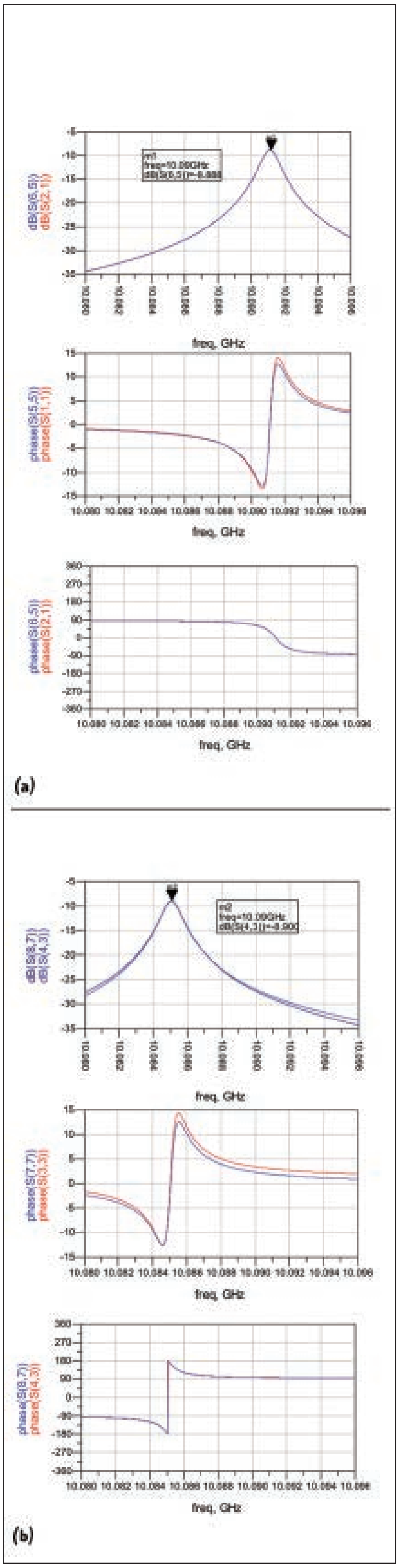

▲ *Fig. 11 HFSS simulation for the two-port DR cavity with both ports on the same side, using the Figure 10b network (a). HFSS simulation for the two-port with ports on opposite sides, using the Figure 10d network (b).*

Proven Performance

GORE-FLIGHT™ Microwave Assemblies, 6 Series are ruggedized, lightweight and vapor-sealed airframe assemblies that withstand the challenges of aerospace.

With GORE-FLIGHT™ Microwave Assemblies, 6 Series, a fit-and-forget philosophy is now a reality – providing the most cost-effective solution that ensures mission-critical system performance for military and civil aircraft operators.

Find out why at:
www.gore.com/GORE-FLIGHT

GORE
Creative Technologies Worldwide

precision lightweight durability

Follow us on

References

1. J. K. Plourde, H. M. O'Bryan, Jr., D.F. Linn and H. J. Thomson, Jr., "Ba2Ti9O20 as a Microwave Dielectric Resonator," *Journal of the American Ceramic Society*, Vol. 58, pp. 418–420, Sept.-Oct. 1975.
2. D. J. Passeand and R. A. Pucel, "A Temperature-Stable Bandpass Filter Using Dielectric Resonators," *Proceeding of the IEEE*, pp. 730, June 1972.
3. K. Wakko, T. Nishikaw, S. Tarnura and Y. Ishikawa, "Microwave Bandpass Filters Containing Dielectric Resonators With Improved Temperature Stability and Spurious Response," *IEEE International Microwave Symposium Digest*, pp. 63–65, 1975.
4. J. K. Plourde and D. F. Linn, "Microwave Dielectric Resonator Filters Utilizing Ba2Ti9O20 Ceramics," *IEEE International Microwave Symposium Digest*, pp. 290–293, 1977.
5. Kajfez and P. Guillon, "Dielectric Resonators," 2nd Edition, SciTech Publishing, 1998, ISBN 1-884932-05-3.
6. J. K. Plourde and C. L. Ren, "Application of Dielectric Resonators in Microwave Components," *IEEE Trans. on Microwave Theory Tech.*, Vol. MTT-29, pp. 754, Aug. 1981.
7. S. J. Fiedziuszko, "Dual-mode Dielectric Resonator Loaded Cavity Filters," *IEEE Trans. on Microwave Theory Tech.*, Vol. MTT-30, pp. 1311, Sep. 1982.
8. Y. Kobayashi and M. Minegishi, "Precise Design of a Bandpass Filter Using High-Q Dielectric Resonators," *IEEE Trans. on Microwave Theory Tech.*, Vol. MTT-35, pp. 1156, Dec. 1987.
9. S. W. Chen and K. A. Zaki, "Dielectric Ring Resonators Loaded in Waveguide and on Substrate," *IEEE Trans. on Microwave Theory Tech.*, Vol. MTT-39, pp. 2069, Dec. 1991.
10. Xiang-Peng Liang and K. A. Zaki, "Modeling of Cylindrical Dielectric Resonators in Rectangular Waveguides and Cavities: *IEEE on Microwave Theory and Tech.*, Vol. MTT-41, pp. 2174, Dec. 1993.
11. Ji-Fuh Liang, K. A. Zaki and Ali E. Atia, "Mixed Modes Dielectric Resonator Filters," *IEEE Trans. on Microwave Theory Tech.*, Vol. MTT-42, pp. 2449, Dec. 1994.
12. Ji-Fuh Liang and William D. Blair, "High- TE01 Mode DR Filters for PCS Wireless Base Stations," *IEEE Trans. on Microwave Theory Tech.*, Vol. 46, No. 12, December 1998.
13. S. A. Vitusevich, K. Schieber, I. S. Ghosh, N. Klein and M. Spinnler, "Design and Characterization of an All-Cryogenic Low Phase-Noise Sapphire K-Band Oscillator for Satellite Communication," *IEEE Trans. Microw. Theory Tech.*, Vol. 51, No. 4, pp. 163–169, Jan. 2003.
14. M. E. Tobar, D. Cros, P. Blondy and E. N. Ivanov, "Compact, High Q, Zero Temperature Coefficient, TE011 Sapphire-Rutile Microwave Distributed Bragg Reflector Resonators," *IEEE Trans. Ultrason., Ferroelectr. Freq. Control*, Vol.

48, No. 3, pp. 821–829, May 2001.

15. J. D. Anstie, J. G. Hartnett, M. E. Tobar, E. N. Ivanov and P. L. Stanwix, "Second Generation 50 K Dual-Mode Sapphire Oscillator," *IEEE Trans. Ultrason., Ferroelectr. Freq. Control*, Vol. 53, No. 2, pp. 284–288, Feb. 2003.
16. E. N. Ivanov and M. E. Tobar, "Low Phase-Noise Microwave Oscillators With Interferometrics Signal Processing," *IEEE Trans. Microw. Theory Tech.*, Vol. 54, No. 8, pp. 3284–3294, Aug. 2003.
17. L. Zhou, Z. Wu, M. Sallin and J. K. A. Everard, "Broad Turning Ultra Low Phase Noise Dielectric Resonator Oscillators Using SiGe Amplifier and Ceramic-Based Resonators," *IET Microwave Antennas Propag.*, Vol. 1, No. 5, pp. 1064–1070, Oct. 2007.
18. D. Y. Jung, K. C. Eun and C. S. Park, "High-Q Circular LTCC Resonator Using Zigzagged Via Posts and a λ/4 Short Stub for Millimeter Wave System on Package Applications," *IEEE Trans. Adv. Packag.*, Vol. 32, No. 1, pp. 216–222, Feb. 2009.
19. L. Zhou, R. Chu, Z. Wu, W.Y. Yin and J. F. Mao, "Broad Tuning Low Noise Ku-Band Dielectric Resonator Oscillators," *Asia-Pacific Microwave Conf.*, Dec. 2008, pp. 1–4.
20. P. Rice, M. Moor, A. R. Barnes, M. J. Uren, N. Malbert and N. Labat, "A 10 GHz Dielectric Resonator Oscillator Using GaN Technology," *IEEE MTT-S International Microwave Symposium Digest*, Vol. 3. Jun. 2004, pp. 1497–1500.
21. P. Stockwell, D. Green, C. Mcneilage and J. H. Searls, " A Low Phase Noise 1.3 GHz Dielectric Resonator Oscillator," *IEEE Int. Freq. Control Symp.*, May 2006, pp. 882–885.
22. A. Warburton, "A Phase Tuned, Fixed Frequency Dielectric Resonator Oscillator Design," in *Proc. Eur. Microw. Conf.*, Oct. 2005, pp. 1–4.
23. C. Florian, P. A. Traverso, G. Vannini and F. Filicori, "Design of Low Phase Noise Dielectric Resonator Oscillators With GaInP HBT Devices Exploiting a Non-Linear Noise Model," *IEEE MTT-S International Microwave Symposium Digest*, June 2007, pp. 1525–1528.
24. J. F. Gravel and J. S. Wight, "On the Conception and Analysis of a 12 GHz Push-Push Phase Locked DRO," *IEEE Trans. Microwave Theory Tech.*, Vol. 54, No. 1, pp. 153–159, Jan. 2006.
25. O. Llpois, G. Cibiel, Y. Kersale, M. Regis, M. Chaubet and V. Giordano, "Ultra Low Phase Noise Sappire-SiGe HBT Oscillator," *IEEE Microwave Wireless Compon. Lett.*, Vol. 12, No. 5, pp. 157–159, May 2002.
26. K. Hosoya, K. Ohata, M. Funabashi, T. Inoue and M. Kuzuhara, "V-Band HJFET MMIC DROs With Low Phase Noise, High Power and Excellent Temperature Stability," *IEEE Trans. Microw. Theory Tech.*, Vol. 51, No. 11, pp. 2250–2258, Nov. 2003.

INVITED PAPER

Designing Next-Generation AESA Radar

Gent Paparisto and David Vye
National Instruments, Austin, Texas

Recent trends in active electronically scanned arrays (AESA) are targeting new radar payloads for satellites and unmanned aerial vehicles (UAV). These payloads, along with updated ground, airborne and shipborne radar, will help military planners meet changing operational requirements and the need for better situational awareness through improved intelligence, surveillance and reconnaissance (ISR) systems. These radar payloads are driving size and performance requirements, which are being addressed through novel architectures and system capabilities made possible through improvements in microwave and signal processing technologies such as GaN power amplifiers (PA), new monolithic microwave integrated circuits (MMIC) and "extreme" MMIC devices, heterogeneous "more than Moore" integration, cost reductions for transmit/receive (T/R) modules, new millimeter wave (mmWave) silicon ICs and electro-optic integration.[1]

Behind these development efforts are a host of evolving electronic design automation (EDA) technologies that support designers with system architecture, component specifications, physical design of individual components and verification prior to prototyping. This article will discuss these technology trends and present several examples where advances in EDA tools are supporting next-generation AESA and phased array radar development.

PHASED ARRAY TECHNOLOGY

An AESA radar, also known as an active phased array radar (APAR), consists of individual radiating elements (antennas), each with a solid-state T/R module containing a low noise receiver, PA and digitally-controlled gain and phase (or delay) elements. Phase and amplitude control of the input signal to the individual elements provides steerable directivity of the antenna beam over both azimuth and elevation, which allows the radar to "aim" the main lobe of the antenna in the desired direction. Unlike a mechanically-steered radar, a phased array can rotate its pattern in space with practically no delay. Digital control of the module transmit/receive gain and timing permits the design of an antenna with beam steering agility, interleaving radar modes and extremely low sidelobes, which provides a significant reduction in antenna radar signature compared to passive electronically scanned arrays (ESA) and mechanically-steered antennas.[2] The width of the beam depends on the number of elements in the array. By increasing the number of elements (or sensors), the beam becomes sharper and more efficient in detecting smaller size targets. Today's AESA radars

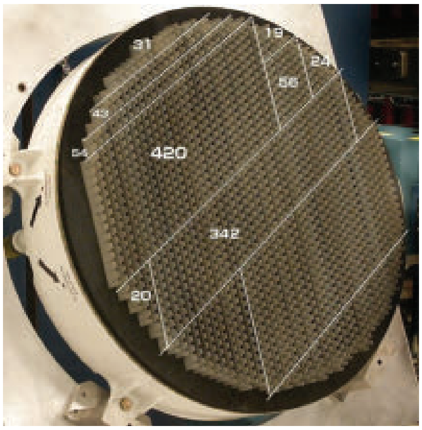

▲ *Fig. 1 AN/APG-80 F-16 AESA radar built by Northrop Grumman, showing partial view of the individual array elements.*

typically consist of thousands of individual elements, electrically interconnected through increasingly complex structures designed for reduced size and weight and better performance (in other words, lower loss).

At RF frequencies below 10 GHz, where a longer wavelength increases the antenna size and spacing, the RF, IF and baseband signal routing can be addressed with discrete components and off-the-shelf MMICs on printed circuit boards (PCB). The impact of longer traces will be offset by the lower PCB losses at these frequencies, and the interface to the antenna can be considered independent of the IC unit cell, due to the relatively flexible packaging requirements. However, at mmWave frequencies (i.e., above 30 GHz), physically short antenna spacings (~λ/2 < 5 mm), packaging losses and manufacturing challenges with impedance-controlled, multi-layer packaging interconnects make high functionality ICs and sophisticated integration more attractive. Designing these complex packaging schemes for high frequency signaling must be addressed with circuit simulation and electromagnetic analysis that is specialized for RF and microwave electronics.[3]

While actively steered phased array antennas have many advantages, they are extremely complex, and their nonrecurring development and production costs are significantly higher than a conventional antenna design. The higher development costs are driven by the inclusion of hundreds to thousands of active electronic modules per production unit (see ***Figure 1***), often implemented with custom GaAs MMIC designs (typically 5 to 10 designs per system).

INCREASING INTEGRATION

Initially funded and developed through U.S. Department of Defense (DoD) support in the 1980s and 1990s, GaAs MMIC technology was the only viable option for manufacturing the densely packed (cross section < 1 cm) T/R modules operating at 10 to 20 GHz. Advances in MMIC design have been enabled by the greater availability of powerful simulation software and inexpensive computing, which allows engineers to design increasingly complex circuits with greater accuracy and to develop libraries of frequently used RF building blocks. Where earlier MMIC development addressed the challenge of combining tens to hundreds of active and passive components (i.e., transistors, PIN diodes, resistors, capacitors and inductors on a single GaAs substrate), integrating AESA functionality scales in complexity when combining RF blocks such as low noise amplifiers (LNA), PAs, and

switching and phase shifters onto a single or multi-channel MMIC. Ever greater functionality and density are being developed through multi-chip modules (MCM) that utilize revolutionary materials, devices and advanced integration techniques.

The Defense Advanced Research Projects Agency (DARPA) Microsystems Technology Office sponsored two programs to investigate next-generation device integration. The DARPA Compound Semiconductor Materials on Silicon (COSMOS) program focused on developing new methods to tightly integrate compound semiconductor (III-V) technologies within state-of-the-art silicon CMOS circuits. The DARPA Diverse Accessible Heterogeneous Integration (DAHI) program continues this work by developing heterogeneous integration processes to intimately combine advanced III-V devices using emerging materials and devices with high density silicon CMOS.[4]

Integration technology has made significant advances over the past 10 years. In 2006, for the DARPA Integrated Sensor is Structure (ISIS) program, Georgia Tech Research Institute developed a four channel X-Band SiGe T/R module with the control circuitry on a single chip and a per-T/R module cost of ~$10. In 2008, researchers at the University of California San Diego (UCSD) achieved a huge leap in performance and integration density with the demonstration of the first SiGe RF-beamforming IC: a 6 to 18 GHz, 8-element phased array receiver with 5-bit phase control and an on-chip 8:1 combiner.[5] In 2009, UCSD followed this with a demonstration of the first 16-element, 45 to 50 GHz phased array transmitter. By 2013, UCSD reported a 110 GHz, 4×4 wafer-scale phased array transmitter with high efficiency on-chip antennas,[6] successfully demonstrating a single chip solution (see ***Figure 2***).

While phased array antennas are evolving into silicon core chips that support multiple radiating elements, preferred solutions frequently combine silicon with III-V front-ends for applications that require the best possible performance, especially for figures of merit such as noise figure (NF) and output power. Increasingly, GaN is displacing GaAs as the material of choice for high power or broadband front ends. For a fixed power level, a GaN MMIC can be one third to one quarter the size of an equivalent power GaAs MMIC, a power density that is enough to offset the higher material cost of GaN compared to GaAs. While the finished GaN wafer (including material) costs twice that of GaAs, the resulting GaN solution is only 50 to 66 percent of the cost per RF watt gen-

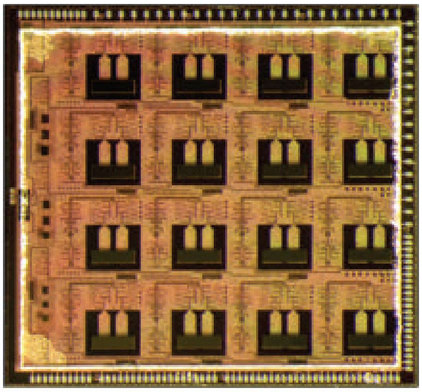

▲ *Fig. 2 110 GHz, 4×4 wafer-scale phased array transmitter.*

erated with a GaAs solution. As the cost of GaN continues to decrease, the elimination of GaAs from phased antennas can be expected for many applications.[7]

Continued investment in wide bandgap (WBG) semiconductors is expected to take "more than Moore" power electronics to another level. Researchers are looking to enhance GaN technology by heterogeneously integrating GaN on top of silicon wafers. The integration of GaN onto larger silicon wafers and the use of standard semiconductor manufacturing processing will provide significant functionality and performance advantages at much lower cost. All these technology options require that designers have an efficient way to understand trade-offs between individual technologies and the impact on overall performance.

Even though the density of a GaAs MMIC is much lower than that of competitive silicon digital ICs, high frequency electronic design requires careful attention to interconnect technology and "EM aware" simulation that is able to predict the parasitic behavior that leads to performance failures. The physical arrangement or layout of components and interconnects is such a critical part of RF/microwave circuit design that software should utilize a unified data model (UDM) to inherently link schematic-based electrical elements to EM simulation-ready layout. This level of analysis is increasingly critical to successful MMIC development, as the technology and integration levels evolve.

While the integration of III-V and Si technologies addresses the size and functionality requirements of next-generation phased arrays, high density ICs also increase the need for wafer processing quality, since losing one transistor out of a hundred due to a fabrication defect amounts to losing the entire, costly die. As a result, the design of a complete microwave RF circuit on a chip requires established RF design rules for the layout of components and interconnections. Robust design, by way of yield/corner analysis, must also be incorporated into the design stage, to study the impact of manufacturing tolerances.

SIMULATION TOOLS

System engineering plays a key role in the convergence of silicon at mmWave frequencies. As the industry shifts toward highly integrated, feature-rich core chips, it is increasingly important that RFIC developers have in-house system expertise to fully examine the trade-offs in architecture and available technologies. System simulation that links circuit simulation to the analysis of radio and signal processing behavioral models enables the system designer to select the optimum monolithic process(es) for the application and perform early architecture definition and component specification.

One contributor to design failure and the resulting high cost of development is the inability of high level system tools to accurately model the interactions between the multitude of electrically interconnected channels that are separately specified. Constructing full or partial phased array systems to investigate these unforeseen interactions is also very

- Amplifiers – Solid State
- Attenuators – Variable/ Programmable
- Couplers (Quadrature, 180° & Directional)
- Detectors – RF/Microwave
- DLVAs, ERDLVAs & SDLVAs
- DTOs, VCOs, PLO, DROs, & Frequency Synthesizers
- Filters & Switched Filter Banks
- Form, Fit, Functional Products & Services
- Frequency Discriminators & IFMs
- Integrated MIC/MMIC Assemblies (IMAs)
- IQ Vector Modulators
- Limiters – RF/Microwave
- Log Amplifiers
- Millimeter Wave Components (Up to 50 GHz)
- Miscellaneous Products
- Multifunction Integrated Assemblies (MIAs)
- Monopulse Comparators
- Phase Shifters & Bi-Phase Modulators
- Power Dividers/Combiners (Passive & Active)
- Pulse Modulators (SPST)
- Rack & Chassis Mount Products
- Receiver Front Ends & Transceivers
- SDLVAs, ERDLVAs & DLVAs
- Single Side Band Modulators
- SMT & QFN Products
- Switch Matrices
- Switched Filter Banks
- Switches – Solid State
- Systems – Fly Eye Radars
- Threshold Detectors
- USB Products

Planar Monolithics Industries, Inc.

High Power Solid-State Switches

PMI offers a full line of High Power Solid-State Switches that range from DC to 50 GHz with power handling up to 130 Watts CW, 5 kW peak. A wide range of standard models with various options are available.

http://www.pmi-rf.com/Products/Switches/standardmodels.htm

Model: P2T-1G1R1G-25-R-SFF-100W

Frequency	1.0 to 1.1 GHz
Isolation	25 dB Min - Measured 40.09 dB
VSWR	1.5:1 Typ
Insertion Loss	0.8 dB Max - Measured 0.49 dB
RF Input Power	100 Watts CW Max / 5 kW peak – Tested to 100 W CW
Switching Speed	100 ns Max – Measured 61.6 ns
Temperature	-45 ºC to +85 ºC Operating

Package Size:
4.22” x 2.98” x 0.70”
Connectors: TNC (F)
DC Voltage:
+5 VDC @ 135 mA
-50 VDC @ 17 mA

Model: PSM-1G1R1G-TRSW-2500W

Frequency	1.0 to 1.1 GHz
Isolation	25 dB Min (J2-J3) - Measured 38 dB 60 dB Min (J2-J4) - Measured 65 dB
VSWR	1.4:1 Typ
Insertion Loss	1.0 dB Max (Tx Mode) - Measured 0.67 dB 0.8 dB Max (Rx Mode) - Measured 0.54 dB
RF Input Power	2.5 KW Peak (J1 Only)
Switching Speed	385 ns Typ - Measured 300 ns @ 2 kHz Switching Rate Max
Temperature	-45 ºC to +85 ºC Operating

Package Size:
7.750” x 3.000” x 0.575”
Connectors: SMA (F)
DC Voltage:
+5 VDC @ 360 mA
+50 VDC @ 30 mA

Model: P2T-1G18G-10-R-528-SFF-HIP10W

Frequency	0.1 to 18.0 GHz
Isolation	25 dB Min - Measured 25.73 dB
VSWR	2.0:1 Max - Measured 1.76:1
Insertion Loss	3.5 dB Max - Measured 2.66 dB
RF Input Power	10 Watts CW Max - Tested at 10 W CW
Switching Speed	200 ns Max - Measured 60 ns
Temperature	-54 ºC to +100 ºC

Package Size:
1.2” x 1.0” x 0.5”
Connectors: SMA (F)
DC Voltage:
+5 VDC @ 2.19 mA
-28 VDC @ 2.25 mA

Model: PEC-9R510R7-100W-SFF-SPDT

Frequency	9.5 to 10.7 GHz
Isolation	40 dB Min - Measured 44.49 dB
VSWR	2.0:1 Max - Measured 1.42:1
Insertion Loss	1.5 dB Max - Measured 1.34 dB
RF Input Power	120 Watts CW
Switching Speed	400 ns Max - Measured <300 ns
Temperature	-55 ºC to +85 ºC Operating

Package Size:
2.12” x 1.18” x 0.51”
Connectors: SMA (F)
DC Voltage:
+5 VDC @ 135 mA
-28 VDC @ 5 mA

West Coast Operation:
4921 Robert J. Mathews Pkwy, Suite 1
El Dorado Hills, CA 95762 USA
Tel: 916-542-1401
Fax: 916-265-2597

East Coast Operation:
7311-F Grove Road
Frederick, MD 21704 USA
Tel: 301-662-5019
Fax: 301-662-1731

sales@pmi-rf.com • www.pmi-rf.com

ISO9001-2008 REGISTERED

expensive, because of the costs of fabrication and testing the interactions of hundreds to thousands of channels. This challenge will only increase with the continuing integration of the antenna array and beam steering control electronics.

Since fabrication and test iterations during design are cost prohibitive, development is typically limited to one prototype in a Phase I or Phase II proof-of-concept demonstration. Failure to meet the specifications leads to an unacceptable number of design and test iterations of the complete antenna/electronics system, making simulation that incorporates the entire system a necessity. Since phased array performance is not driven purely by the behavior of the antenna or microwave electronics, simulation must capture their combined interaction to accurately predict the overall system.

While EDA tools for individual circuit spaces are mature, the adoption of tools to evaluate the overall system performance as a function of combined subsystems is not as widespread. Often, the high level system analysis is performed using custom implementations by way of spreadsheets (e.g., Excel) or generic mathematical calculations using products such as MATLAB. Typically, these custom solutions vary in complexity from company to company, even among different projects within the same company. Such custom tools are generally used to specify the performance requirements of the underlying subsystems (i.e., MMICs, antennas, RF passives and control elements).

A more robust analysis combines the performance metrics of each of the subcomponents of a phased array system to provide a more accurate accounting of the high level system performance. Initially, the analysis is used to specify the overall system component topology and performance requirements of the individual subsystems. As more detailed models of the subsystems become available, these subsystem models and/or measurements can be integrated into the full system analysis to obtain a better understanding of the overall system performance.

System analysis enables designers to:

- Evaluate array performance over a range of power levels and frequencies
- Perform various budget analysis measurements, such as cascaded gain, NF, output power (e.g., P1dB), gain-to-noise temperature (G/T)
- Evaluate sensitivity to imperfections and hardware impairments via yield analysis
- Perform end-to-end system simulations using a complete model of the phased array.

Parametric analysis also allows the designer to efficiently study changes to the system to balance cost vs. performance. Examples of parametric studies are T/R module specifications, phase shift resolution (i.e., number of bits) and errors, combiner/divider topologies, resistive vs. reactive amplitude shaping, the number of antenna elements and antenna element spacing.

PHASED ARRAY ANALYSIS WITH VSS

As an example of this approach, new capabilities for full system analy-

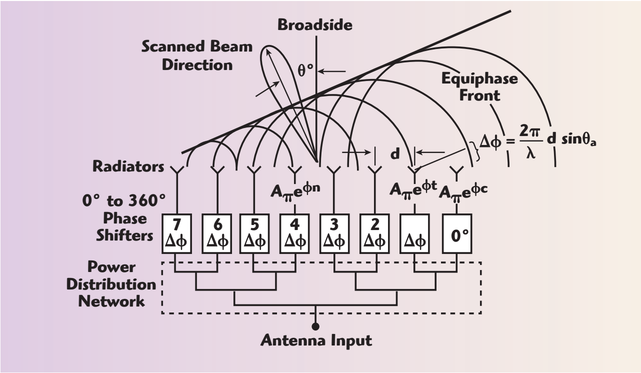

Fig. 3 Gain and phase tapering used for beam shaping, steering and sidelobe control.

sis of AESAs have been added to Visual System Simulator™ (VSS), the system level simulator that operates within the NI AWR Design Environment platform. The simulator provides full system performance as a function of steered beam direction, the antenna design and active and passive circuit elements used to implement the electronic beam steering. The current version of VSS enables modeling of phased arrays with thousands of antenna elements. It allows array configuration using various standards, as well as custom geometries. Previously, phased arrays were implemented using basic individual blocks, and their sizes were limited to several hundred elements, each modeled as a single input/single output block. Now, the phased array's behavior can easily be defined through the parameter dialog box or a data file containing configuration parameters, such as gain and phase offset, θ/φ angles of incidence, X/Y location (either in absolute length or lambda) and signal frequency. The phased array model can be set to either transceiver (Tx) or receiver (Rx) mode. In Tx, the signal power exciting each element is calculated based on the signal setting defined by the user, including:

- Lossless, which excites all array elements by the power of the input signal
- Power divider, where the input signal is divided equally among all array elements
- Voltage divider, where the input signal is divided equally among all array elements, such that the sum of their voltages equals the input signal.

Amplitude excitation through gain tapering is often used to control beam shape and reduce sidelobe levels. A number of commonly used gain tapers are implemented in the phased array block. Gain taper coefficient handling defines whether the gain taper is normalized; if it is, the taper is normalized to unit gain. Standard gain tapers in the phased array model include Dolph-Chebyshev, Taylor Hansen and uniform. The user can also define custom gain tapers by specifying the gains and phases for each array element (see ***Figure 3***).

Along with various signal distribution schemes and support for frequency-dependent operation, the model allows users to simulate array imperfections caused by manufacturing flaws or element failure. All gain and phase calculations are performed

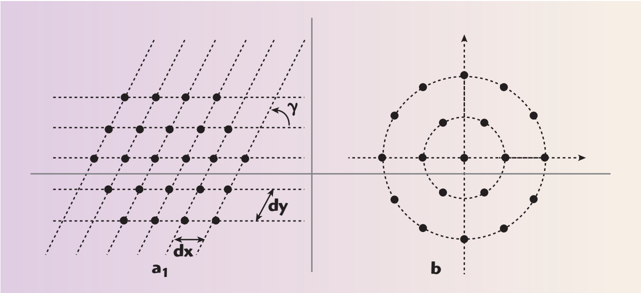

▲ *Fig. 4 Lattice (a) and circular (b) phased array geometries.*

internally, and yield analysis can be applied to the block to evaluate sensitivity to variances of any of the defining phased array parameters.

The parameter dialog box enables the user to quickly define the antenna array architecture using standard or custom geometries. The lattice option (see ***Figure 4a***) allows configuration of the phased array in a lattice pattern, which is configured using the number of elements along the X and Y axes (NX and NY), element spacing along these axes (dx and dy) and the angle between these axes (γ). Any positive value for γ may be used to configure the lattice. Setting γ to 90° results in a rectangular lattice, while γ= 60° creates a triangular lattice. The circular option (see ***Figure 4b***) configures circular phased arrays with one or more concentric circles. The number of elements in each concentric circle and the radius of each circle can be defined as vectors by variables NC and R. Alternately, the user-defined option allows for custom array architectures using the number of array elements, N, and their X and Y locations.

Designers can define gains or full radiation patterns for each antenna element in the phased array. This allows them to use different radiation patterns for internal, edge and corner elements. The radiation pattern of each antenna element will often be affected by its position in the array. These patterns may be measured in the lab or calculated in an electromagnetic (EM) simulator such as AXIEM for planar EM and Analyst™ for 3D FEM analysis, simulators within NI AWR software. A simple approach is to use a 3 × 3 phased array and excite one element — the internal element, one of the edge elements or one of the corner elements — and terminate all others. This will provide the internal, edge and corner element radiation patterns, respectively, which can automatically be stored in data files using the NI AWR software output data file measurements. This approach includes the effect of mutual coupling from first-order neighbors. A 5 × 5 element array may be used to extend the mutual coupling to second-order neighbors.

Another new feature in VSS is the capability to model the RF links of individual elements in the phased array. This is an important functionality, since RF links are not ideal and can cause array behavior to deviate significantly from ideal. As an example, gain tapers are commonly used in phased arrays; however, using identical RF links for all antenna elements

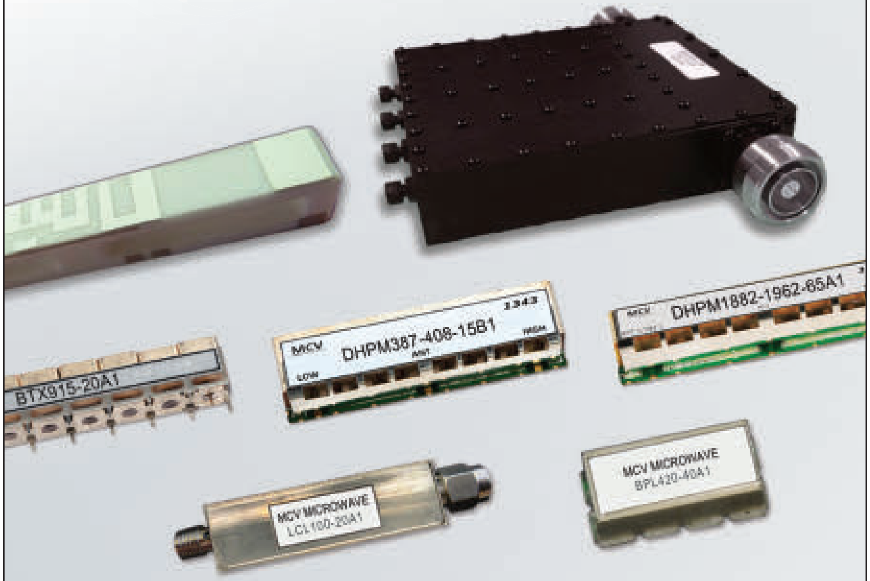

may cause certain elements (the ones with higher gain) to operate near or in compression, while the others will be linear. Array performance will be affected by how close to compression the elements operate. Alternatively, based on the gain tapers that are used, designers may choose different RF link designs for different elements. While this is more complicated, it results in more efficient phased arrays, and the VSS modeling allows designers to achieve this.

CONCLUSION

The capability to design and verify the performance of individual components, as well as the entire signal channel of an AESA radar, becomes a necessity as element counts and the integration of the antenna with the electronics increase. Using circuit simulation, system-level behavioral modeling and electromagnetic analysis within a single design platform enables development teams to investigate system performance and component-to-component interaction prior to costly prototyping. Being able to predict performance and modify the RF design so that requirements are met is one of the capabilities that modeling functionality of VSS offers. ■

References

1. Thomas E. Kazior, "Beyond CMOS: Heterogeneous Integration of III–V Devices, RF MEMS and Other Dissimilar Materials/Devices with Si CMOS to Create Intelligent Microsystems," www.ncbi.nlm.nih.gov/pmc/articles/PMC3928903/.
2. Carlo Kopp, "Active Electronically Steered Arrays, A Maturing Technology," www.ausairpower.net/aesa-intro.html.
3. Xiaoxiong Gu et al., "W-Band Scalable Phased Arrays for Imaging and Communications," *IEEE Communications Magazine*, Vol. 53, Issue 4, April 2015, pp. 196–204.
4. Sanjay Raman et al., "The DARPA Diverse Accessible Heterogeneous Integration (DAHI) Program: Towards a Next-Generation Technology Platform for High-Performance Microsystems," CS MANTECH Conference, April 23–26, 2012, Boston, Mass.
5. "An Eight-Element 6 to 18 GHz SiGe BiCMOS RFIC Phased-Array Receiver," *Microwave Journal*, May 4, 2007, www.microwavejournal.com/articles/4757-an-eight-element-6-to-18-ghz-sige-bicmos-rf-ic-phased-array-receiver.
6. "Researchers Develop First Silicon Wafer-Scale 110 GHz Phased Array Transmitter," PhysOrg.com, April 6, 2012, www.phys.org/news/2012-04-silicon-wafer-scale-ghz-phased-array.html.
7. Mike Harris et al., "GaN-Based Components for Transmit/Receive Modules in Active Electronically Scanned Arrays," CS MANTECH Conference, May 13–16, 2013, New Orleans, La.


because close
is not always
good enough

UAV/Drone Detection System

Aaronia AG
Strickscheid, Germany

The rapid proliferation of micro/mini UAVs is a growing concern. Easy to make, cheap to buy, simple to fly, and hard to detect, commercial and non-commercial drones are one of the most quickly evolving technological threats to military and civilian interests. Military communications links often exploit techniques such as frequency agility in order to reduce the probability of interception, but the designers of UAVs are trying to field an inexpensive commercial product. As a result, UAV communications links are low-cost, unsophisticated sub-systems that have no clandestine qualities. To address this issue, Aaronia has spent four years developing the new Drone Detector, which exploits RF radiation emitted by the UAV's onboard systems and by the operator's control unit. Real-time RF signal detection, combined with what the company terms 'pattern triggering,' provides rapid warning of any UAV or UAV control unit that is operating within the area being monitored.

▲ *Fig. 1 The basic drone detector configuration is best suited to mobile operation, teaming a single antenna with an XFR V5 PRO portable unit.*

Two types of 3D direction-finding antennas are offered by the Drone Detector — the IsoLOG 3D 80 and IsoLOG 3D 160. These have eight sectors with 16 antennas, and 16 sectors with 32 antennas respectively. Both cover the 680 MHz to 6 GHz range and extenders are

available should VLF (9 kHz to 680 MHz) and 6 to 20 GHz coverage be required. For field use these antennas must be teamed with either an XFR V5 PRO, shown in ***Figure 1***, when used for portable installations, or an RF Command Centre for stationary use. For fixed remote installations or multi-unit grid installations Aaronia offers the waterproof 'Remote BOX'. All RTSA receivers cover frequencies from 9 kHz to 20 GHz, this includes the frequencies commonly used for UAV control and video links — typically 433 MHz, 900 to 915 MHz, 1.3 GHz, 2.4 GHz and 5.8 GHz.

NO EXPORT LICENSE

In its standard form, the Drone Detector has a real-time bandwidth of 80 MHz. Optionally, this can be extended to 160 or 175 MHz. Also, the standard system can be shipped without the need for an export license, but this is not the case if the customer requires a 175 MHz bandwidth unit. Using these basic components, the user can opt for systems of varying complexity. The simplest consists of a single IsoLOG 3D antenna and a stationary or mobile spectrum analyzer. This is already sufficient for the surveillance of a wide area up to approximately 3 km diameter.

If a fully mobile solution is required, the system can be installed on a vehicle and operated on battery power. The Drone Detector's antennas are

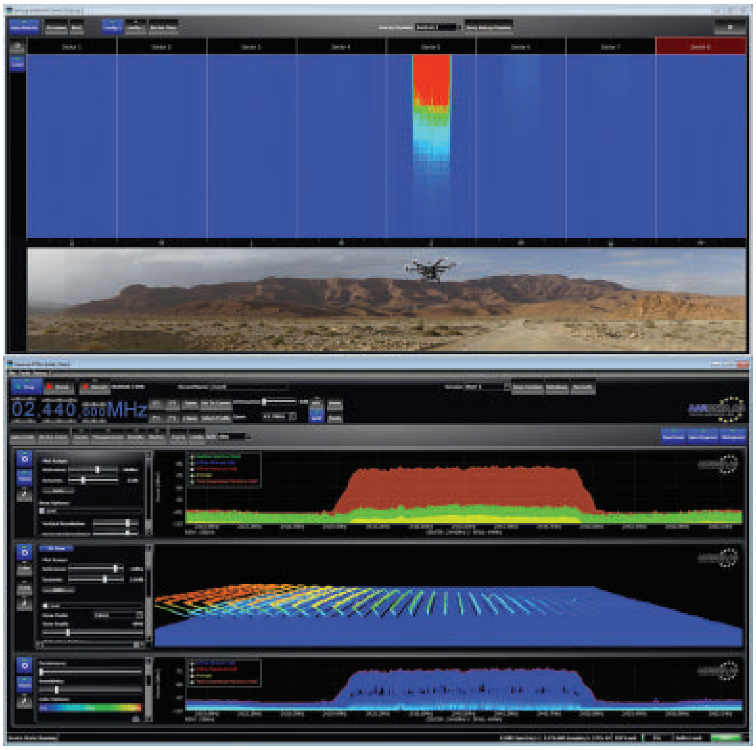

▲ *Fig. 2 Aaronia's custom software shows the presence of a UAV directly to the south of a detector installation. If the drone changes position, the red indication on the display will move to the right or left.*

SUMITOMO ELECTRIC
Device Innovations USA

Radar, Base Stations, SATCOM, Point to Point, and Space

You Have Many Choices for GaN Devices Only One Stands Above the Rest

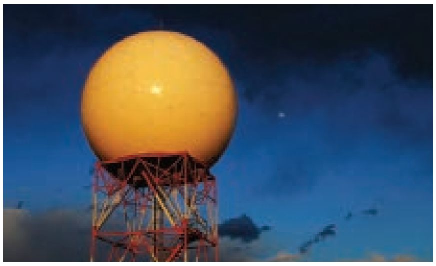

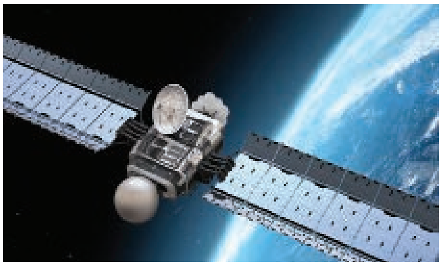

GaN for BTS

Macro Cells
UHF to 2.7 GHz
50/80/120/180/240/360W

3.6 GHz
50/80/120/180/240W

Small Cells
UHF to 3.8 GHz
10/15/20/30/40W

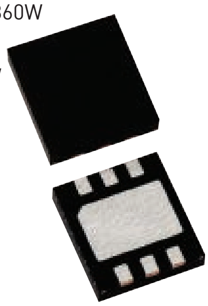

GaN for Radar

X-band (8.5 to 9.8GHz)
50/100/200/300W Discrete 30W Module

S-band
2.7-2.9GHz 600W
2.7-3.1GHz 500W
2.9-3.3GHz 500W
All Single-Ended, Discrete

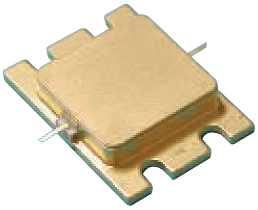

C-band (5.2-5.9GHz), Upcoming
50/100/200W

To learn more, contact
mw@sei-device.com

GaN for Satellites

UHF to S-band
2/10/40/75/150/200W

X-band
6/20/25/50W

C-band (3.7-4.2GHz), Upcoming
30/100/200W

www.sei-device.com

SUMITOMO ELECTRIC GROUP

resistant to the effects of salt water splashes or spray, enabling deployment on a boat. Once a signal has been detected, its approximate bearing will be shown to an accuracy that depends on which model of antenna is being used. With the standard IsoLOG 3D 80, the bearing accuracy will be at least within the 45° coverage of a single antenna sector but is often much higher (via software approximation up to 10° or even 5°).

When larger areas must be covered, several antennas and spectrum analyzers can be connected to a single centralized PC, which manages these simultaneously. The larger the area to be covered, the greater the number of antennas and analyzers that must be deployed. Any threat signal is likely to be received by several antennas, so the results can be triangulated to provide detailed information on the location of the UAV and/or its operator. ***Figure 2*** offers a physical example of the information generated.

The drone detection software offers an intuitive layout combined with powerful tracking, trigger and display options helping to identify, capture and track any RF emissions from drones/UAVs or other RF sources up to 20 GHz. Each sector/antenna gets its own real-time view, which enables the exact direction that the drone is coming from to be identified. Customizable alarms or pop-ups guarantee early warning for the operator/user.

NO FALSE ALARMS

Since the system is designed to recognize the RF signals specifically associated with UAVs by observing their frequency and other characteristics, it will not provide false alarms when faced with other types of RF signals. When faced with several UAVs, the system can detect these, no matter if the intruders are of the same type or different.

The average time needed for the detection of a UAV is between 10 µs and 500 ms. It depends on factors such as the complexity of the deployed system and the number of antenna arrays being used. While a clear line of sight between the antennas and the UAV or its operator gives the best results, the system can detect RF signals whose source is obscured by trees, bushes or a crowd of people. The system is passive, emitting no signals of its own that could interfere with the normal operation of nearby assets such as airports, or give the UAV operator warning of its presence. System performance is unaffected by darkness or poor weather —if meteorological conditions allow UAVs to fly, they can be detected.

The drone detection system can be used virtually anywhere. Typical use scenarios are the protection of residential areas, governmental buildings and commercial/industrial areas like nuclear plants. Available as a single-side or multiple-side solution, the system is adjustable to the characteristics of the terrain to be monitored.

VENDORVIEW

Aaronia AG
Strickscheid, Germany
www.aaronia.com


DELTA
Electronics Mfg. Corp.
Interconnect Solutions
ARROW
Aerospace & Defense
A.E. Petsche Co.
SMP & SMPM
High Performance
Connectors to 65 GHz
Create
Collaborate
Connect
“Fully customizable cost effective solutions”
Distributed by A.E. Petsche Co.
A Delta Channel Partner
contactAEP@aepetsche.com
www.aepetsche.com
(844) AEP-7600
(844) 237-7600

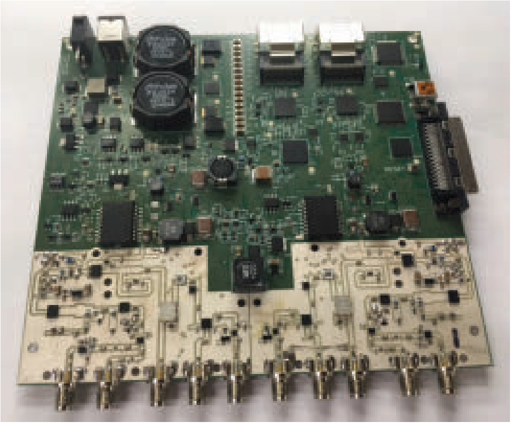

1.8 to 2.7 GHz, 2×2 MIMO Front-End and SDR Transceiver

NewEdge Signal Solutions
Shirley, Mass.

As the number of frequency bands and waveforms continue to expand in commercial and government wireless networks, the need for a high power, software defined radio (SDR) RF front-end has never been greater. NewEdge Signal Solutions is bringing the frequency and waveform agility that already exists in baseband and transceiver ICs to both the high power RF power amplifier (PA) and filter components of the system. NewEdge has developed two products to fulfill this emerging need (see ***Figure 1***):

- ETX108, a ×2 multiple-input-multiple-output (MIMO) RF front-end that transmits 7 W of average power per channel, using either 4G or a constant envelope (CE) waveform across 1.8 to 2.7 GHz
- ETX117, an SDR transceiver system developed in collaboration with Ettus Research.

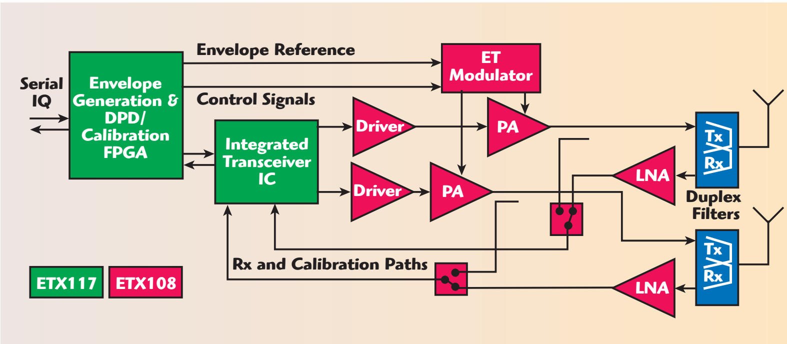

▲ *Fig. 1 RF front-end and SDR transceiver reference design. EGI, CFR and DPD code by NewEdge Signal Solutions.*

The ETX108 front-end is broadband, covering 1.8 to 2.7 GHz in transmit and 1.7 to 2.7 GHz in receive. The PA provides 44 W peak or 7 W average output power per channel, assuming 8 dB peak-to-average power ratio (PAPR). The PA comprises all gain stages, power sequencing and supplies. With both channels at full output, it consumes less than 40 W. The receiver has a noise figure less than 1 dB and an input 1 dB compression point of 1.5 dBm. The compact front-end, measuring 5.25" × 5.75", can be configured for envelope tracking (ET) or constant voltage operation. It supports either frequency division duplex (FDD) or time division duplex (TDD) LTE and, running NewEdge firmware on the ETX117 transceiver system, complies with 3GPP (LTE) ACLR1.

The ETX117 SDR transceiver system is comprised of the Ettus Research N230 SDR transceiver board with NewEdge firmware, which includes the envelope generation interface (EGI), crest factor reduction (CFR) and digital predistortion (DPD). This board is designed to work from 300 MHz to 6 GHz and can accept I/Q data via an Ethernet link, when the modem is remote, or directly from a number of baseband systems on a chip (SoC) via an adaptor cable. Most importantly, the board

ProductFeature

operates via Ettus Research's universal software radio protocol hardware driver (UHD). The UHD architecture is compatible with GNU Radio, C++/Python API, Amarisoft LTE 100, OpenBTS and other third-party software and frameworks.

MULTIPLE WAVEFORM SUPPORT

Supporting network provider and operators that want hardware easily upgraded in the field, the ETX108/ETX117 combination may be configured to operate in FDD LTE, TDD LTE and constant envelope modes. For best efficiency, the ET modulator on the ETX108 board should be used for high peak-to-average power ratio waveforms (e.g., FDD and TDD LTE). When running in TD-LTE mode, as defined by 3GPP TS 36.104, the PA in each channel can be disabled, meeting the 3GPP requirement that the transmit output must shut down to below -85 dBm/MHz within 17 µs.

Onboard programmable resources within the ETX108 are available to control the TD-LTE T/R switch from a single TDD control line for each transmit channel. This guarantees accurate T/R switch timing, to minimize transition time and avoid "hot switching," which can damage the switch. Onboard T/R switch control also ensures accurate enable/disable timing of the receive port.

For networks running legacy or lower peak-to-average ratio waveforms, such as FM or GSM, the ET modulator on the ETX108 board may be configured to act as a standard DC-DC converter and will operate the final stage RF power transistor at a fixed voltage.

ET EASY TO USE

In developing the ETX108/ETX117 combination, NewEdge has solved the challenges historically associated with ET:

- Access to the original modem data stream is required so that the envelope and RF signals may be separate, enabling envelope generation and RF delay management to be performed in the digital domain.
- RF PA implementation must take the ET modulator bias network into account, as traditional approaches to bias choke and matching network design are incompatible with ET modulator requirements. Wide signal bandwidth waveforms dictate that the ET modulator and PA be highly integrated and developed as one functional block.
- For modern high peak-to-average waveforms, DPD and CFR firmware is really a "must-have" for average power levels greater than 1 to 2 W. NewEdge provides an ET compatible DPD/CFR solution that is part of the ETX117 SDR firmware.

The system allows users to bring their digital I/Q data over Ethernet (if the modem is based in the cloud, for example) or via a special adapter cable that brings the I/Q data from many popular baseband SoCs.

The ETX108/ETX117 combination quickly gets users up and running for evaluation, field trials and moderate volume applications. NewEdge Signal Solutions will be developing small form-factor and lower cost variations of this combination to meet additional customer requirements.

NewEdge Signal Solutions
Shirley, Mass.
www.newedges2.com

14 and 16-bit AWGs for Automated and Remote Applications

Spectrum Instrumentation has a new line of arbitrary waveform generators (AWG), based on the LXI instrumentation standard, and available for immediate delivery. Seven new instruments in the generatorNETBOX series use the latest digital-to-analog converter (DAC) technology to generate signals from DC to 400 MHz, with full remote control through an Ethernet interface. The generatorNETBOX instruments offer two, four or eight fully synchronous channels. Each channel is clocked using a precision phase locked loop (PLL) control system that can be generated internally or from an external reference. To generate long and complex waveforms, the AWGs combine their large on-board memories with operating modes such as single-shot, loop, FIFO, gating and sequence replay.

The top of the range is the DN2.66x series: fast, high resolution AWGs using 16-bit DACs, output rates to either 1.25 GSPS or 625 MSPS and large on-board memories (up to 2 × 4 GB). For lower frequency applications — up to 60 MHz frequency content — Spectrum offers the DN2.60x series, which has 14-bit DACs and output signal rates to 125 MSPS.

The instruments are self-contained, with all the tools necessary to generate an almost unlimited variety of waveforms. Spectrum's SBench6-Pro software, standard with every unit, controls all the operating modes and hardware settings from a simple and easy-to-use graphical user interface. Available drivers allow users to write their own control programs using popular programming languages.

Small and compact, the generatorNETBOX products can be used on a benchtop or rack mounted. For mobile applications, they can be powered by an optional 12 or 24 V DC source.

Spectrum Instrumentation
Grosshansdorf, Germany
www.spectrum-instrumentation.com

500 W L/S-Band GaN SSPA

Teledyne Paradise Datacom has added a 500 W, 1.75 to 2.12 GHz solid-state power amplifier (SSPA) to its line of compact outdoor GaN SSPAs. With a size of 10" × 19" × 6.5", the HP-AS2-500 has the smallest footprint available for a high power SSPA operating in L/S-Band — only slightly larger than a shoe box and weighing 44 lbs. The amplifier is available in single thread or fully redundant configurations.

Using the latest GaN device technology, the SSPA delivers higher power density, efficiency, reliability and thermal resiliency, as well as wide instantaneous bandwidth. The amplifier provides 500 W saturated output power or 250 W linear (e.g., where the third-order intermodulation products are < –25 dBc for two tones separated by 5 MHz). The design has an integrated reflected power monitor and true RMS power detection. Developed for outdoor operation, the SSPA withstands extreme environments, with an operating temperature range from –40° to +60°C. If required by the application, the low end of the temperature range can be extended to –55°C.

The family of Teledyne Paradise Datacom SSPAs cover a range of bands — L, S C, X, Ku and Ka — providing output power levels from 100 through 500 W. They can be deployed in applications traditionally reserved for older traveling wave tube amplifier (TWTA) technology.

Teledyne Paradise Datacom
State College, Pa.
www.paradisedata.com

HIGH POWER
100 MHz to 20 GHz

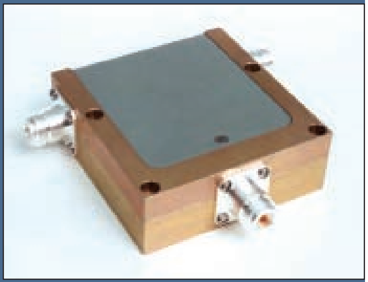

For Military/Radar Applications.

Isolators/Circulators

As one of the leading suppliers of ferrite components in the industry, UTE Microwave has pioneered innovative designs, quality craftsmanship and exceptionally high quality products. Custom designs, standards...many of them off-the-shelf, are the result of over 35 years of experience in the industry. UTE Microwave continues this tradition with new products for ever changing applications. Our broad line of HIGH POWER, low loss circulators and isolators spans the spectrum from below 100 MHz in coax/stripline units to waveguide devices at 18 GHz for both peak and average powers.

325 MHz NEW HIGH POWER Circulator for Radar & UHF Frequencies

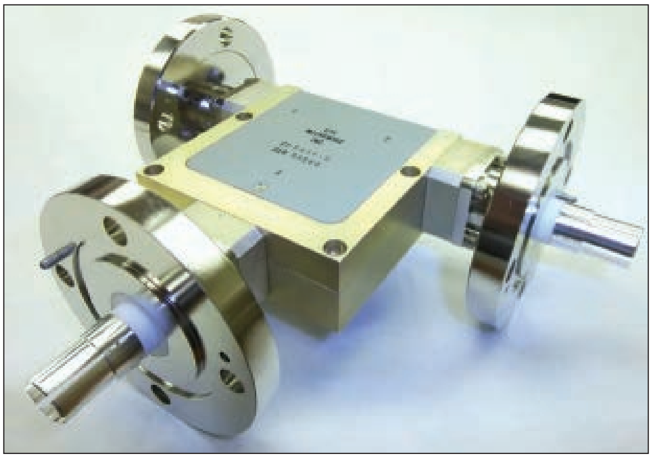

Model CT-1864-S is rated at 60kW peak and 600W average power at 325 MHz. The unit provides 20 dB minimum isolation, 0.2 dB insertion loss and 1.20:1 maximum VSWR. Its extremely compact design has flange to flange insertion length of only 6-3/4" and a height of 5-1/4". For use in radar applications, it has 1-5/8" EIA connectors. It is also available at other UHF frequencies and connector types.

HIGH POWER Drop-in Series

A broad line of low loss HIGH POWER Drop-in circulators are available from VHF to Ku band including Kilowatt average power levels at VHF thru S band. L and S band radar are a specialty. A few of these are shown here.

A) 2.7–3.1 GHZ 1 kW pk, 100 W av

B) 1.2–1.4 GHZ 3 kW pk, 300 W av

C) UHF TV Band 5 kW pk, 500 W av

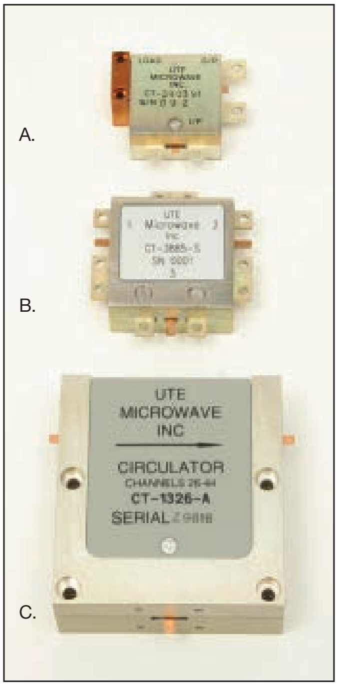

Our "POWER-LINE" serves the COMMUNICATIONS, TELECOM, MEDICAL, SCIENTIFIC, TV, PCS and INDUSTRIAL markets.

The following models are examples of our High Power units

Model No.	Power	Connectors	Freq. Range
CT-1542-D	10 Kw Pk 1 Kw Av	DIN 7/16	420–470 MHz
CT-2608-S	3 Kw Pk 300 W Av	"Drop-in"	1.2–1.4 GHz
CT-3877-S	2.5 Kw Pk 250 W Av	"Drop-in"	2.7–3.1 GHz
CT-3838-N	5 Kw Pk 500 W Av	N Conn.	2.7–3.1 GHz
CT-1645-N	250 W Satcom	N Conn.	240–320 MHz
CT-1739-D	20 Kw Pk 1 Kw Av	DIN 7/16	128 MHz Medical

Broadband Units • Common Band Devices • High Isolation Units • Multiport Devices • Drop-In Devices • Wireless/PCN Devices • High-Power Industrial/Medical Iso Adaptors Waveguide Junctions • High-Power TV Units • VHF and UHF Devices

sales@utemicrowave.com

FEATURES:

- **Power levels to 5 KW CW, 75 KW Pk.**
- **Low Intermod Units**
- **Low Loss Options**
- **Extended Octave Bandwidths**
- **Power Monitors and DC Blocks**
- **Iso Filter-Monitor Assemblies**

UTE MICROWAVE INC.

3500 Sunset Ave., Asbury Park, NJ 07712
Tel: 732-922-1009 Fax: 732-922-1848
E-mail: info@utemicrowave.com

Contact us for more information on our extensive product line and current catalog. We accept Visa, MC, Amex

6 GHz Three-Stage Down-Converter

SignalCore's SC5307A and SC5308A are three stage down-converters with an input frequency range from 100 kHz to 6 GHz. The SC5307A is packaged in a PXIe form factor, while the SC5308A is a core-module with serial interface. These high performance down-converters can be used in a variety of applications: instrumentation, wireless communication, signal intelligence, satellite links and software-defined radio (SDR).

The output IF frequency of both products can be set to 1250 MHz or tuned to center between 100 and 500 MHz, with IF bandwidths of 80, 160 or 320 MHz. IF output IP3 is typically better than 35 dBm, with an input noise floor less than –160 dBm/Hz with the input preamplifier enabled. The down-converter has a programmable gain range greater than 60 dB. The tunable RF LO uses an internal YIG oscillator, which provides excellent phase noise and contributes negligible noise to the down-converted RF. The LO signals are synthesized from an internal 10 MHz TCXO, which has better than ±0.1 ppm stability. To increase stability, the down-converter module can be programmed to phase lock to an external reference, such as a Rubidium or oven-controlled crystal oscillator.

Driver and development software is provided with the hardware, as well as a software GUI that allows the user to easily control the unit without having to write any control software.

The SC5307A occupies two PXIe slots and is useful for systems that are space constrained. The SC5308A benchtop unit requires a single +12 V supply and can be controlled via a USB, SPI or RS232 interface.

SignalCore
Austin, Texas
www.signalcore.com

Software and Mobile Apps

AR App of Knowledge

VENDORVIEW

AR RF/Microwave Instrumentation's mobile app is available as a free download from Apple iTunes and Google Play. This application is a quick and easy tool to access a variety of content from AR. The home screen icons allow easy navigation to view basic and full product descriptions, app notes, AR's literature library, YouTube videos, contact information and social media activity — all from your mobile device. To download the app, visit www.arww-rfmicro.com/html/ar-moblie-app.asp.

AR RF/Microwave Instrumentation
www.arworld.us

Filter Wizard

K&L Microwave's Filter Wizard® filter synthesis and selection tool streamlines identification of filter products meeting customer specifications across a large portion of K&L's standard product offerings. Filter Wizard accelerates user progress from specification to RFQ for RF and microwave filters spanning an ever-increasing range of response types, bandwidths and unloaded Q values. Provide the application with your desired specifications, and the software will return a list of products that match — placing response graphs, outline drawings and downloadable S-parameters at your fingertips.

K&L Microwave
www.klfilterwizard.com

BenchVue Software Applications

VENDORVIEW

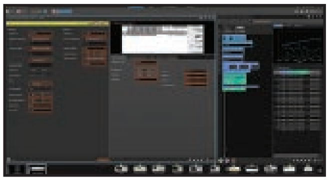

Keysight's new BenchVue software applications enable users to control and obtain data from signal generators and FieldFox handheld signal analyzers. These new applications, along with Test Flow, the built-in BenchVue automation app, enable users to speed up control and automation of instruments by eliminating the need for time-consuming instrument programming. BenchVue software allows users to create custom, automated test sequences within the BenchVue environment, streamlining measurement tasks on hundreds of Keysight's broad range of test and measurement instruments.

Keysight Technologies Inc.
www.keysight.com/find/benchvue

Release 2016a

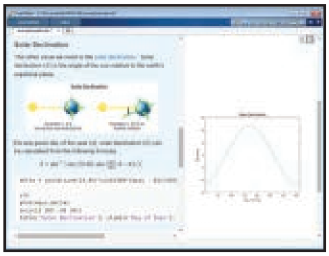

MathWorks introduced Release 2016a (R2016a). This release includes the MATLAB Live Editor, which offers the ability to write, run and modify code in a single interactive environment to accelerate exploratory analysis; and App Designer, an environment that simplifies the process of building MATLAB apps. R2016a also includes a number of new features in Simulink to help speed model development and simulation, as well as updates and bug fixes for all other products.

MathWorks
www.mathworks.com

COMPLETE Library v16.1

VENDORVIEW

Modelithics released the latest version of The Modelithics® COMPLETE Library, version 16.1, formatted for use with NI AWR Design Environment™. Version 16.1 adds 33 new models from 13 different vendors to the existing collection of highly accurate simulation models with unique and powerful scalability features. Other significant features include a simulation mode that has been incorporated into most CLR models. Modelithics' models with pad parameters are now compatible with NI AWR software iCell intelligent microstrip components and users can now adjust the license expiration warning.

Modelithics Inc.
www.modelithics.com

USim Version 2.2

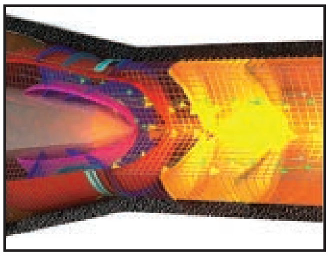

Tech-X Corp. announced the release of USim Version 2.2. USim is a fluid plasma modeling framework that simulates the dynamics of charged fluids or neutrals. USim 2.2 new and updated features include: preconditioners for diffusion-type problems; reduced memory footprint for finite volume operators; many bug fixes throughout the simulation engine, documentation and user-interface; and improved user interface including better run output, vector plots and better controls for license. Request your free simulation evaluation today.

Tech-X Corp.
www.techxcorp/usim

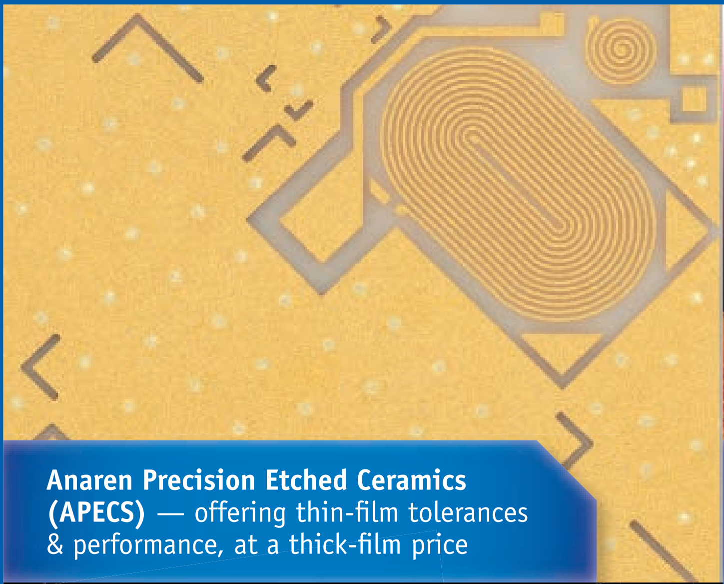

Anaren Precision Etched Ceramics (APECS) — offering thin-film tolerances & performance, at a thick-film price

Space/Mil-grade Xinger® couplers — proven in Mars missions & ready for tough terrestrial settings, too

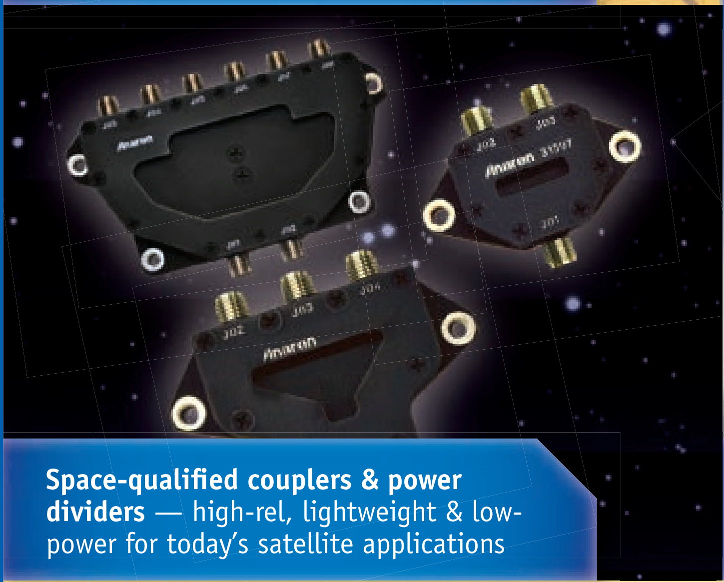

Space-qualified couplers & power dividers — high-rel, lightweight & low-power for today's satellite applications

RF solutions for next-gen AESAs — including manifolds, T/R modules & beam-formers for air, sea, and land platforms

Isn't it time to put Anaren innovations like these to work for *you*?

Fast-approaching our 50th anniversary — and this year celebrating our 1 billionth Xinger®-brand coupler sold! — today's Anaren continues to drive innovative, best-in-class RF technology for the world's most demanding space, defense, wireless, and consumer electronics customers.

> **Our Space & Defense Group** offers a fast-growing range of passive and active solutions, including multichip modules, IMAs, and custom solutions for today's digital radars. Exciting, new PCB and ceramic substrates and multilayer packaging techniques. And a growing line-up of space-grade components and high-temperature modules.

> **Our Wireless Group** continues to reinvent the passive components category. From new, Femto-sized and mil-grade Xinger®-brand SMTs. To subminiature baluns and couplers for consumer products. To our growing family of Anaren Integrated Radio (AIR) modules and other solutions for the wireless IoT.

To learn more about how today's Anaren can make you more competitive tomorrow — visit **www.anaren.com** or email us at **sales@anaren.com** today!

Anaren®
What'll we think of next?®
800-411-6596 > www.anaren.com

INSPIRE • ENVISION • INNOVATE

EMC+SIPI

★ WASHINGTON, DC ★

AUGUST 7-11 • 2017

2017 IEEE INTERNATIONAL SYMPOSIUM ON

ELECTROMAGNETIC COMPATIBILITY, SIGNAL AND POWER INTEGRITY

EMC+SIPI is the leading event to provide education of EMC and Signal and Power Integrity techniques to specialty engineers. The Symposium features five full days of innovative sessions, interactive workshops/ tutorials, experiments and demonstrations, and social networking events.

Join your colleagues August 7 – 11, 2017 at the EMC + SIPI Symposium in National Harbor, Maryland just outside of Washington D.C.

Gaylord National Resort & Convention Center
National Harbor, Maryland

CALL FOR PAPERS

Get Your Ideas Published!

EMC 2017 is a Technical Symposium. Technical Papers are the essence of our Technical Program. Original, unpublished papers on all aspects of EMC & SIPI are invited.

- **Preliminary Full Paper Manuscript:** November 1, 2016 - January 16, 2017
- **Notification of Acceptance:** February 21, 2017
- **Final Paper Due:** May 3, 2017

Call for Experiments & Demonstrations

Experiments and demonstrations utilize hardware and software to demonstrate a principle or phenomena of EMI/EMC. The presentations are informal and non-commercial; they are usually conducted in specific areas within the Exhibit Hall.

To schedule, contact:
Bob Scully - **bob.scully@ieee.org**
Sam Connor - **sconnor@ieee.org**

Call for Abstract Reviewed Papers

Abstract Reviewed Papers provide opportunities to exchange experiences and ideas. Only an abstract is required for initial submission, papers are included in the conference proceedings; however, these papers are not published in the IEEE XPlore.

Proposals Accepted: November 1, 2016 - February 21, 2017
Acceptance Notification: March 27, 2017
Final Paper Due: May 3, 2017

Call for Special Sessions

Special Sessions focus on areas of interest not addressed in Technical Papers. Acceptance criteria are the same as for Technical Papers.

Proposals Accepted: November 1, 2016 - December 20, 2016
Notification of Acceptance: January 8, 2017
Preliminary Papers Due: March 6, 2017
Final Papers Due: May 3, 2017

Call for Workshops & Tutorials

Workshops and Tutorials are informal, interactive educational presentations, typically addressing the practical side of understanding and solving EMC issues. These sessions are held on Monday and Friday.

Proposals Accepted: November 1, 2016 - January 16, 2017
Notification of Acceptance: February 21, 2017
Final Presentations Due: May 3, 2017

Commercial Vendor Demonstrations

Please note: Commercial Demonstrations are presented by vendors and are not committee reviewed.

To schedule, contact:
Mark Maynard – **mmaynard@ieee.org**

IEEE | EMC SOCIETY

www.emc2017.emcss.org

eLEARNING center

Presented by: Microwave Journal

Scan page using layar app

November Short Course Webinars

Technical Education Training
Performing On-Wafer VNA Measurements from 70 kHz to 110 and 145 GHz
Sponsored by: Anritsu
Live webcast: 11/1/16

Wireless Communications and Connectivity
Unlocking Wideband 5G & mmWave Insights to 110 GHz
Presented by: Keysight Technologies
Live webcast: 11/2/16

CST Webinar
Analyzing HF & LF RadHaz Scenarios with 3D EM Simulation
Live webcast: 11/3/16

Technical Education Training
Tackling the Challenges of Next Generation ADAS Vehicle Architectures
Sponsored by: National Instruments
Live webcast: 11/3/16

CST Webinar
EMC Simulation for Space Applications with CST STUDIO SUITE
Live webcast: 11/10/16

RF/Microwave Training
Passive Components
Sponsored by: Mini-Circuits
Live webcast: 11/10/16

Technical Education Training
AntSyn
Sponsored by: National Instruments/AWR
Live webcast: 11/16/16

CST Webinar
Transformer Simulation
Live webcast: 11/17/16

Technical Education Training
Ampleon Brings RF Power Innovations Towards Industrial Heating Market
Sponsored by: Ampleon
Live webcast: 11/17/16

CST Webinar
Antenna Analysis and Design with Characteristic Mode Analysis
Live webcast: 11/22/16

Register to attend at mwjournal.com/webinars

Past Webinars On Demand

Technical Education Training Series
- Design of an 800 W GaN Power Amplifier Stage for Pulsed L-Band Applications Using Simulated Load Pull
- Preparing for the Autonomous Car: Developing a 5G Network and Integrating Sensors
- Innovative Passives and Substrates Enable RF Power Amplifier Designs for Cooking Applications
- VCO Fundamentals
- On the Road to 5G, Advances in Enabling Technology: A Materials Perspective
- Vector Network Analyzers as a Tool for Signal Integrity in High Speed Digital Systems

RF/Microwave Training Series
Presented by: Besser Associates
- Mixers and Frequency Conversion

Innovations in EDA
Presented by: Keysight Technologies
- How to Design Phased Arrays for 5G, Radar and Satellite
- Advances in High Power RF Design

Keysight in Aerospace/Defense
- Real-Time Recordings and Post-Processing of Wide-Bandwidth EW Signals

NEW PRODUCTS

FOR MORE NEW PRODUCTS, VISIT WWW.MWJOURNAL.COM/BUYERSGUIDE
FEATURING VENDORVIEW STOREFRONTS

COMPONENTS

High-Reliability Ferrite Beads

AEM announced the release of their HRB-US series of high-reliability ferrite beads that meet the stringent requirements of the Defense Supply Center Columbus (DSCC) specification 03024. AEM is the only ferrite chip manufacturer whose parts are approved by the Defense Logistics Agency (DLA) to the DSCC 03024 specification. The innovative HRB-US process up-screens commercially available parts utilizing AEM's proprietary techniques to selectively certify additional ferrite beads to the DSCC standard.

AEM
www.aem-usa.com

RF Switches

CEL is offering new GaAs RF switches to replace the discontinued Renesas Electronics RF switch devices. These new drop-in replacements support frequencies up to 6 GHz and are ideal for dual-band wireless LAN applications. The switches, which have miniature packages, are available in different configurations and have evaluation boards to help engineers speed up their circuit designs.

California Eastern Labs
www.cel.com/RF

ISM Band, Bandpass Filter

This TX/RX filter dramatically reduces adjacent and out-of-band interference to the ISM Band (902 to 928 MHz), allowing higher data rates and improved range. Features include high Q, low loss, extremely sharp lowside cutoff limits 800 MHz cellular-band noise and interference. They are available with SMA adapter board or stand-alone. Designed for infrastructure ISM Band users, this filter features automated data collection, dedicated monitoring and data links. For more information, contact Integrated Microwave at (858) 259-2600.

Integrated Microwave
www.imcsd.com

RF Microwave Isolators

VENDORVIEW

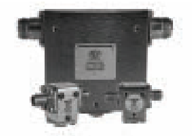

MECA's isolators are optimized for excellent performance across microwave and millimeter wave bands, covering VHF to EHF and MHz to GHz frequencies, in N, SMA and 2.92 mm connectors. Also available are attenuators, power dividers, terminations and couplers. Their rugged construction makes them ideal for telecommunications, aerospace and test equipment systems. Made in the U.S. and 36-month warranty.

MECA Electronics Inc.
www.e-MECA.com

mmWave YIG-Tuned Filters

Micro Lambda Wireless Inc. announced the production release of two new millimeter wave YIG-tuned filter models. This expands Micro Lambda Wireless' millimeter wave filter product offering to the largest in the market today. The new 4-stage standard models operate over 2 to 40 GHz and 8 to 40 GHz. Units operate over the standard 0 to +65°C temperature range, but military versions covering -40° to +85°C are available on special order.

Micro Lambda Wireless Inc.
www.microlambdawireless.com

18 to 40 GHz Down-Converter

This millimeter wave frequency converter has a single RF input and two IF outputs at 4 to 18 GHz. The unit has integrated LO sources and down-converts 18 to 26.5 GHz and 26.5 to 40 GHz simultaneously. A positively sloping gain across the frequency range compensates for other system losses.

Norden Millimeter Inc.
www.nordengroup.com

Waveguide Directional Couplers

VENDORVIEW

Pasternack introduced a new family of waveguide directional couplers displaying highly accurate performance up to 33 GHz. These waveguide couplers are commonly used for signal sampling and other general purpose applications in wireless transmit/receive systems, satellite communications, radar systems, point-to-point backhaul and telecom. Pasternack's latest release consists of 74 unique models spanning a frequency range of 5.85 to 33 GHz across eight popular frequency bands.

Pasternack
www.pasternack.com

Two Pole Transfer Switch

VENDORVIEW

PMI's Model No. PXS-1G2G-80-T-SFF is an absorptive, high speed, two pole transfer switch capable of switching within 100 ns max. This switch has > 80 dB isolation. Features include SMA female connectors. Unit size is 1.2" × 1.2" × 0.5" with painted blue finish. Frequency is 1 to 2 GHz. Impedance is 50 Ω. Other features are input power +30 dBm (1 W) max, input VSWR 1.5:1 maximum – measured 1.35:1, insertion loss 1 dB maximum – measured 0.76 dB, isolation 80 dB minimum – measured 97.82 dB, switching speed 100 ns maximum – measured 30 ns, DC voltage: +5 VDC – measured 43 mA, -15 VDC (±3 V) – measured 72 mA and control solder pin, TTL logic.

Planar Monolithics Industries Inc.
www.pmi-rf.com

Reflective Coaxial SP2T Switch

Key features are wide-band operation DC to 12 GHz, TTL compatible driver included, fast switching speed 50 ns, low insertion loss and high isolation and a temperature range of -45° to +85°C. Customization available upon request. Hermetically sealed package up to 60,000 ft. available upon request. Primary applications are military, airborne, wireless infrastructure, satellite communications and medical applications.

RF Lambda
www.rflambda.com

NewProducts

Low PIM Switches

RLC Electronics introduced a series of low PIM switches, with offerings from SP2T to SP12T. Switches are available in any frequency range from DC up to 65 GHz, and the low PIM designs offer the customer the ability to reduce intermodulation in active devices in order to reduce system interference. Typical performance ranges from -160 to -175 dBc, and the high isolation minimizes cross-talk between channels to ensure signal integrity. Customer applications include DAS, surveillance and communication systems.

RLC Electronics Inc.
www.rlcelectronics.com

Low PIM Switch

VENDORVIEW

The low Passive Inter-Modulation (PIM) switch is a double-pole, double-throw switch that aims to revolutionize equipment testing. It is claimed to enable users to tap potential savings in the order of about 90% compared to conventional methods. It is designed for those wanting to use a switch in a calibrated test system that will continue to work through hundreds of thousands of cycles without requiring any maintenance.

SPINNER GmbH
www.spinner-group.com

CABLES & CONNECTORS

RF Orange Test Cable

The MegaPhase RF Orange test cable has earned a reputation as the best overall value in phase and amplitude stable performance. With its patented GrooveTube technology, this rugged test cable provides a long service life with repeatable performance. Designed for the DC to 67 GHz bandwidth, this is the ideal test cable whether you're in a lab, production environment or building an ATE. Fewer calibrations mean less downtime, resulting in the MegaPhase promise of Lowest Cost Per Measurement™.

MegaPhase
megaphase.com/tm/orange

Coaxial PCB Connectors

SV's complete line of coaxial PCB connectors meet the industry need for high-performing, easy-to-use compact designs. Current configurations include single-port and multi-port 1.85 mm, 2.92 mm, 2.4 mm, SMA, SMP, SMPM and SMPS edge launch, board mount and thru-hole connectors. SV Microwave's PCB connector designs are ideal for high density applications, while allowing for axial and radial misalignment to compensate for tolerance stack up.

SV Microwave
www.svmicrowave.com

AMPLIFIERS

Solid-State Amplifier

VENDORVIEW

Model 300S1G6AB is a solid-state; 300 W class AB amplifier that instantaneously covers 0.7 to 6 GHz in one unit with an input power level of 0 dBm. This wideband output power amplifier is approximately half the size of a traditional Class A design, more efficient, and offers a more economical price. Typical uses include wireless and EW applications.

AR RF/Microwave Instrumentation
www.arworld.us/post/300S1G6AB.pdf

Solid-State RF PA Module

VENDORVIEW

High efficiency, high power and compact with proven GaN technology, the VSC3645 can be easily combined to create high power C-Band radar transmitters. CPI BMD's solid-state power amplifiers are reliable, highly-efficient and easy to maintain. The VSC3645 solid state power amplifiers are designed for use in maritime surveillance and weather radar transmitters and cover 5.2 to 5.9 GHz. GaN transistors are combined into a 4.2 kW output and are air cooled.

CPI Beverly Microwave Division
www.cpii.com/bmd

Solid-State Power Amplifier Module

COMTECH PST introduced a new high power density solid-state RF module. Comtech's latest development continues to expand on its proven innovative integrated RF GaN power amplifier designs by further increasing the RF power density. Comtech's latest GaN-based, 6 to 18 GHz RF amplifier is consistent with the company's planned technology development roadmap. This highly integrated design is ideal for use in communication, electronic warfare and radar transmitter systems where space, cooling and power are limited.

COMTECH PST
www.comtechpst.com


SQ-, TQ-, IQ-, BQ-, CQ- =
connecting 4, 7, 8, 10 or 12 coaxial RF-Lines at once
RQ23-DC26 =
connecting 23 coax RF-
& 26 Signal Lines at once
Spectrum
Elektrotechnik GmbH
when Quality is needed
Hermetically
Sealed Adapters
2.92mm, TNC, N, Feedthroughs
with venting holes for Vacuum Test Chambers
Phase-Adjusters
360° @ 1 GHz
230° @ 12 GHz
350° @ 18 GHz
500° @ 26 GHz
590° @ 40 GHz
400° @ 50 GHz
600° @ 63 GHz
85° @ 2 GHz
520° @ 12 GHz
770° @ 18 GHz
Big and Small,
we have 'em all
Almost any Waveguide to almost any Coax Connector
WG Materials : Aluminum, Copper, Brass
Connectors : 1.92mm ...SMA....
TNC....N...7/16
www.spectrum-et.com
Telephone: +49-89-3548-040
Email: Sales@Spectrum-et.com
Facsimile: +49-89-3548-0490

NewProducts

AMP1064 Module

VENDORVIEW

Exodus introduced the AMP1064 module covering the entire instantaneous 20 to 6000 MHz frequency range at 20 W CW minimum and 25 W CW typical with flatness of less than 4 dB peak to peak. Using state-of-the-art GaN devices and operating from a 50 VDC source at less than 3 amp consumption, this module is suitable for use with all single channel modulations standards and applications requiring high power and ultra-wide band coverage. It has built-in protection circuits, high reliability and ruggedness. Typical applications include high power testing, EMI/RFI, EW and communications.

Exodus Advanced Communications
www.exoduscomm.com

Solid-State GaN Power Amplifiers

Fairview Microwave Inc. released a new line of solid-state GaN amplifiers. These new amplifiers offer designers a unique solution of off-the-shelf components, typically requiring months of lead time to acquire. The high thermal conductivity of gallium nitride helps to dissipate heat more effectively which results in amplifier designs that have significantly higher output power levels over broadband and narrowband frequencies. Common applications include commercial and military radar, jamming systems, medical imaging, communications and electronic warfare.

Fairview Microwave Inc.
www.fairviewmicrowave.com

300 W GaN Transistor

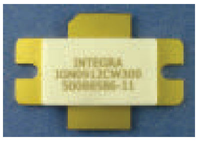

Integra Technologies Inc., a designer and manufacturer of high-power RF transistors, pallets and amplifiers, announced the release of a 300 W GaN transistor, IGN0912CW300, for CW communications. IGN0912CW300 operates over the instantaneous bandwidth of 960 to 1215 MHz. Under continuous wave (CW) conditions, it supplies a minimum of 300 W of output power with typically >13.5 dB gain and 70% efficiency from a 36 V supply voltage.

Integra Technologies Inc.
www.integratech.com

Ultra-High Dynamic MMIC Amplifier

VENDORVIEW

Mini-Circuits' LHA-1H+ MMIC amplifier delivers ultra-high dynamic range for broadband applications from 0.05 to 6 GHz. Fabricated using E-PHEMT process technology, the amplifier provides +41 dBm IP3, 2.1 dB noise figure, 13.9 dB gain and +22.5 dBm P1dB. It provides excellent matching over its full frequency range without the need for external matching components. Industry leading IP3 performance relative to device size and power consumption makes this model ideal for use in driver amplifiers for complex waveform up-converter paths, drivers in linearized systems, and secondary amplifiers in high dynamic range receivers.

Mini-Circuits
www.minicircuits.com

GaN Power Amplifiers

VENDORVIEW

Richardson RFPD, Inc. announced the availability and full design support capabilities for two new X-Band GaN power amplifiers from Qorvo. The TGA2622-SM and TGA2624-SM operate from 9 to 10 GHz and are offered in 7 mm × 7 mm air-cavity, laminate-based QFN packages. For both devices, the RF ports are internally DC blocked and matched to 50 Ω, enabling simple system integration. Ideally suited for pulsed applications, the new GaN power amplifiers offer superior power, PAE and gain performance.

Richardson RFPD
www.richardsonrfpd.com

1 W Power Amplifier

Model ASP40-3530 is a 26.5 to 40 GHz power amplifier that provides a minimum output power of +30 dBm P-1 dB; while maintaining a typical IP3 of +39 dBm. The small signal gain level is 35 dB with a maximum gain flatness of ± 3.5 dB and a typical noise figure of +7 dB. This standard product power series amplifier consists of gain blocks of 25 and 35 dB.

Wright Technologies
www.wrighttec.com

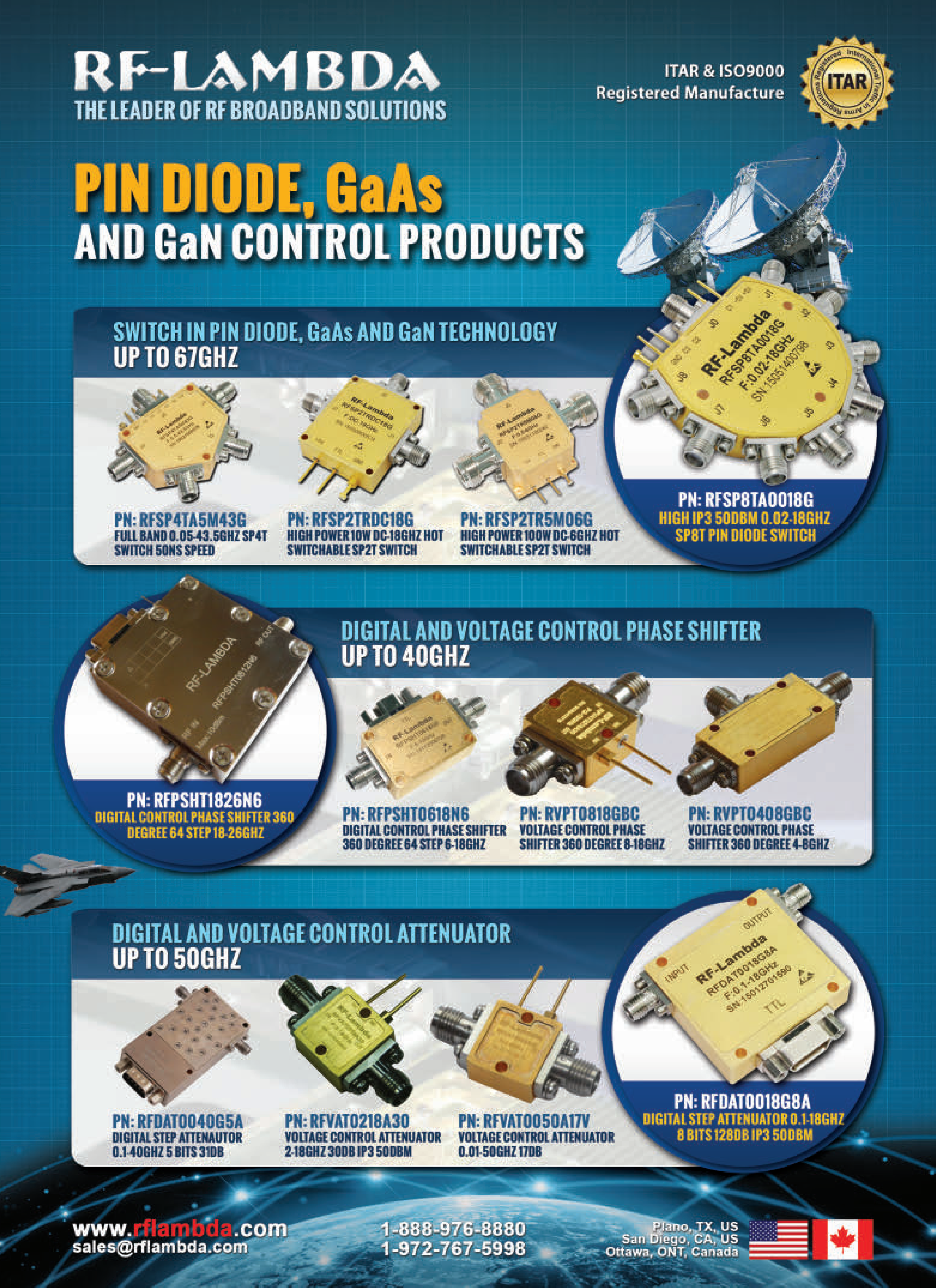
RF-LAMBDA
THE LEADER OF RF BROADBAND SOLUTIONS
ITAR & ISO9000
Registered Manufacture
ITAR
PIN DIODE, GaAs
AND GaN CONTROL PRODUCTS
SWITCH IN PIN DIODE, GaAs AND GaN TECHNOLOGY
UP TO 67GHZ
PN: RFSP4TA5M43G
FULL BAND 0.05-43.5GHZ SP4T SWITCH 50NS SPEED
PN: RFSP2TRDC18G
HIGH POWER 10W DC-18GHZ HOT SWITCHABLE SP2T SWITCH
PN: RFSP2TR5M06G
HIGH POWER 100W DC-6GHZ HOT SWITCHABLE SP2T SWITCH
RF-Lambda
RFSP8TA0018G
F:0.02-18GHz
PN: RFSP8TA0018G
HIGH IP3 50DBM 0.02-18GHZ
SP8T PIN DIODE SWITCH
DIGITAL AND VOLTAGE CONTROL PHASE SHIFTER
UP TO 40GHZ
RF-LAMBDA
PN: RFPSHT1826N6
DIGITAL CONTROL PHASE SHIFTER 360 DEGREE 64 STEP 18-26GHZ
PN: RFPSHT0618N6
DIGITAL CONTROL PHASE SHIFTER 360 DEGREE 64 STEP 6-18GHZ
PN: RVPT0818GBC
VOLTAGE CONTROL PHASE SHIFTER 360 DEGREE 8-18GHZ
PN: RVPT0408GBC
VOLTAGE CONTROL PHASE SHIFTER 360 DEGREE 4-8GHZ
DIGITAL AND VOLTAGE CONTROL ATTENUATOR
UP TO 50GHZ
PN: RFDAT0040G5A
DIGITAL STEP ATTENAUTOR 0.1-40GHZ 5 BITS 31DB
PN: RFVAT0218A30
VOLTAGE CONTROL ATTENUATOR 2-18GHZ 30DB IP3 50DBM
PN: RFVAT0050A17V
VOLTAGE CONTROL ATTENUATOR 0.01-50GHZ 17DB
OUTPUT
INPUT
RF-Lambda
RFDAT0018G8A
F:0.1-18GHz
TTL
PN: RFDAT0018G8A
DIGITAL STEP ATTENUATOR 0.1-18GHZ
8 BITS 128DB IP3 50DBM
www.rflambda.com
sales@rflambda.com
1-888-976-8880
1-972-767-5998
Plano, TX, US
San Diego, CA, US
Ottawa, ONT, Canada

NewProducts

SYSTEMS

RF Drone Detection System

VENDORVIEW

This RF Drone Detection System (DDS) is based on the company's IsoLOG 3D tracking array antenna, a rugged, remote-controllable spectran V5 real-time spectrum analyzer and specialized RTSA suite software. It exploits the RF radiation emitted by the UAV's onboard systems and by the operator's control unit. Highlights of the system are the coverage of several kilometers, a detection time of 10 µS to 500 ms and the ability to track the drone operator. The DDS can also be used for spectrum monitoring and other RF signal tracking applications covering 9 kHz to 20 GHz.

Aaronia AG
www.aaronia.com

10-Gigabit Wireless Ethernet Link

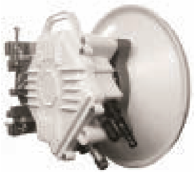

ELVA-1, manufacturer of ultra-high capacity wireless infrastructure links since 2006, announced the availability of its new PPC-10GE, 10-Gigabit radio to U.S. commercial customers. The PPC-10GE is an IP radio link operating at 70/80 GHz (E-Band), and supports QAM 256 modulation. Easy aggregation up to 4 × 10 Gbps (total 40 Gbps) is achievable. For further information, contact ELVA-1's U.S. business agent, Gilland Electronics, at elva@gilland.com.

ELVA-1
www.elva-1.com

SOURCES

OEM Signal Generator

VENDORVIEW

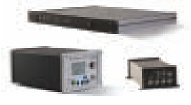

Berkeley Nucleonics released a user-customizeable OEM signal generator platform for RF/microwave systems requiring brand singularity or system integration. This platform leverages proven designs at 20 GHz and 26.5 GHz frequencies. The fast switching (FS) option for the 845 line of signal generators allows for extremely fast digital sweeps. In combination with the trigger system, FS equipped systems can generate very accurate and fast frequency and power ramps as fast as 10 µs or better.

Berkeley Nucleonics
www.berkeleynucleonics.com

7 to 12 GHz Surface-Mount Frequency Synthesizer

The HFS-12000-XA is a 7000 to 12000 MHz surface-mount frequency synthesizer designed as a high performance down-converter LO for RADAR digital signal processors. The design also features low phase noise (<-90 dBc/Hz @ 100 KHz offset) and fast switching capability (<750 µec, band-edge to band-edge) critical for signals intelligence applications.

EM Research
www.emresearch.com

RF Synthesizers/PLLs

The 8V97053 and 8V97053L RF synthesizers/PLLs offer an industry-leading combination of high performance, low spurious noise, low power consumption and wide tuning range. Ideal for applications such as GSM RF cards and instrumentation, these devices feature a VCO with a large tuning range capable of providing multiband LO frequency synthesis, limiting the need for multiple narrow band RF synthesizers/PLLs. The reduced BOM and design complexity help reduce costs of developing RF products.

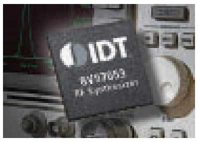

Integrated Device Technology
www.idt.com/go/RF-Synth

Phase Locked Ultra-Low Noise Synthesizer

Synergy Microwave Corp. introduced a series of ultra-low phase noise frequency synthesizers. Model KSS-LO238286-128 covers 2380 to 2860 MHz in 128 MHz step size and offers excellent phase noise of -90 dBc/Hz at 100 Hz offset and -133 dBc/Hz at 100 kHz offset. Step size and reference input options are available. These synthesizer models include SPI input programming inputs and lock alarm and are packaged in a 2.25" × 2.25" housing. Frequencies available to 30 GHz with an optional piggyback doubler.

Synergy Microwave Corp.
www.synergymwave.com

ANTENNAS

Circularly Polarized Omni Antennas

VENDORVIEW

Southwest Antennas introduced their new small form factor "Turbo Cloverleaf" family of circularly polarized (CP) Omni antennas in 1.98 to 2.2 GHz and 2.3 to 2.5 GHz frequencies. These new and innovative antenna products deliver substantial increases in high data rate throughput and signal-to-noise ratio (SNR) in a very compact, rugged radome that measures two inches or less on each side. Each antenna in the new family of products also features an integrated 3" RF coaxial gooseneck assembly with ruggedized, non-rotating RF connector options.

Southwest Antennas
www.southwestantennas.com

MICRO-ADS

New**Products**

TEST EQUIPMENT

RF Power Meter/Signal Generator

DS Instruments introduced an all-new version of the TT7000, a portable auto-calibrating RF power meter with integrated low phase-noise RF gignal generator and a full stand-alone interface. Full USB remote operation with simple serial commands. Power meter reaches 7 GHz and signal generator pushes past 9.5 GHz.

DS Instruments
www.dsinstruments.com

The EMxpert ERX+

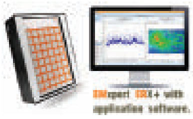

The EMxpert ERX+ has been the fastest high-resolution scanner in the market since its launch. Thanks to the relentless efforts of EMSCAN's R&D team, the EMxpert ERX+ is now 3 times faster than the earlier model. Now you can scan an area of 3 cells × 3 cells at level 7 (0.1 mm) in only 10 minutes.

EMSCAN
www.emscan.com

Digital Microscope

The IRIS DM-S7 is a revolutionary new high-performance digital microscope inspection system that allows image capturing without a computer. A 10.1" capacitive touch screen allows users to take pictures directly from the screen. The use of a digital microscopes is becoming essential as the components of the boards are becoming smaller, enabling the PCB to hold more components. This new digital microscope will improve quality and increase output efficiency.

Innovative Microscopes
www.innoscopes.com

Open-Architecture Semiconductor Test Solution

Marvin Test Solutions' new TS-960e is a flexible, open-architecture semiconductor test solution which offers PXI express performance and digital, mixed-signal and RF test capabilities in a compact, single-chassis footprint. ATEasy® test development/test executive software provides an easy-to-use integrated software environment to reduce development time. The TS-960e is now available with Keysight Technologies' comprehensive portfolio of PXIe RF instrumentation to address a range of RF applications including WLAN, Bluetooth, cellular, EW and RF transceivers.

Marvin Test Solutions
www.MarvinTest.com

Exceptional
Phase Noise Performance
Dielectric Resonator Oscillator

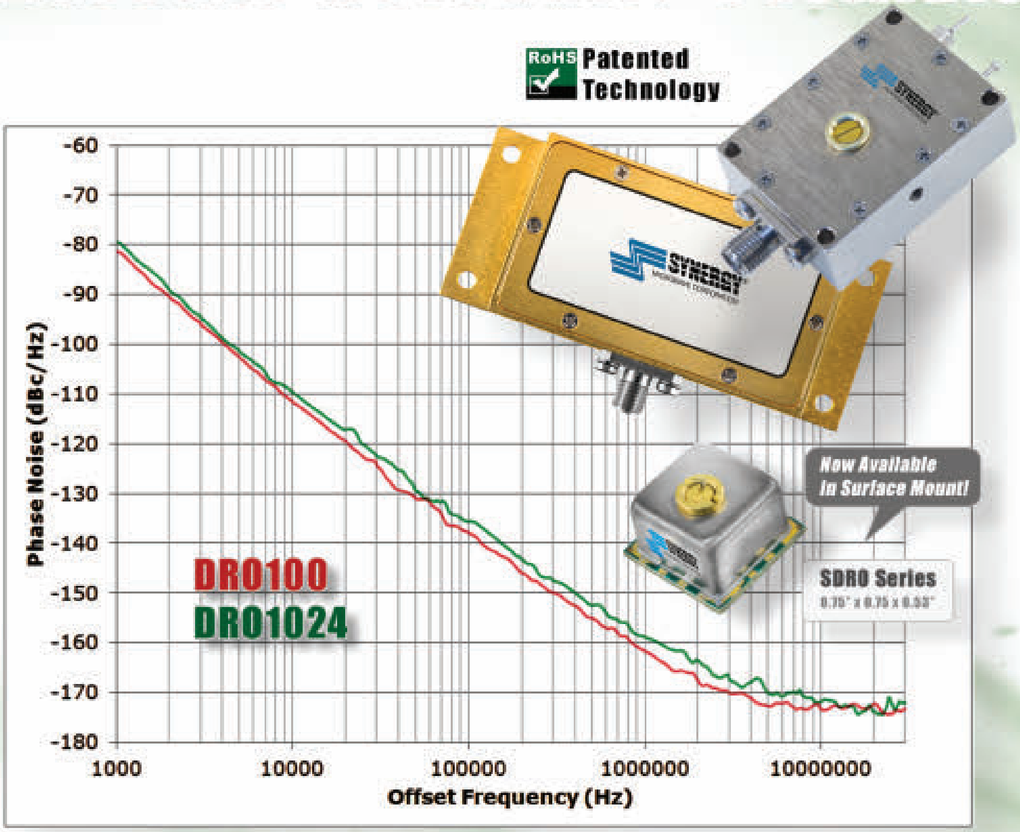

Model	Frequency (GHz)	Tuning Voltage (VDC)	DC Bias (VDC)	Typical Phase Noise @ 10 kHz (dBc/Hz)
Surface Mount Models				
SDRO1000-8	10	1 - 15	+8 @ 25 mA	-107
SDRO1024-8	10.24	1 - 15	+8 @ 25 mA	-111
SDRO1250-8	12.50	1 - 15	+8 @ 25 mA	-105
Connectorized Models				
DRO100	10	1 - 15	+7 - 10 @ 70 mA	-111
DRO1024	10.24	1 - 15	+7 - 10 @ 70 mA	-109

Model	Center Frequency (GHz)	Mechanical Tuning (MHz)	Supply Voltage (VDC / Current)	Typical Phase Noise @ 10 kHz (dBc/Hz)
Mechanical Tuning Connectorized Model				
KDRO145-15-411M	14.5	±4 MHz	7.5 V / 90 mA (Max.)	-88

Talk To Us About Your Custom Requirements.

SYNERGY® MICROWAVE CORPORATION

Phone: (973) 881-8800 | Fax: (973) 881-8361
E-mail: sales@synergymwave.com
Web: WWW.SYNERGYMWAVE.COM
Mail: 201 McLean Boulevard, Paterson, NJ 07504

IEEE MTT-S

IMS

Connecting Minds. Exchanging Ideas.

2017 INTERNATIONAL MICROWAVE SYMPOSIUM

4 – 9 JUNE 2017 HONOLULU, HAWAI'I

CALL FOR PAPERS

COME JOIN US IN HONOLULU AND ENJOY THE FLAGSHIP MICROWAVE THEORY AND TECHNIQUES SOCIETY (MTT-S) CONFERENCE IN THE ALOHA STATE OF HAWAI'I

PHOTO BY NEAL MIYAKE

The IEEE Microwave Theory and Techniques Society's 2017 International Microwave Symposium (IMS2017) will be held 4 - 9 June 2017 at the Hawai'i Convention Center in Honolulu, Hawai'i as the centerpiece of Microwave Week 2017. IMS2017 offers technical sessions, interactive forums, plenary and panel sessions, workshops, short courses, industrial exhibits, application seminars, historical exhibits, and a wide variety of other technical and social activities including a guest program. As usual, the Microwave Week 2017 technical program also comprises the RFIC Symposium (**www.rfic-ieee.org**) and the ARFTG Conference (**www.arftg.org**).

With over 8000 participants and 500 industrial exhibits of state-of-the-art microwave products, Microwave Week is the world's largest gathering of radio-frequency (RF) and microwave professionals and the most important forum for the latest research advances and practices in the field. IMS2017 offers something for everyone:

- The first-ever IMS Hackathon and IMS 3-Minute Presentation Competitions
- A 5G Summit showcasing next-generation wireless technologies
- An Executive Forum to discuss the latest in 5G and Internet of Things (IoT)
- RF Boot Camp – a three-quarter day course on RF/microwave basics
- The first-ever IMS Exhibitor Workshops for exhibitors to present the technology behind their products
- Networking events for Young Professionals and Women in Microwaves
- Student Design, Student Paper, Best Industry Paper, and Best Advanced Practice Paper Competitions
- Project Connect for under-represented minority engineering students, and the PhD Student Initiative for new PhD students
- *Teaching that inspires...students that aspire* – an exciting STEM program exposing middle school and select high school students, as well as their teachers, to RF/microwave technology

IMS2017 will include a comprehensive portfolio of events featuring recent 5G developments, including a plenary session, focus session, workshops, panel session, and a technology-development pavilion.

Paper Submission: Authors are invited to submit technical papers describing original work and/or advanced practices on RF, microwave, millimeter-wave, and terahertz (THz) theory and techniques. The deadline for submission is 5 December 2016. A double-blind review process will be used to ensure anonymity for both authors and reviewers. Detailed instructions on submitting a double-blind compliant paper can be found at **www.ims2017.org**. Papers will be evaluated on the basis of originality, content, clarity, and relevance to IMS.

Emerging Technical Areas: IMS2017 enthusiastically invites submission of papers that report state-of-the-art progress in technical areas that are outside the scope of those specifically listed in this Call for Papers, or that may be new to IMS, but are of interest to our attendees.

Workshops, Short Courses, Focus and Special Sessions, Panel and Rump Sessions: Topics being considered for these areas include Next-Generation Wireless Systems (5G and beyond), Internet of Space, Latest Technologies for RF/Microwave Measurements, and Advances in RFIC Technology. Please consult **www.ims2017.org** for a more detailed list of topics and instructions on how to prepare a proposal. Proposals must be received by 6 September 2016.

MicroApps and Exhibitor Workshops: The Microwave Application Seminars (MicroApps) serve as a forum for IMS exhibitors to present technology behind their commercial products and special capabilities. New for IMS2017 are Exhibitor Workshops, which offer IMS exhibitors a chance to present in-depth technical topics, via two-hour sessions, in a meeting room off the exhibit floor. Both presentation formats are open to all conference and exhibit attendees – MicroApps are free of charge and Exhibitor Workshops require a nominal fee. Please visit **www.ims2017.org** for details on submitting MicroApps and Exhibitor Workshop presentation ideas.

HAWAI'I 5G Catch the Wave!

Symposium Chairs
W. Shiroma (General Chair), K. Miyashiro (Co-Chair), V. Lubecke (Vice Chair)

Technical Program
O. Boric-Lubecke (Co-Chair), R. Miyamoto (Co-Chair), T. Itoh (Senior Advisor), A. Crahan (Administrator)

Electronic Paper Management
J. Hacker, M. DeLisio, S. Owens

Workshops and Short Courses
C. Hang, Y.-C. Shih, K. Leong, B. Wu, C. Song, L. Dunleavy, K. Hall, S. Kumar

Panel, Rump, Focus, and Special Sessions
C. Jackson, R. Kagiwada, A. Oki, T. LaRocca, Y. Wang, C. Rodenbeck

Interactive Forum
D. Bibb, G. C. Huang, R. Perron

Plenary Session and 5G Summit
V. Lubecke, D. Choudhury, T. LaRocca, D. Zuckerman

Technical Program Competitions
R. Gough, E. Yavari, X. Gao, A. Rahman, P. Orel, S. Rosenau, J. Bandler, E. Kiley

TPC At Large
J. Lin, H. Okazaki

Publicity, Promotions, and Publications
M. Watanabe, K. Kogasaka, J. Roque, A. Scacchitti

Website and Program Book
C. Brough, D. Goshi, M. Moorefield

Social Media
K. Cho, J. Hofer, M. Visitacion, J. Warner

Microwave Magazine
I. Mostafanezhad, A. Singh

Local Arrangements / Operations
J. M. Akagi, A. Noveloso, Z. Bardai, M. Tamamoto, J. T. Akagi, B. Lei, G. Uyeda, A. Ohta, A. Combs

Finance and Registration
D. Goshi, K. Leong, T. Fujishige, R. Alongi, N. Jordan

Student Volunteer Coordination
A. Morishita, J. Dang, T. Chun

Focus Groups
R. Pang, R. Iwami, B. Lei

Young Professionals
A. Zamora, K. Lu, W. Tonaki, T. Sharma, K. Allen

Women in Microwaves
C. Kitamura, J. Nakatsu, A. Pham, S. Yamada

STEM and Project Connect
C. Ishii, K. Matthews, D. Ah Yo, R. Mukai, A. Noveloso, K. Lau, G. Zhang

MicroApps and Exhibitor Workshops
J. Guzman-Vazquez, G. Uekawa, J. Weiler, B. Wu

Historical and University Exhibits
A. Combs, J. Hausner, J. Navarro, K. Sarabia

Global Ambassadors
K. Wu, D. Zimmerman

Conference and Exhibition Management
E. Vega, L. Wood, S. Horn, D. Waldron

Senior Advisors
T. Weller, S. Kanamaluru

UNITED STATES POSTAL SERVICE

Statement of Ownership, Management, and Circulation (All Periodicals Publications Except Requester Publications)

1. Publication Title: Microwave Journal	2. Publication Number: 3 9 6 - 2 5 0	3. Filing Date: September 30, 2016
4. Issue Frequency: Monthly	5. Number of Issues Published Annually: 12	6. Annual Subscription Price: Domestic: $120.00 Foreign: $200.00
7. Complete Mailing Address of Known Office of Publication (Not printer) (Street, city, county, state, and ZIP+4®): HORIZON HOUSE PUBLICATIONS, INC. 685 Canton Street Norwood, MA 02062-2610		Contact Person: Barbara Walsh Telephone: 781-769-9750 x2025

8. Complete Mailing Address of Headquarters or General Business Office of Publisher (Not printer)

same as above

9. Full Names and Complete Mailing Addresses of Publisher, Editor, and Managing Editor (Do not leave blank)

Publisher (Name and complete mailing address)

Carl S. Sheffres, Horizon House Publications, Inc., 685 Canton Street, Norwood, MA 02062-2610

Editor (Name and complete mailing address)

Patrick Hindle, Horizon House Publications, Inc., 685 Canton Street, Norwood, MA 02062-2610

Managing Editor (Name and complete mailing address)

Jennifer DiMarco, Horizon House Publications, Inc., 685 Canton Street, Norwood, MA 02062-2610

10. Owner (Do not leave blank. If the publication is owned by a corporation, give the name and address of the corporation immediately followed by the names and addresses of all stockholders owning or holding 1 percent or more of the total amount of stock. If not owned by a corporation, give the names and addresses of the individual owners. If owned by a partnership or other unincorporated firm, give its name and address as well as those of each individual owner. If the publication is published by a nonprofit organization, give its name and address.)

Full Name	Complete Mailing Address
Horizon House Publications, Inc.	685 Canton Street, Norwood, MA 02062-2610
William M. Bazzy, CEO	" " " " " " "
Ivar A. Bazzy, President	" " " " " " "
Jared M. Bazzy, Vice President	" " " " " " "
Joan B. Egan, EVP	" " " " " " "

11. Known Bondholders, Mortgagees, and Other Security Holders Owning or Holding 1 Percent or More of Total Amount of Bonds, Mortgages, or Other Securities. If none, check box ✓ None

Full Name	Complete Mailing Address

12. Tax Status (For completion by nonprofit organizations authorized to mail at special rates) (Check one)
The purpose, function, and nonprofit status of this organization and the exempt status for federal income tax purposes:
☑ Has Not Changed During Preceding 12 Months
☐ Has Changed During Preceding 12 Months (Publisher must submit explanation of change with this statement)

13. Publication Title: Microwave Journal		14. Issue Date for Circulation Data Below: YTD	September 30, 2016
15. Extent and Nature of Circulation: 50K		Average No. Copies Each Issue During Preceding 12 Months	No. Copies of Single Issue Published Nearest to Filing Date
a. Total Number of Copies (Net press run)		40,377	41,340
b. Paid Circulation (By Mail and Outside the Mail)	(1) Mailed Outside-County Paid Subscriptions Stated on PS Form 3541. (Include paid distribution above nominal rate, advertiser's proof copies, and exchange copies)	31,393	31,829
	(2) Mailed In-Country Paid Subscriptions Stated on PS Form 3541 (include paid distribution above nominal rate, advertiser's proof copies and exchange copies)	0	0
	(3) Paid Distribution Outside the Mails Including Sales Through Dealers and Carriers, Street Vendors, Counter Sales, and Other Paid Distribution Outside USPS®	5,265	5,567
	(4) Paid Distribution by Other Classes of Mail Through the USPS (e.g. First-Class Mail®)	0	0
c. Total Paid Distribution (Sum of 15b(1), (2), (3), and (4))		36,658	37,396
d. Free or Nominal Rate Distribution (By Mail and Outside the Mail)	(1) Free or Nominal Rate Outside-Country Copies included on PS Form 3541	790	794
	(2) Free or Nominal Rate In-Country Copies Included on PS Form 3541	0	0
	(3) Paid Distribution Outside the Mails Including Sales Through Dealers and Carriers, Street Vendors, Counter Sales, and Other Paid Distribution Outside USPS®	0	0
	(4) Free or Nominal Rate Distribution Outside the Mail (Carriers or other means)	2,739	3,132
e. Total Free or Nominal Rate Distribution (Sum of 15d (1), (2), (3) and (4))		3,530	3,926
f. Total Distribution (Sum of 15c and 15 e)		40,188	41,322
g. Copies not Distributed (See Instructions to Publishers #4 (page #3))		190	18
h. Total (Sum of 15f and g)		40,377	41,340
i. Percent Paid (15c divided by 15f times 100)		91.22%	90.50%

16. Publication of Statement of Ownership
✓ If the publication is a general publication, publication of this statement is required. Will be printed in the November, 2016 issue of this publication. ☐ Publication not required.

17. Signature and Title of Editor, Publisher, Business Manager, or Owner	Date
Carl S. Sheffres, Publisher	September 30, 2016

I certify that all information furnished on this form is true and complete. I understand that anyone who furnishes false or misleading information on this form or who omits material or information requested on the form may be subject to criminal sanctions (including fines and imprisonment) and/or civil sanctions (including civil penalties).

PS Form 3526, September 2007 (Page 2 of 3)

BookEnd

On-Wafer Microwave Measurements and De-Embedding

Errikos Lourandakis

On-wafer RF measurements are central to the RF/microwave semiconductor industry, from model development to IC design and, in many cases, IC production. "On-Wafer Microwave Measurements and De-Embedding" is a comprehensive treatment of making on-wafer measurements and processing the raw data to extract device performance from the measurement artifacts.

With any discussion of a narrow technical topic, the author must decide whether to assume prior knowledge of the broader technical landscape. In this case, Errikos Lourandakis chose to make the book readable to those with no prior knowledge of RF/microwave theory. Before delving into the intended subject, he briefly discusses AC signals, the electromagnetic spectrum and frequency and time domain analysis.

The focus of the book begins with on-wafer measurement equipment, including open, short, thru and load calibration standards. A chapter is devoted to network analyzer basics and calibration, including error models and on-wafer calibration methods. Subsequent chapters cover de-embedding methods applied to passive silicon devices and CMOS circuits. Three appendices provide additional reference material on network theory (e.g., S-, T-, Y- and Z-parameters); even/odd mode analysis; and MATLAB code for various de-embedding algorithms, as well as code for calculating inductor, capacitor and transmission line metrics. Written for "hands on" engineers, the information is concise and practical. Ample references are provided at the end of each chapter, should the reader wish to probe deeper.

Lourandakis is a senior engineer at Helic Inc., where he works on modeling high frequency electromagnetic phenomena and developing electronic design automation tools for silicon devices. He is an "expert user" of Helic's 70 GHz silicon characterization laboratory and manages the physical characterization of silicon devices and circuits. He received a Ph.D. from the Institute for Electronics Engineering in Erlanger, Germany.

To order this book, contact:

Artech House
www.artechhouse.com
ISBN-13: 978-1-63081-056-6
240 pages
$169
Available in hardcover and eBook formats

Advertising**Index**

Advertisers in blue are enabled with the layar app

Sales Representatives

Microwave Journal
Frequency Matters.

Eastern and Central Time Zones
Chuck Boyd
Northeast Reg. Sales Mgr.
(New England, New York, Eastern Canada)
685 Canton Street
Norwood, MA 02062
Tel: (781) 619-1942
FAX: (781) 769-5037
cboyd@mwjournal.com

Michael Hallman
Eastern Reg. Sales Mgr.
(NJ, Mid-Atlantic, Southeast, Midwest, TX)
4 Valley View Court
Middletown, MD 21769
Tel: (301) 371-8830
FAX: (301) 371-8832
mhallman@mwjournal.com

Pacific and Mountain Time Zones
Brian Landy
Western Reg. Sales Mgr.
(CA, AZ, OR, WA, ID, NV, UT, NM, CO, WY, MT, ND, SD, NE & Western Canada)
144 Segre Place
Santa Cruz, CA 95060
Tel: (831) 426-4143
FAX: (831) 515-5444
blandy@mwjournal.com

International Sales
Richard Vaughan
International Sales Manager
16 Sussex Street
London SW1V 4RW, England
Tel: +44 207 596 8742
FAX: +44 207 596 8749
rvaughan@horizonhouse.co.uk

Germany, Austria, and Switzerland (German-speaking)
WMS.Werbe- und Media Service
Brigitte Beranek
Gerhart-Hauptmann-Street 33,
D-72574 Bad Urach
Germany
Tel: +49 7125 407 31 18
FAX: +49 7125 407 31 08
bberanek@horizonhouse.com

Korea
Young-Seoh Chinn
JES Media International
2nd Floor, ANA Bldg.
257-1, Myungil-Dong
Kangdong-Gu
Seoul, 134-070 Korea
Tel: +82 2 481-3411
FAX: +82 2 481-3414
yschinn@horizonhouse.com

China
Shenzhen
Michael Tsui
ACT International
Tel: 86-755-25988571
FAX: 86-10-58607751
michaelt@actintl.com.hk

Shanghai
Linda Li
ACT International
Tel: 86-21-62511200
lindal@actintl.com.hk

Beijing
Cecily Bian
ACT International
Tel: +86 135 5262 1310
cecilyb@actintl.com.hk

Hong Kong, Taiwan, Singapore
Mark Mak
ACT International
Tel: 852-28386298
markm@actintl.com.hk

Japan
Katsuhiro Ishii
Ace Media Service Inc.
12-6, 4-Chome,
Nishiiko, Adachi-Ku
Tokyo 121-0824, Japan
Tel: +81 3 5691 3335
FAX: +81 3 5691 3336
amskatsu@dream.com

Ed Kiessling Traffic Manager/Inside Sales • 685 Canton Street Norwood, MA 02062 • Tel: (781) 619-1963 FAX: (781) 769-6178 • ekiessling@mwjournal.com

ULTRA-REL™ CERAMIC MMIC AMPLIFIERS

10 MHz to 7 GHz

Low NF from 0.5 dB   *High IP3 up to +42 dBm*   *Low DC current 65 mA*   from $7.45 ea. (qty 20)

When failure is not an option! Our CMA family of ceramic MMIC amplifiers is expanding to meet your needs for more critical applications. Designed into a nitrogen-filled, hermetic LTCC package just 0.045" high, these rugged models have been qualified and are capable of meeting MIL standards for a whole battery of harsh environmental conditions:

Qualified for: *(see website for complete list and details)*

Gross and Fine Leak	*HTOL (1700 hours @ +105°C)*
Mechanical Shock	*Steam Aging*
Vibration	*Solder Heat Resistance*
Acceleration	*Autoclave*
PIND	*And More!*

**Gross leak only*

Robust performance across wide bandwidths makes them ideal for military and defense applications, hi-rel instrumentation, and anywhere long-term reliability adds bottom-line value. Go to minicircuits.com for all the details today, and have them in your hands as soon as tomorrow!

Electrical Specifications *(-55 to +105°C)*

3 x 3 x 1.14 mm

Model	Freq. (GHz)	Gain (dB)	P_{OUT} (dBm)	IP3 (dBm)	NF (dB)	DC (V)	Price $ ea. (qty 20)
CMA-81+	DC-6	10	19.5	38	7.5	5	8.95
CMA-82+	DC-7	15	20	42	6.8	5	8.95
CMA-84+	DC-7	24	21	38	5.5	5	8.95
CMA-62+	0.01-6	15	19	33	5	5	7.45
CMA-63+	0.01-6	20	18	32	4	5	7.45
CMA-545+	0.05-6	15	20	37	1	3	7.45
CMA-5043+	0.05-4	18	20	33	0.8	5	7.45
CMA-545G1+	0.4-2.2	32	23	36	0.9	5	7.95
CMA-162LN+	0.7-1.6	23	19	30	0.5	4	7.45
CMA-252LN+	1.5-2.5	17	18	30	1	4	7.45

RoHS compliant

Mini-Circuits®

www.minicircuits.com   P.O. Box 350166, Brooklyn, NY 11235-0003   (718) 934-4500   sales@minicircuits.com

FABS and LABS

Wireless Innovation Tackles Problems, Forges Partnerships – Even Bumblebees

Photo credit to Matthew Burgos / WPI.

Before you can pronounce his name, Alexander Wyglinski has introduced himself and is showing us around. Words streaming in a New York minute, he is totally engaged, gesturing, writing on the white board, smiling, laughing, enthusiasm bubbling. Wyglinski (pronounced: wig-lin-skee) is the director — father — of the Wireless Innovation Laboratory at Worcester Polytechnic Institute, or WPI, as the locals call it.

The WI Lab was born with Wyglinski's arrival at WPI during the summer of 2007. He was recruited to set up a research facility focusing on wireless communication systems. Wyglinski says the lab's mission is "to advance the current state-of-the-art in wireless communication, coming up with practical solutions to technological challenges that are facing the wireless sector and society in general." The WI Lab chooses high-risk projects with a five-year horizon, fundamental and applied research across a range of wireless applications: wireless communication systems engineering, cognitive and software defined radio, satellite communication, electromagnetic spectrum security and connected vehicles. Mirroring WPI's project-oriented curriculum, the lab's projects are "hands on"— meaning they build and test lots of prototype hardware. The lab typically has five externally-sponsored projects underway, keeping six to seven Ph.D., one or two master's and about 10 undergraduate students busy.

The list of company and government labs sponsoring WI Lab projects is impressive: Analog Devices, MathWorks, MITRE, Raytheon, Toyota, the Air Force Research Laboratory (AFRL), National Science Foundation (NSF), Naval Research Laboratory (NRL) and the Office of Naval Research (ONR). Such collaboration is symbiotic: enabling meaningful research that neither company nor WPI can do alone, extending the R&D horizon beyond what most quarterly-driven companies can tackle, providing research for advanced degrees and identifying future technical talent for the sponsoring organizations.

One of Wyglinski's keen interests is autonomous driving. He can talk at length about the technical, regulatory and human factors challenges to be solved — no surprise that he's the president-elect of the IEEE Vehicular Technology Society. In one of WPI's labs, students work on a golf cart outfitted with the various subsystems required for autonomous driving. It's definitely a prototype, with a mix of wires, circuit boards and computer monitor juxtaposed with the seats and frame.

Reading about research in WPI's biology and biotechnology department, Wyglinski wondered whether vehicle-to-vehicle (V2V) communication could learn from bumblebees. How bumblebees collect information and make decisions is analogous to a cognitive radio. In a highway of autonomous vehicles, each will need to quickly identify the most reliable and low latency communications channel. Seeing if bumblebees can help solve that cognitive radio challenge led to collaboration with two biology professors, supported by three Ph.D. candidates and a $300,000 NSF grant. We'll likely never know what's buried in the code of the autonomous vehicles our children or grandchildren will ride in; however, it may bear the legacy of WPI's bumblebees.

Wyglinski says "nine of 10 ideas don't pan out, yet you have to pursue them all to yield the one success." His enthusiasm is undiminished.

http://ecewp.ece.wpi.edu/wordpress/wireless/

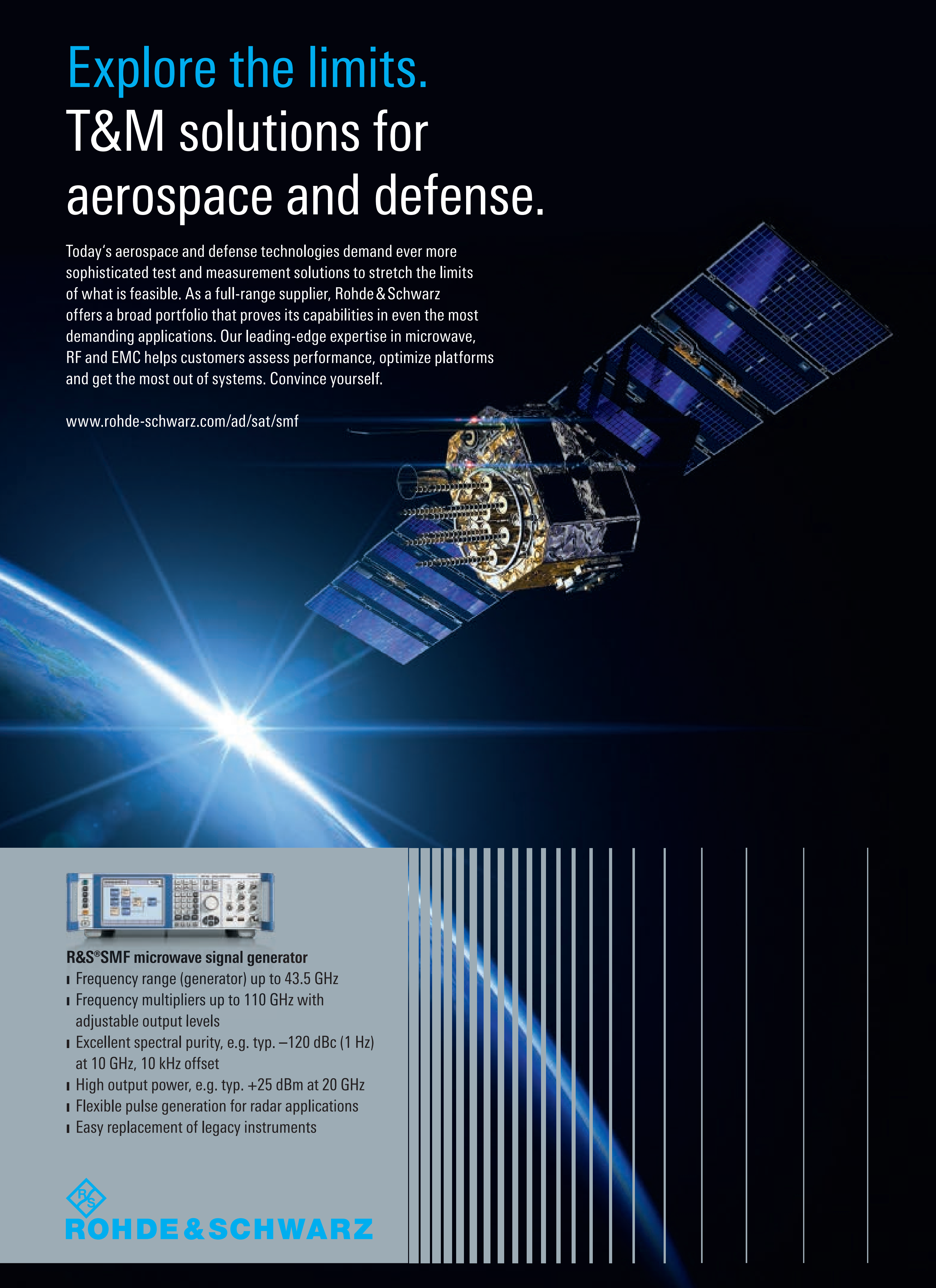
Explore the limits.
T&M solutions for aerospace and defense.
Today's aerospace and defense technologies demand ever more sophisticated test and measurement solutions to stretch the limits of what is feasible. As a full-range supplier, Rohde & Schwarz offers a broad portfolio that proves its capabilities in even the most demanding applications. Our leading-edge expertise in microwave, RF and EMC helps customers assess performance, optimize platforms and get the most out of systems. Convince yourself.
www.rohde-schwarz.com/ad/sat/smf
R&S®SMF microwave signal generator
Frequency range (generator) up to 43.5 GHz
Frequency multipliers up to 110 GHz with adjustable output levels
Excellent spectral purity, e.g. typ. –120 dBc (1 Hz) at 10 GHz, 10 kHz offset
High output power, e.g. typ. +25 dBm at 20 GHz
Flexible pulse generation for radar applications
Easy replacement of legacy instruments
ROHDE&SCHWARZ

WERLATONE®

We Are High Power

Absorptive Filters

Werlatone Absorptive Filters are NON-Reflective!

Out-of-Band Signals are NOT reflected back to the source.

- Out-of-Band signals are **internally terminated.**
- Electrical Specifications are less susceptible to temperature change.
- Reduces the dependency of the system on the length of interconnecting cable between two non-perfect components.

Model AF9350

Werlatone Absorptive Filters Eliminate:

- Instability of power amplifiers at out-of-band frequencies.
- Excessive In-Band ripples due to out-of-band reflected energies.
- False trigger of power detector circuitry due to reflected harmonics.
- Potential damage to power amplifiers due to reflection of high power out-of-band energies.

Model AF10200

Low Pass Absorptive Filters

Model	Frequency (MHz) Pass Band	Frequency (MHz) Stop Band	Power (W CW) Pass Band	Power (W CW) Stop Band	Insertion Loss(dB) Pass Band	Rejection(dB) Stop Band	VSWR Pass Band	VSWR Stop Band	Size (Inches)
AF10200	0-2.5	4.5-30	500	150	0.5	45	1.30:1	1.60:1	12 x 5.6 x 3.25
AF10201	0-4.2	7.5-50	500	150	0.5	45	1.30:1	1.60:1	12 x 5.6 x 3.25
AF10202	0-7	12.6-100	500	150	0.5	45	1.30:1	1.60:1	12 x 5.6 x 3.25
AF10203	0-12	21-150	500	150	0.5	45	1.30:1	1.60:1	12 x 5.6 x 3.25
AF10204	0-19	34-200	500	150	0.5	45	1.30:1	1.60:1	12 x 5.6 x 3.25
AF10205	0-30	57-250	500	150	0.5	45	1.30:1	1.60:1	12 x 5.6 x 3.25
AF10502	0-2.5	4.5-25	1,500	400	0.5	45	1.30:1	1.60:1	15 x 6.1 x 3.5
AF10503	0.-4.1	7.4-41	1,500	400	0.5	45	1.30:1	1.60:1	15 x 6.1 x 3.5
AF10504	0-6.7	12.1-67	1,500	400	0.5	45	1.30:1	1.60:1	15 x 6.1 x 3.5
AF10505	0-11	19.8-110	1,500	400	0.5	45	1.30:1	1.60:1	15 x 6.1 x 3.5
AF10506	0-18	32-180	1,500	400	0.5	45	1.30:1	1.60:1	15 x 4.6 x 3.5
AF10507	0-30	54-300	1,500	400	0.5	45	1.30:1	1.60:1	15 x 4.6 x 3.5
AF9438	1-30	50-380	5,000	250	0.5	45	1.30:1	1.60:1	20 x 16.9 x 3.5
AF9349	10-150	270-1500	500	25	0.4	50	1.35:1	1.60:1	4.5 x 1.75 x 1.1
AF9187	10-490	850-3000	100	10	0.5	45	1.40:1	1.90:1	2.5 x 1.3 x 1
AF9350	10-500	750-3000	400	25	0.5	45	1.25:1	1.60:1	4.2 x 1.75 x 1.1
AF9960	10-500	750-3000	600	25	0.5	45	1.25:1	1.60:1	4.2 x 1.75 x 1.1
AF9680	10-520	1040-3000	160	10	0.6	60	1.25:1	1.60:1	4.2 x 1.75 x 1.1
AF9313	10-870	1700-4000	100	10	0.6	53	1.30:1	1.60:1	2.5 x 1.3 x 1

5G & IoT
2016

A SPECIAL SUPPLEMENT TO

Microwave Journal

5G & IoT

Table of Contents

AUGMENTED REALITY: HOW IT WORKS

STEP 1
Download the free Layar app from the iTunes (iOS) or Google Play (Android) store.

STEP 2
Launch the app to view enhanced content on any page with the layar logo.

STEP 3
Frame the entire page in the screen and tap to experience enhancements (tap screen again for full screen view).

Look for the Layar logo on participating pages. AR pages may expire after 30 days.

Staff

Publisher: Carl Sheffres
Editor: Patrick Hindle
Technical Editor: Gary Lerude
Managing Editor: Jennifer DiMarco
Associate Technical Editor: Cliff Drubin
Multimedia Staff Editor: Leslie Nikou
Multimedia Staff Editor: Barbara Walsh
Contributing Editor: Janine Love
Consulting Editor: Harlan Howe, Jr.
Consulting Editor: Frank Bashore
Consulting Editor: Raymond Pengelly

Electronic Marketing Manager: Chris Stanfa
Digital Content Production Specialist: Lauren Tully
Audience Development Manager: Carol Spach
Traffic Manager: Edward Kiessling
Director of Production & Distribution: Robert Bass
Art Director: Janice Levenson
Graphic Designer: Sachiko Stiglitz

EUROPE
International Editor: Richard Mumford
Office Manager: Nina Plesu

CORPORATE STAFF
CEO: William M. Bazzy
President: Ivar Bazzy
Vice President: Jared Bazzy

INVITED PAPER

Fingertip Gesture Control Interface for 'Invisible' Devices

Suresh Ram and Jagjit Singh Bal
Infineon Technologies, Milpitas, Calif.

In the last decade, automotive sensor systems emerged as the largest single market for compact radar systems. Standardization of frequencies and the economics of chip-scale production made the technology practical in mid-range and long-range sensor applications, resulting in market adoption at a pace approaching annual volume of tens of millions of chipsets. Now, recently developed single-chip radar that meets size and performance thresholds needed for a much wider range of consumer electronics devices is set to trigger an exponential increase in the use of radar.

A key driver for this growth is the rapid evolution of the Internet of Things (IoT). By the end of this decade, we will be surrounded by IoT devices. Many will be sensors that operate with no human intervention. Yet many others will be designed for interaction with users. These new types of devices, beginning with wearables, require a new type of user interaction. One of the most exciting new interaction methods is gesture control.

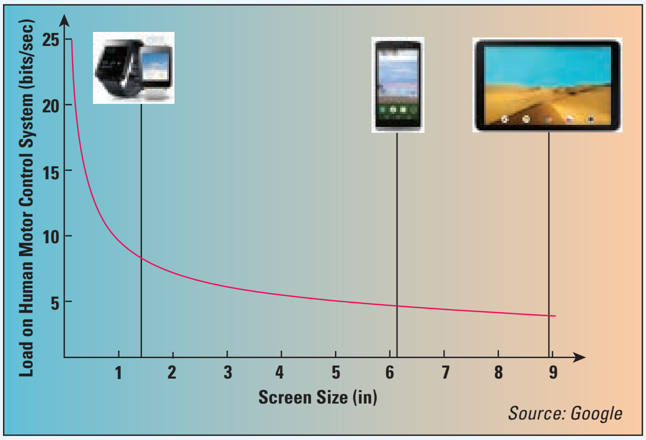

▲ *Fig. 1 Touch interaction challenges vary with screen size. Source: From Soli Team at Google ATAP.*

For wearable electronics, such as smartwatches, use of conventional physical controls and/or interaction on a tiny screen interface is a detriment to the user experience. Precise control of tiny devices using even a simple graphic interface or set of physical controls is difficult to achieve without dedicating a large part of the available surface of the device to the interface. Interaction is increasingly challenging as devices get smaller in size and the available real estate for a touch display screen shrinks.

As shown in ***Figure 1***, researchers at Google's Advanced Technology and Projects (ATAP) Group demonstrated that the load on the human motor control system increases exponentially when screen sizes smaller than 2"× 2". As a result, gestures are becoming relevant to human-machine interaction as a replacement or addition to touch screens and voice control. A gesture interface is very well suited to wearable electronics with limited real estate for controls. It also allows control in high ambient noise environments where voice may be ineffective. When the scope of applications is expanded from wearables to the types of 'invisible' sense and control systems envisioned for the IoT, the value of a gesture-based interface is amplified.

The technologies available to implement gesture control include capacitive, visible and infrared light, ultrasonic and radar. While each is useful for specific applications, radar-based human-machine interaction may prove to be the most flexible and widely deployed. Capaci-

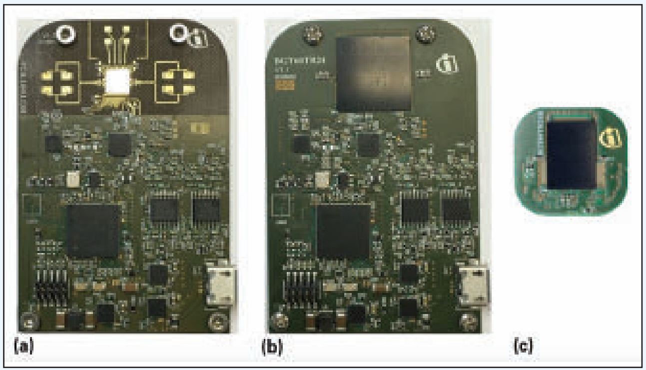

▲ *Fig. 2 Infineon reference designs for different BGT60TR24: first generation with bare die (a) second generation in a 14 mm × 14 mm² package (b) third generation in a smaller 9 mm × 12.5 mm² package (c).*

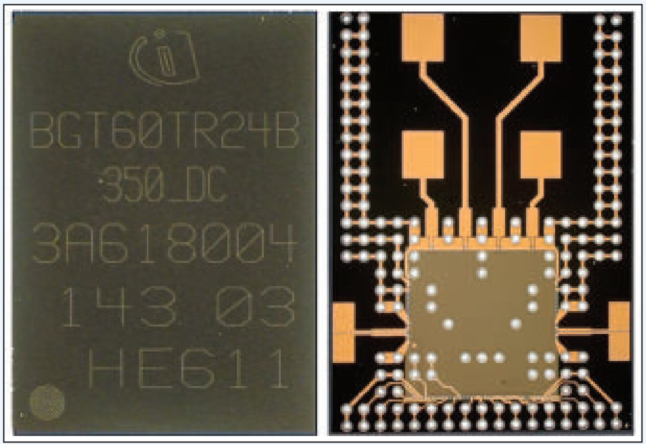

▲ *Fig. 3 Infineon's Soli chipset BGT60TR24B (top and bottom views).*

tive sensing is short range, while light and sound-based sensors are sensitive to environmental conditions like noise, rain, wind and temperature changes. These types of sensors also cannot be mounted invisibly and tend to introduce constraints for the industrial design of the end product. Finally, each of these alternatives has limited flexibility in terms of directional capability and distance measurement.

Millimeter wave (mmWave) radar's capabilities as a sensor for gesture control applications overcome these limitations. It can operate in all lighting conditions, can transmit through many materials (e.g., polycarbonate) and is resistant to moisture, dirt and temperature variations that limit infrared, ultrasonic and laser-based sensor systems.

When compared to microwave frequency bands, a V-Band (57 to 64 GHz) sensor has several additional advantages. One of them is the range resolution, i.e., the ability of the radar sensor to distinguish two closely spaced targets as separate targets. There is 7 GHz bandwidth available in the unlicensed V-Band, which theoretically results in range resolution of 2 cm.

This can be extended to sub-millimeter scale resolution using advanced signal processing techniques. At mmWave frequencies the wavelength (5 mm at 60 GHz) is small enough to allow easy integration of multiple antennas in a package. A mmWave sensor also has better Doppler sensitivity, as the Doppler shift caused by a moving object is proportional to the operating frequency of the sensor. In the 57 to 64 GHz band, the corresponding Doppler shift is comparatively easier to detect and process than microwave bands. This eases detection of slow moving objects. Another advantage of a mmWave sensor is that the path loss at these frequencies is very high (1m = 68 dB @ 60 GHz). As the signal suffers large attenuation, it does not cause interference with other systems operating nearby.

The combined advantages of mmWave technology led the Google ATAP researchers to partner with Infineon on a project to engineer a radar sensing system with the size, power consumption and resolution needed for gesture control applications in consumer electronics products. The combination of Infineon's two decades of experience in high-frequency RF technology and the cross-functional expertise at ATAP contributed to a remarkably fast development process for the Alpha DevKit.

FROM CONCEPT TO SINGLE-CHIP

Beginning with a benchtop concept in July 2014, a collaborative engineering team developed a series of hardware prototypes, iterating through designs using off-the-shelf, multi-chip radar components and ultimately producing a proof of concept IC. Demonstrated for the first time in May 2015, this single-chip radar and associated system components were released on a limited basis as the Soli Alpha Development Kit to developers for concept application development.

In the Soli Alpha development kit, the Soli radar chipset is paired with Google-developed algorithms for signal processing and a gesture library for developers that runs on an application processor. The sensor software abstracts signals in real-time and analyzes the signals at up to 10,000 fps to precisely determine position and motion and ultimately recognize gestures. Most of the gestures are designed so that haptic feedback is provided by the sensation of fingers moving against each other, which makes each gesture feel natural and responsive. The sensitivity of the Soli radar allows recognition of overlapping fingers and gestures in a 3D space. The radar has sub-millimeter resolution allowing the recognition of a range of gestures from large sweeping hand motions to micro gestures. This common language helps developers to quickly implement system designs and will let users learn to interact with Soli-powered devices in an easy-to-learn and consistent way.

The device still required a standalone PC to process the data gathered by the sensor and drew 1.2 W in operating mode. Also this early iteration of the device was a bare-die that required special PCB material to have low losses at 60 GHz, involved a lot of design effort for the on-board antennas, required wire-bonding for assembly and had a larger form factor.

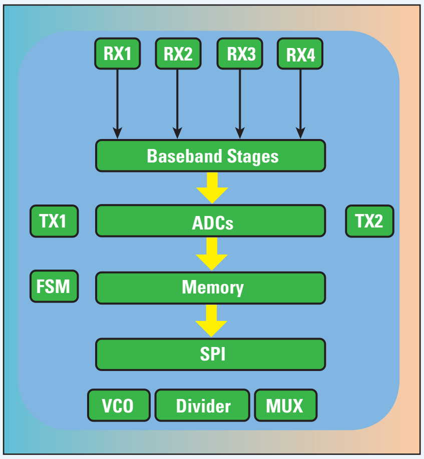

▲ *Fig. 4 BGT60TR24B block diagram.*

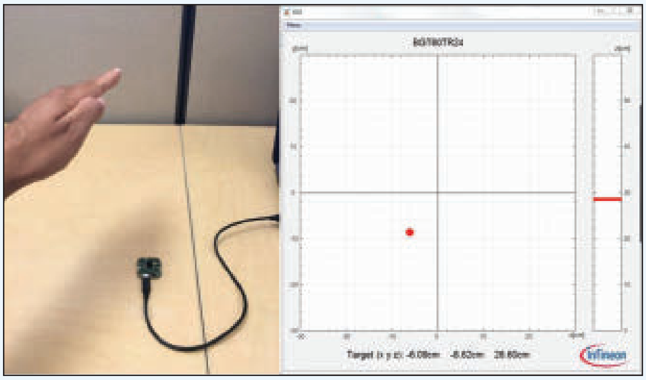

▲ *Fig. 5 GUI view showing the location of the hand in XYZ coordinates.*

So the team continued its work to reduce power requirements and size while enhancing system integration, as shown in ***Figure 2***.

The result of this effort is integrating Soli, a new sensing technology, into one of the world's smallest radars to detect touchless gesture interactions. The chip, shown in ***Figure 3***, and its corresponding software suite bring precise gesture control capability to consumer electronic products. Fabricated in Infineon's BiCMOS process, the highly integrated chipset contains the complete RF front-end, baseband and ADCs, as well as memory, state machine and a programmable serial interface for communication with any application processor, as shown in ***Figure 4***. The high level of integration, small form factor and overall efficiency of the BGT60TR24B ensure that it can fit into space constrained devices, for example a wearable band.

BGT60TR24B has effective isotropic radiated power (EIRP) of up to 10 dBm. The output power level can be varied by the integrated VGA in the transmit chain. As per the FCC rules, 10 dBm EIRP is the maximum allowable power limit for a field disturbance sensor covering the 57 to 64 GHz bandwidth. Recently the FCC[1] also made amendments to Section 15.255 of its rules that would allow for the field disturbance sensors to operate over an even wider bandwidth (57 to 71 GHz).

Phase noise of the integrated VCO has a major impact on the sensing system. In a Frequency Modulated Continuous Wave (FMCW) system the targets are detected at a certain offset from the carrier frequency. As the received signal level from a far-off target has low level, it could be masked by the phase noise of the carrier and may not be detected. This is more likely if the target is far away and has low radar cross section, such as a human body or hand. With its phase noise of -80 dBc/Hz @ 100 kHz offset, the Soli radar chip improves the system SNR to allow detection of farther away targets.

In FMCW systems, the range to the target is proportional to the difference in frequency between the received and emitted signal, which is referred to as the beat frequency. This is typically a couple of MHz depending on modulation parameters and target range. The lower flicker noise corner of BGT60TR24B ensures that the beat frequencies from the target of interest are not degraded by the flicker noise.

The single chip radar also can easily interface via standard SPI to the existing processor inside the device. The fast SPI of the sensor enables raw data from the sensor to be fed to the signal processing pipeline running on the processor at the very high frame rate necessary for the end application to achieve real time-like performance.

The BGT60TR24B is housed in an embedded Wafer Level Ball (eWLB) Grid array package with ball pitch of 500 μm and can be mounted on a standard low cost FR4 PCB. The packaged IC has dimensions of 9 mm × 12.5 mm × 0.8 mm. It has two transmit channels; four receive channels and corresponding antennas to detect objects and motions up to 10 m distant. The four RX antennas are placed in 2×2 array to minimize grating lobes. The RX channels can be used to implement digital beam forming for tracking the objects in both the azimuth and elevation planes. The chip is designed with the flexibility to enable and disable several integrated blocks. For example, in application scenarios where only one receive channel is sufficient to detect a target the others can be turned off in order to extend battery life of the device.

The chipset also has an idle mode in which most of the integrated blocks are switched off. This mode is especially useful in cases when the sensing application running on the device is not used frequently. The complete radar system uses a 1.8 V power supply and draws 0.054 W in sensing mode. This low power consumption and thermal dissipation makes the integration of radar sensors into wearable devices practical, while assuring a comfortable end-user experience of the device. In addition to wearables, the integration and flexibility of the solution allows for cost effective implementation in a wide range of applications like gaming, virtual reality and mobile devices.

OPERATING PRINCIPLES

Infineon produced its first single-chip radar system, a 24 GHz device integrating a single transmit and two receive channels in a 4.5 mm × 5.5 mm footprint, in early 2014[2]. The Soli chip applies this experience in a higher frequency, high bandwidth, high integration and low power consumption device, and the underlying signal processing and analysis algorithms are tightly linked to the unique characteristics of the hardware.

Antenna design, in particular, plays an important role for effective transmit and receive when the entire array is contained within the confines of the 9 mm × 12.5 mm × 0.8 mm package. The antennas integrated in package cover the complete 57 to 64 GHz bandwidth in order to achieve higher range resolution. The 2×2 RX antennas have gain of 10 dBi and half power beam width (HPBW) is 42° × 45° (E- and H- Plane). The TX antennas have gain of approximately 5 dBi and HPBW is 90° × 65°.

The wider beam width of the transmit antennas ensure that the entire scene in front of the sensor is captured for the signal processing pipeline. The spatial arrangement of two transmit and four receive antennas allows the sensor to precisely scan a 3D area in its field of view. As an example ***Figure 5*** shows a GUI which displays the position of hand in front of sensor in XYZ coordinates. Also, the integration of all antennas in the package makes it easier for developers to design a low-cost PCB as there is no need to route 60 GHz signals on the PCB.

A typical sensor system implementation comprises the blocks shown in ***Figure 6***.

The BGT60TR24B radar chipset handles the RF signals and provides

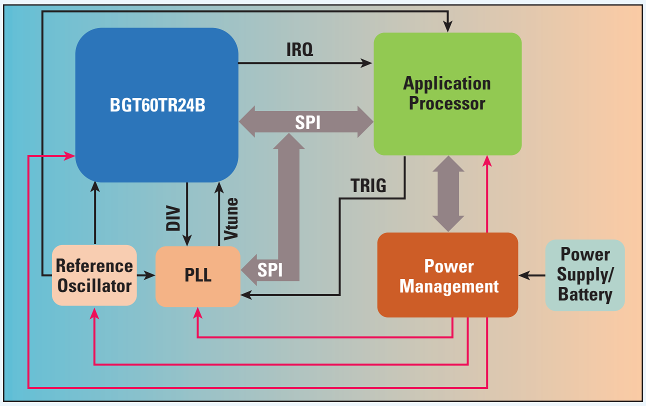

▲ *Fig. 6 Typical implementation of a BGT60TR24B-based sensing system.*

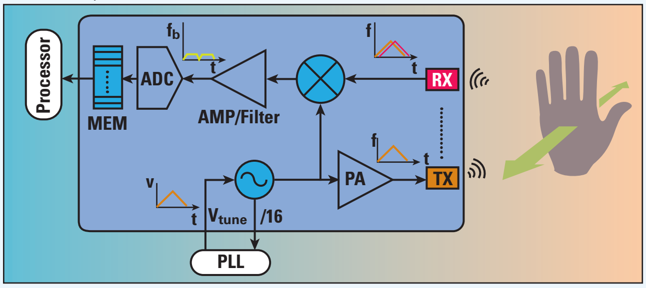

▲ *Fig. 7 FMCW ramp generation using an external PLL and digital data capture with the processor.*

the digitized data to the processor via a digital interface; the application processor gets digitized data from the sensor, processes it and then runs the user application; the PLL locks the carrier of the BGT60TR24B to provide a highly linear FMCW modulated signal; the reference oscillator provides the clock to the chipset and the PLL; and the power management IC provides the required supply voltages to different blocks.

The BGT60TR24B sensor transmits a FMCW signal from 57 to 64 GHz on one of the transmit channels. In order to obtain highly accurate range and velocity information from the target it is required that the FMCW ramp has high linearity over the complete frequency sweep. If this is not the case the beat frequency corresponding to the target will drift, resulting in reduced accuracy of the measurements. On the system evaluation board, a highly linear FMCW sweep is generated by locking the carrier with an external PLL. The BGT60TR24B has an internal divide-by-16-circuit that provides a low frequency (4 GHz @ 64 GHz) signal at its divider output to connect to the external PLL. The transmitted FMCW signal hits the target and a part of it is reflected back to the four receiving antennas of the BGT60TR24B as shown in ***Figure 7***.

The receive channels down-convert the reflected signals to the IF frequency. The frequency of the IF signal corresponds to the distance of the target from the sensor and the modulation parameters, i.e., bandwidth of the transmitted signal and ramp duration of the FMCW chirp. The IF signal passes through filtering and baseband amplification stages in order to have sufficient drive level for the following ADC stage. The gain of the baseband stages can be controlled via the digital interface. The frequency of the IF signal can vary up to MHz range, so the baseband filtering and the ADC sampling rate needs to be adjusted for the application of interest.

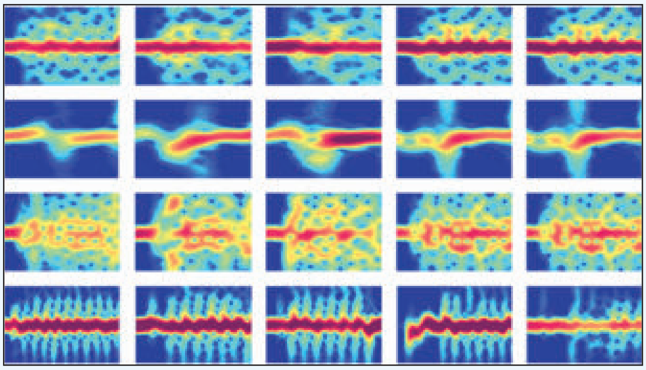

▲ *Fig. 8 Sensor data showing four gestures by five users. Source: From Soli Team at Google ATAP.*

▲ *Fig. 9 Future human-machine interaction enabled by gesture sensing technology.*

The ADCs digitize the IF signal at the set sampling rate and the resulting data is stored in the internal memory of the chipset. The memory is accessed by the external application processor via the digital interface. The application processor is the master controller, which triggers the FMCW ramp and ADC sampling and then captures the raw data when it is available in the memory of the sensor. The amplitude, frequency and phase of the reflected signal contain information about the size, distance, velocity, direction of movement and angular location of the target with respect to the sensor. The application processor runs software and algorithms to extract all target information by analyzing changes in the received signal over time. Based on variations in temporal signal, the system is able to differentiate both deformation in hand shapes and complex finger movements, which are incorporated into a control gesture library.

The gesture recognition pipeline abstracts data from the raw signal through proprietary transformations to determine position and motion data for analysis by image and gesture recognition libraries. A sample of typical data is shown in ***Figure 8***. Most of the defined gestures generate a haptic sensation as a result of finger touch which is a clear advantage over gesture sensing systems like cameras. The consideration of haptic feedback while defining the gesture library results in both the fluidity and precision of natural motions.

In addition to efficacy of the sensor system, the unplugged nature of wearables and many potential IoT applications makes low power operation critical for the single chip radar. Every functional block of the IC is designed to power down outside of its specific duty cycle. Wake-up

(**Fingertip Gesture**, *Continued on page 18*)


Higher. Wider. Faster.
Test solutions for 5G.
The next major step beyond LTE/LTE-Advanced (4G) sets challenging requirements. Rohde & Schwarz is a world leader in all areas of RF and microwave test and measurement equipment. As a technology expert, we have been actively involved in mobile communications since the first generation. We are committed to supporting the wireless communications industry with the solutions needed to investigate, develop and standardize 5G.
Check out our test solutions at www.rohde-schwarz.com/ad/5G
ROHDE&SCHWARZ

INVITED PAPER

Testing 5G: Time to Throw Away the Cables

Moray Rumney
Keysight Technologies, Edinburgh, Scotland

Back in August 2010, *Microwave Journal* published a series of articles called, "Masters of MIMO," opening with an overview article from me called, "The MIMO Antenna: Unseen, Unloved, Untested!" I predicted then that MIMO over the air (OTA) testing was the biggest challenge I had seen in 20 years of standards development. Looking back over the intervening six years, I can now see that I underestimated that challenge as the work within CTIA and 3GPP to develop MIMO OTA test methods are still in the final stages of validation. In the meantime, the sophistication of MIMO standards has grown considerably from the original LTE Release 8 through LTE-Advanced Pro in Release 14. Yet, as I write, antenna designers still don't have basic 2×2 MIMO performance requirements for the receivers of their Release 8 capable devices.

Looking ahead, the focus of this article is describing the test challenges of the next generation, the fifth generation. Having underestimated the difficulty in standardizing basic MIMO OTA testing for 4G (LTE), it is humbling to be making predictions this early for the next generation. But here is my best shot: The emergence of the fifth generation of mobile communications is set to revolutionize everything we know about the design, testing and operation of cellular systems. The primary reason for this is the assumption that to deliver on many key 5G objectives, a new air interface is required, one that will operate in the millimeter wave (mmWave) frequency bands (i.e., 28 GHz and above), with channel bandwidths around 1 GHz and higher. To overcome the radio propagation path losses at these operating frequencies, it is assumed that both the base station and mobile devices will need to incorporate medium or large-scale antenna arrays (sometimes referred to as massive MIMO on the base station side) to maintain a usable link budget. The result will be a 5G air interface that relies on beam-steered antennas at both ends of the link, in what will be a sparse and highly dynamic 3D narrow beam propagation environment.

For 4G, MIMO OTA testing was an obvious and useful evolution from traditional cabled testing, but MIMO OTA was never essential for 4G, since MIMO-enabled devices have been shipping for years. The untested static antennas have at least functioned, even if we don't know how well. However, mmWave devices with massive antenna arrays cannot be tested using cables, because there will be no possibility to add connectors for every antenna element. In addition, the dynamic (active) nature of antenna arrays means it is not possible to extrapolate end-to-end performance from measurements of individual antenna elements. So yes, for testing 5G, it really is time to throw away the cables — whether we want to or not!

Compared to the 4G MIMO OTA test challenge, with its basic 2×2 transmission mode and static 2D geometry, it seems safe to predict that what lies ahead for testing 5G will be a revolution compared to the mere evolution that we saw in the transition from 3G to 4G. To add one final opening point, there is so little time! The industry goal to deploy 5G in the 2020 timeframe demands mmWave OTA test solutions and requirements in little more than half the time taken to develop the basic 4G MIMO OTA test methods we have today — even without performance requirements.

MOVE TO RADIATED TESTING

Table 1 summarizes the different types of device testing across the product lifecycle that

TABLE 1

EVOLUTION OF CABLED/OTA TEST NEEDS

Test Area	History	Today	Future mmWave
Design Verification	Cabled	Predominantly Cabled, OTA in Ascendance	Predominantly Radiated (Non-Spatial and Spatial)
RF/Baseband Conformance	Cabled	Cabled	Radiated (Non-Spatial Cable Replacement)
Radiated Performance	Limited to SAR/ EMC	SISO Established, MIMO Emerging	Radiated 3D Spatial Domain Analysis
Production	Cabled	Predominantly Cabled	Radiated (Non-Spatial Cable Replacement)

the industry needs to address. Each area has its own specific needs, in terms of cost and sophistication. Design verification and production testing will be handled outside of standards bodies, while RF/baseband conformance and radiated performance test methods and requirements will be specified by 3GPP.

In addition to the UE MIMO OTA work that started in 2009, 3GPP also commenced radiated test standards in 2011 for base station active antenna array systems (AAS).[1] Traditionally, as with mobile devices, all base station RF requirements such as output power, sensitivity, blocking/spurious and error vector magnitude (EVM) have been measured at the temporary antenna connectors; the actual base station antenna impact is not considered. However, with the introduction in Release 13 of full dimension MIMO (FD-MIMO), also known as elevation beam forming, it is now accepted that the active nature of base station antennas means cabled testing without the antennas is no longer sufficient. This led 3GPP to develop the first radiated test methods for base stations.

Currently, only total radiated power (TRP) and total radiated sensitivity (TRS) tests at boresight are defined, but more will be developed in the Release 14 evolved AAS (eAAS) work item. Today's AAS scope characterizes the antenna in a static line-of-sight channel using one of four defined test methods, all simpler than UE MIMO OTA test methods using spatial fields. However, the AAS work does point to what will happen with basic 5G device testing when operating frequencies approach mmWave, when there will be multiple antenna elements and no temporary antenna connectors.

Tests which were straightforward using cables become much more involved when carried out OTA. Take blocking, for instance: The requirements for blocking were derived from 2D spatial system simulations, and the base station blocking levels were statistically derived from summing the power from three spatially separate mobiles. In the conducted domain, this just looks like an omnidirectional power to be added to the wanted signal. However, if we move back to the radiated domain, how should the blocking signal be constructed? Recreating the system level parameters implies spatially separate blocking signals interacting with the directional base station antenna, so an exhaustive test of all spatial combinations and frequencies would extend today's already long tests beyond the pale. So there are difficult choices yet to be made about how AAS and ultimately mmWave OTA tests are to be developed.

mmWAVE CHANNEL MODELS

Despite the challenges in AAS and eAAS to replace current RF and demodulation tests with line-of-sight radiated equivalents, the area of performance testing in realistic radio environments presents the greatest test challenge. This is the test area UE MIMO OTA has been occupying since 2009 and is the focus for the rest of this article. Central to useful performance testing is a correct understanding of the radio propagation environment. Traditional cabled performance tests look like omnidirectional faded signals to the receiver, and there are aspects of this type of test that may be retained for mmWave receivers. More important is radiated performance testing which has to take into account the antenna patterns at both ends of the link, as well as the propagation environment, all of which are highly dynamic. By comparison, UE MIMO OTA is not even a walk in the park, it's like sitting on the park bench.

For 4G systems below 6 GHz, the 2D spatial channel extended models (referred to as SCME) were chosen as sufficient,[2] and test methods implementing those have been developed. At mmWave frequencies, new channel models need to be developed, and this was one of the first tasks within 3GPP for the development of the 5G new radio (aka NR, for the time being). The first publication of these models for the 6 to 100 GHz range[3] is based on extending the existing stochastic models developed for under 6 GHz up in frequency. This was a pragmatic response by 3GPP to the tight timescales of the ITU's IMT-2020 (5G) project, so that the next stage of NR development can start. In addition to the stochastic models, the initial set of channel models includes an alternate hybrid model. It is based on using deterministic map-based modeling of the static large scale parameters in the environment, coupled with a stochastic approach for small scale parameters like people or vehicles that are better modeled statistically.

Keysight Technologies, in conjunction with the University of Bristol,

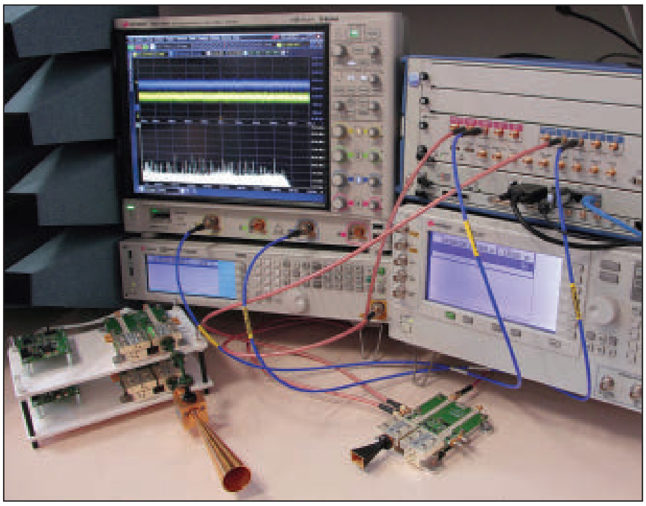

▲ *Fig. 1 60 GHz channel sounding system with 2 GHz real-time channel bandwidth.*

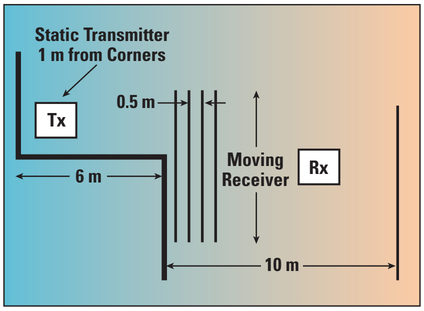

▲ *Fig. 2 Atrium used for corner diffraction measurements at the Merchant Venturers' Building, University of Bristol.*

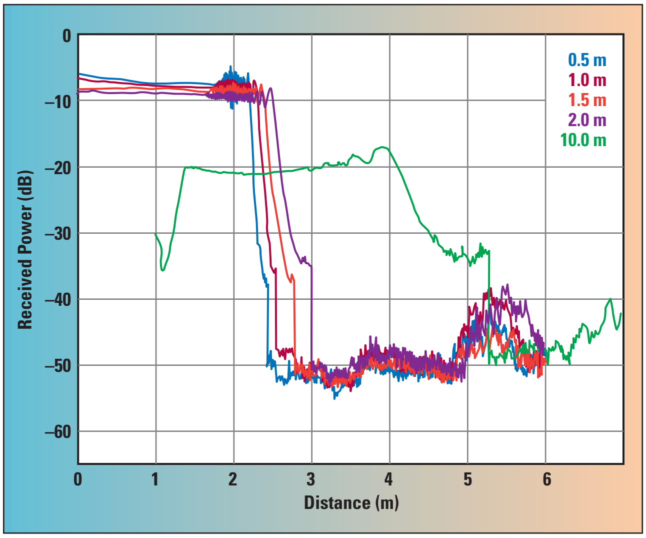

▲ *Fig. 3 Received power vs. distance for all runs of the corner diffraction study.*

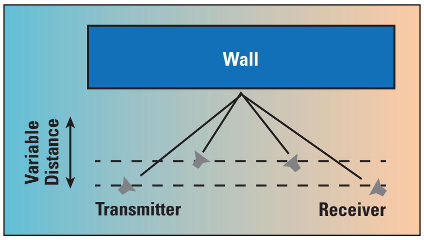

▲ *Fig. 4 Measurement setup for surface scattering measurements.*

and as part of the European Horizon 2020 project mmMAGIC, has been researching many aspects of 5G, including channel modeling, with a view towards what will be required to functionally test mmWave cellular systems. ***Figure 1*** shows a 60 GHz channel sounder used for such research at the University of Bristol. The system provides real-time vector channel analysis with 2 GHz instantaneous channel bandwidth and can readily be adapted for different frequency bands (e.g., 71 to 76 GHz or 28 GHz).[4] The channel sounding function works by repeatedly transmitting a single carrier signal bearing a modulated waveform with excellent auto-correlation properties and a low peak-to-average power ratio. The system, using antennas with a 3 dB beam width of 12 to 15 degrees, has been used to study corner diffraction, diffuse surface scattering and beam pointing algorithms.

Corner Diffraction Study

Figure 2 shows the experimental layout to study corner diffraction. A receiver on a cart was moved past an internal wall in an atrium, at varying distances from the wall, to study the transition from non-line-of-sight to line-of-sight. The results (see ***Figure 3***) indicate that the behavior of the signal is quasi-optical at 60 GHz, with the signal dropping 30 dB over very short distances, around 20 cm. Simulations[4] showed that at a 2 m distance from the wall, 40 cm of travel causes a 25 dB drop at 60 GHz, compared to only 8 dB at 3.5 GHz. This indicates that the speed of signal acquisition and tracking at mmWave frequencies will have to be much faster than at low frequencies.

Mixed Wall Surface Scattering Study

The channel sounding system was mounted on a single trolley to investigate the scattering properties of different surface materials in the local environment (see ***Figure 4***). ***Figure 5*** shows the results for a mixed surface wall containing a window. The received power shows a huge variation that depends on the surface. This is equivalent to a user walking past the window and experiencing only a reflected signal from a transmitter across the street, due to body shadowing. ***Figure 6*** shows the in-channel analysis for the signal reflected from the glass. The power vs. channel bandwidth (2 GHz) of the vertically polarized transmitted signal is shown in yellow in the top left trace. The blue trace (below) shows the residual horizontal power, indicating well-behaved specular reflection with a nearly flat frequency response. This contrasts sharply with the signal reflected from the rough wall, shown in ***Figure 7***. Apart from the significant 25 dB power loss seen for the rough stone, the in-channel analysis in the top left trace shows a complete loss of polarization diversity in the lower 1 GHz of the channel bandwidth, followed by a dominance of the transmitted vertical component in the upper 1 GHz. ***Figure 8*** shows the in-channel analysis at one of the glass-to-wood transitions. The channel flatness in the top left trace shows a 20 dB dropout at mid channel, the result of a strong 1 ns reflection that can be seen in the time domain plot in the lower right. ***Figure 9*** shows the results of this same measurement at a position 8 mm further along the track. Despite the short distance, the frequency response of the channel has completely changed, due to the phase cancellation caused by the 5 mm wavelength at 60 GHz. This is an example of the "ground bound" effect, when two strong signals can reach the receiver with very short (30 cm) differences in path length. Such differences cause large variations in the 2 GHz channel bandwidth, meaning this is a

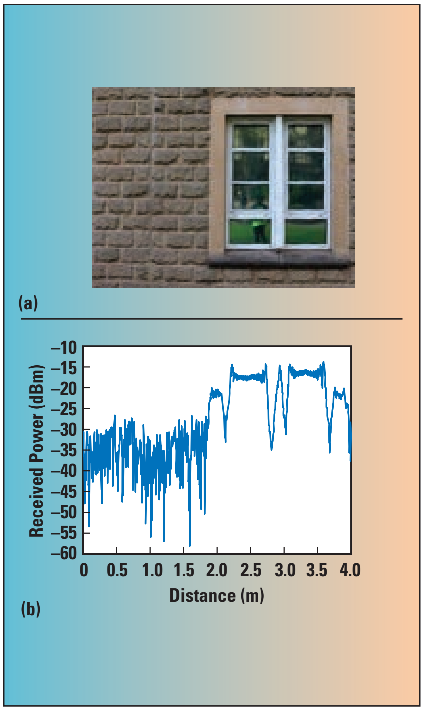

▲ *Fig. 5 Mixed composition surface (a) and measured received power from the first scattered impulse (b).*

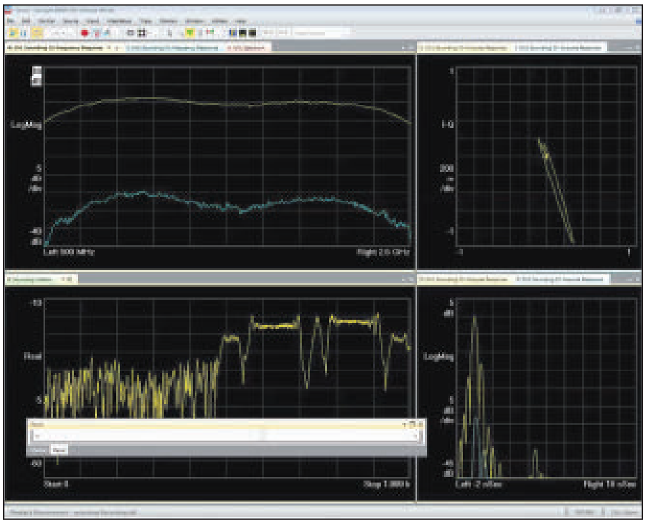

▲ *Fig. 6 In-channel analysis for the signal reflected from glass.*

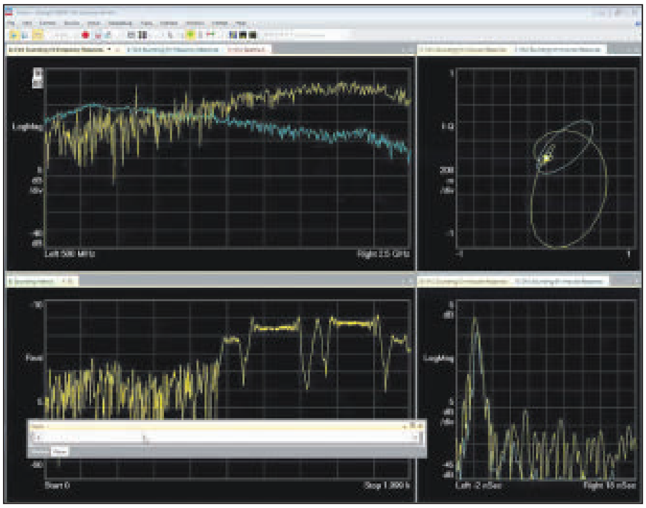

▲ *Fig. 7 In-channel analysis for the signal reflected from a rough wall.*

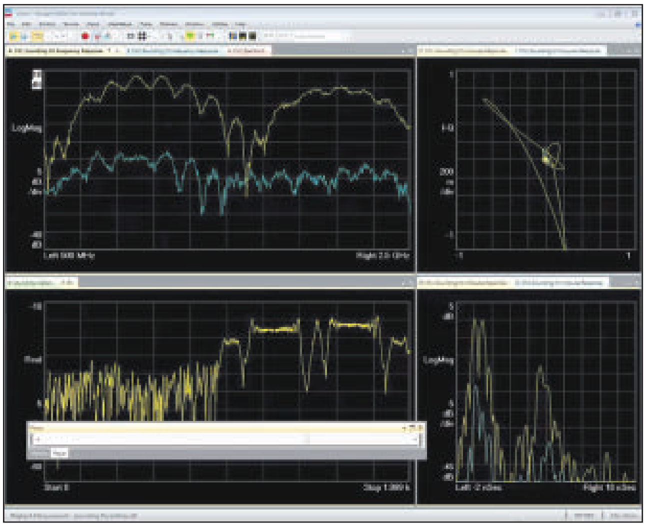

▲ *Fig. 8 In-channel analysis for the glass-to-wood transition.*

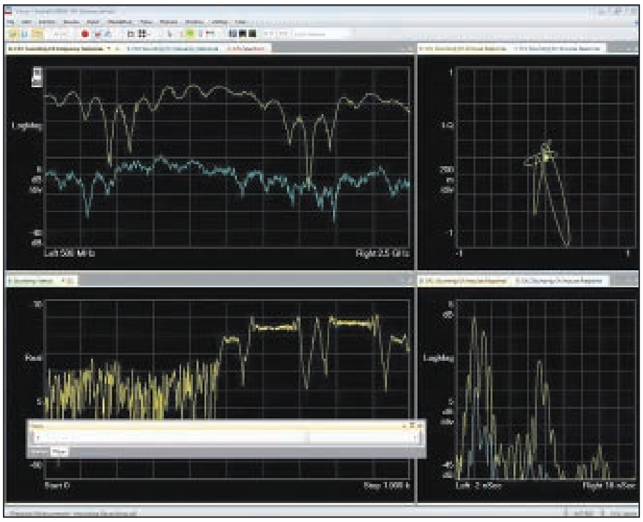

▲ *Fig. 9 In-channel analysis for the glass-to-wood transition, with the trolley in a slightly different position along the track.*

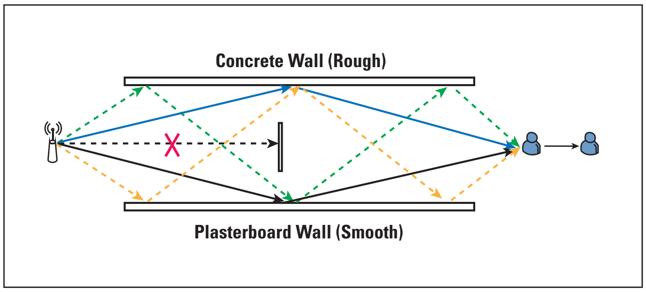

▲ *Fig. 10 Ray tracing in a corridor.*

very difficult signal to demodulate when the user is moving at any speed.

Beam Steering Simulation Study

In this simulation, a user moves 2 m down a corridor, and the specular and diffuse reflections are computed to investigate the benefit of beam steering (see ***Figure 10***). The transmitter (on the left) is blocked by a barrier from line-of-sight to the user (on the right). The upper wall is made of rough concrete, the lower wall smooth sheetrock (plasterboard). The permittivity and K-factor of the wall surfaces used in the simulation were based on measurements of the actual materials. The transmitter has 32 antennas, the receiver 8, giving a potential beam forming gain of 24 dB. Due to its permittivity, the specular reflection from the rough concrete was 6 dB higher than the sheetrock and constant over the 2 m of user movement. However, ***Figure 11*** shows large differences in the diffuse power from each surface as a function of user movement.

Figure 12 illustrates the effect of beam forming. The lower two traces show the available power from the specular and diffuse components (both surfaces combined) using an isotropic antenna (i.e., no beam forming) at both ends of the link. The upper two traces reflect both ends of the link making "ideal" beam forming choices, yielding around 20 dB more power. The simulation shows six beam pointing angles available (see ***Figure 13***). To capture the maximum power as the user moves down the corridor, the transmitter and receiver need to rapidly alter which surface and angle each points to. By performing a cumulative distribution

Futureproofing the wireless smart home.

Consumers worry the smart home products they buy today won't talk to next year's gadgets. Qorvo® can help you futureproof your wireless products now, so your volume takes off. Our ultra-low power IEEE 802.15.4 solutions solve compatibility issues and support the multiple home networking standards of today and tomorrow, with a single chip.

Qorvo's key RF differentiators

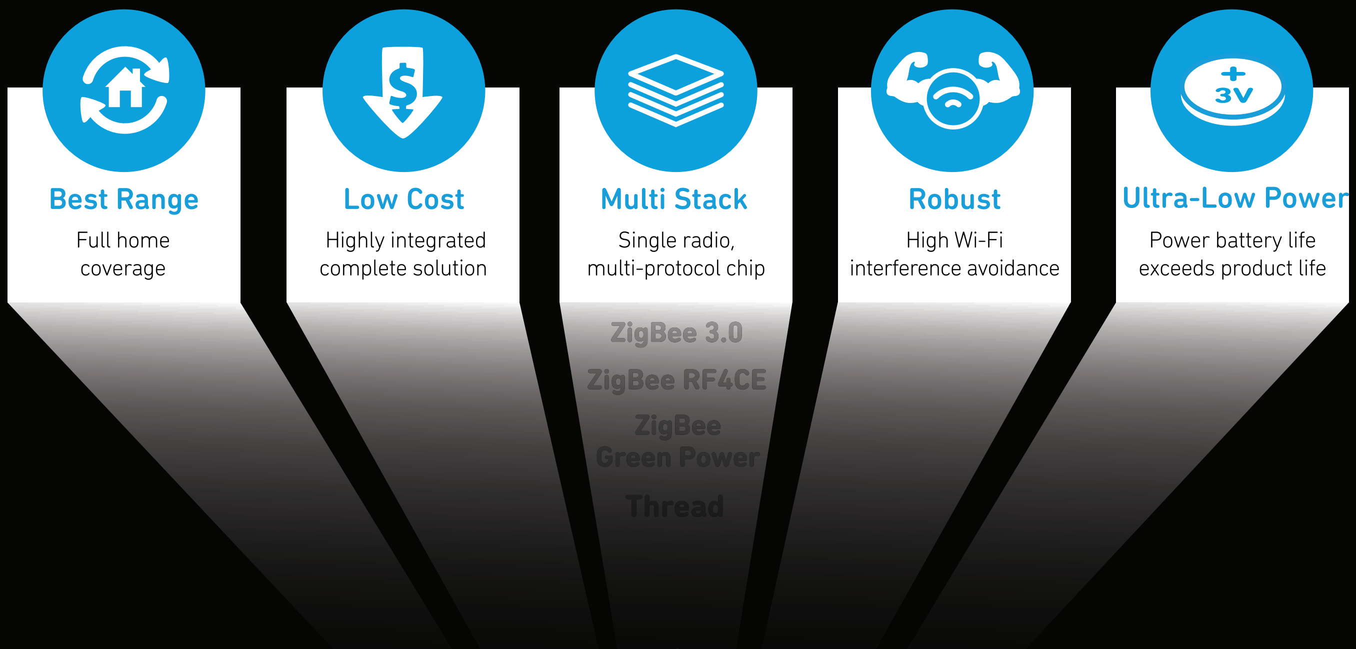

The Internet of Things begins now – learn more at **www.qorvo.com**

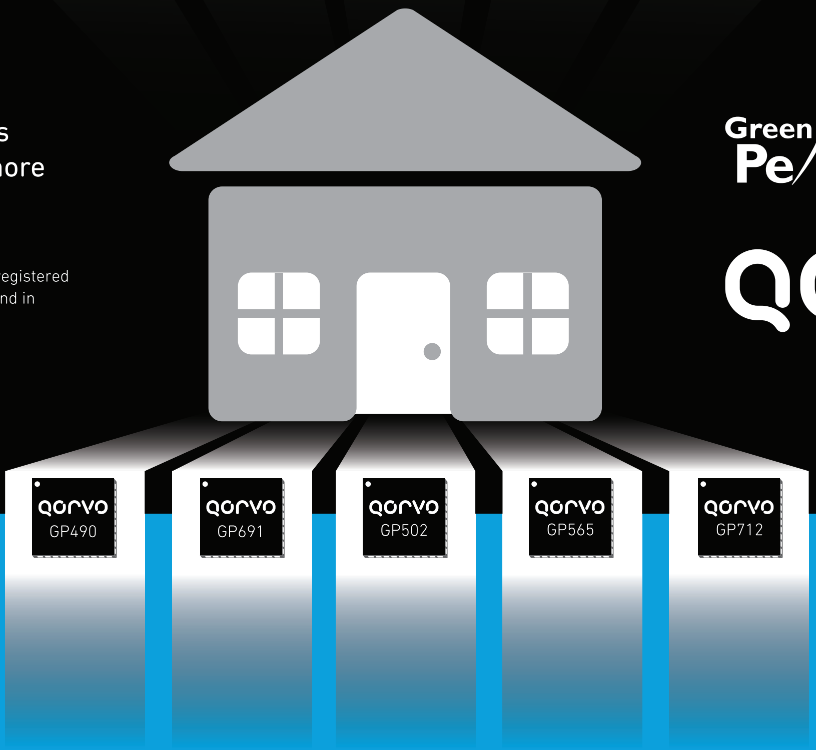

GreenPeak is now qorvo®

function (CDF) analysis of the power distribution using the optimal beam selection as 100 percent, pointing only at the best single concrete wall reflection (beam 2) has a 5 dB loss at 95 percent confidence, while the best single sheetrock reflection (beam 2) has a 17 dB loss.

This simple simulation shows just how dynamic mmWave channels can be, motivating the need for sophisticated beam steering algorithms at both ends of the link to optimize performance. By comparison, recent 3GPP measurements of commercial devices at 2.6 GHz[5] showed that even for the directional SCME urban micro channel model used for MIMO OTA testing, the variation in performance was typically less than 3 dB over a 360 degree rotation. A mmWave device with fixed antennas would only operate for a fraction of the available angles, when the source and receiver signal directions happen to coincide.

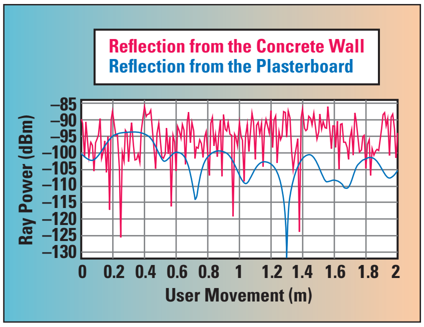

Fig. 11 Diffuse power from the two wall surfaces.

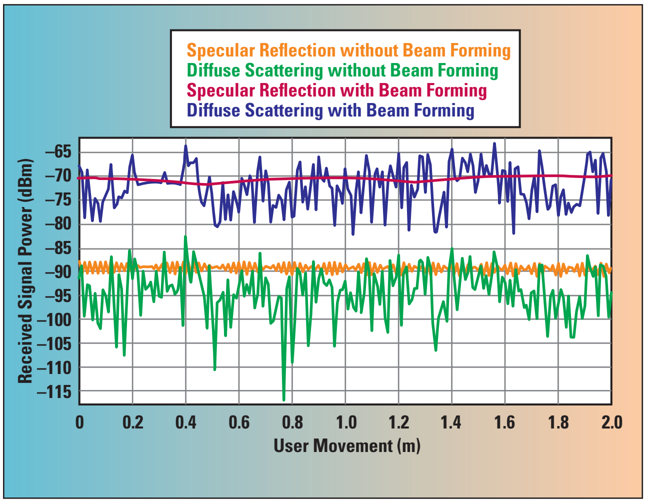

Fig. 12 Ideal beam forming increases the simulated received power by about 20 dB.

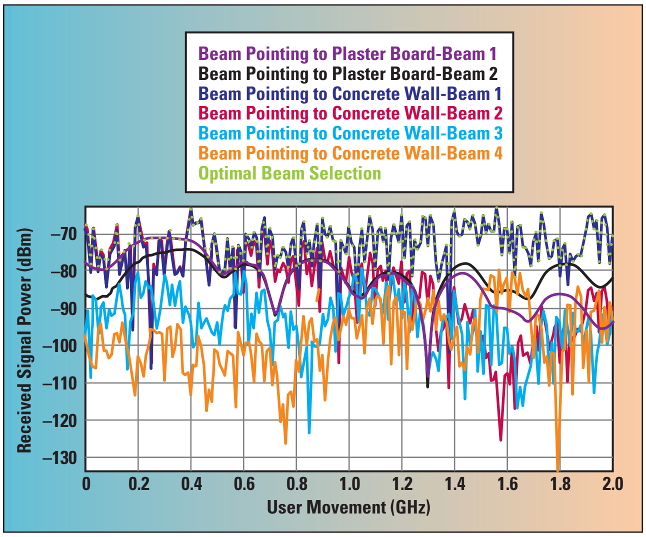

Fig. 13 Received signal power vs. user movement for various beams and surfaces.

PERFORMANCE TESTING AT mmWAVE

The limited examples of mmWave propagation discussed here illustrate the challenge that faces 5G OTA performance testing. Such variability is not yet predicted by the preliminary stochastic channel models, but may be predicted using more advanced hybrid channel models. At RF, the challenge was "how good is my signal"; at mmWave the new question is "where is my signal?" Steerable antennas can only go so far, and it is likely that to provide sufficient quality of service, mmWave networks will have to rely on multi-site connections. This will ensure the UE can simultaneously monitor, acquire and track the available line-of-sight base stations and strong reflections in the environment, with the goal of performing a handover at the subframe level to maintain connectivity and latency. This redundancy is not so different than the soft handover concept built into CDMA systems to handle cell edge signal problems. Falling back to 4G at RF is always possible, but it won't provide 5G performance.

To properly test 5G systems, it will be necessary to first pick appropriate channel conditions that adequately reflect the environment of choice. This must take into account fast-changing in-channel impairments, as well as numerous sources of blocking caused by the physical environment and dynamic factors such as vehicle and device movement and body/hand blocking. Any realistic test system will have to emulate similar conditions, but do the existing test methods specified by 3GPP[6] scale up to mmWave?

The radiated two stage (RTS) method relies on measuring the antenna pattern before convolving this with the channel model to create the signal to be used for device testing in the receiver after the antennas. Since mmWave systems will rely heavily on steerable antennas, the RTS method does not have an obvious role in black box conformance testing of devices; however, it may prove to be useful during device development.[7] The reverberation chamber plus channel emulator (RC + CE) method is capable of creating stochastic reflections, although not with any specific control on direction and limited control of reflection count, controlled by attenuation in the chamber. It is not clear what role reverberation chambers will play at

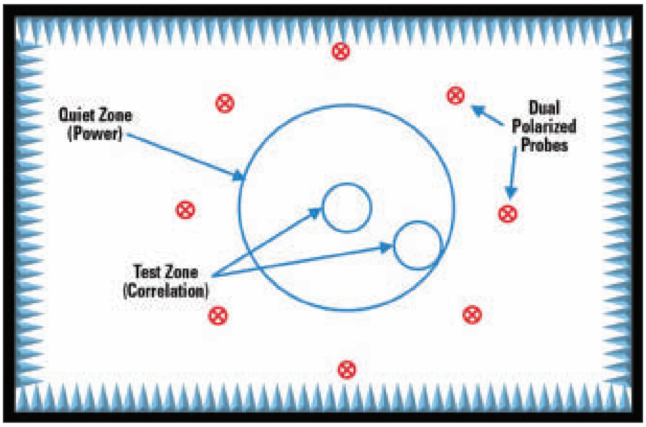

Fig. 14 8×2 MPAC test system.

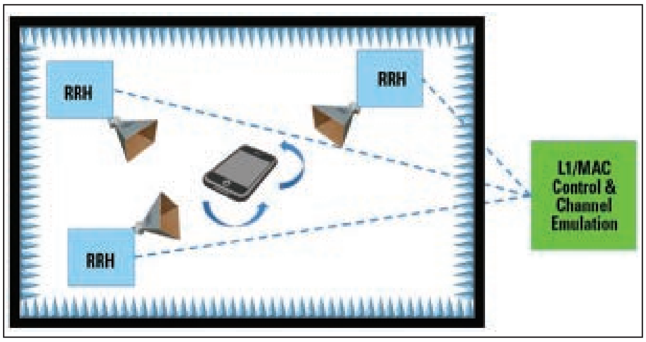

▲ *Fig. 15 Limited scope mmWave test system.*

mmWave, although they may have the potential for some aspects of cable replacement testing where spatial control is not required. The multi-probe anechoic (MPAC) test method has potential for extension to mmWave frequencies. ***Figure 14*** shows a plan view of a typical 8×2 chamber. The usable area within an MPAC system is determined by two properties: the quiet zone and the smaller test zone. The quiet zone is the area within which the power is controlled and is largely determined by the chamber size relative to the signal wavelength. At mmWave frequencies, the quiet zone is not an issue. The smaller test zone is the area within which the correlation of the test signals can be controlled to create arbitrary 2D spatial channels. The size of the test zone is determined by the angular separation of the probes; 8×2 probes provide an ideal test zone of 0.7λ before starting to degrade, rising to 1.6λ with 16×2 probes. Unfortunately, at 60 GHz the wavelength is only 5 mm, which equates to a test zone of just 12.5 mm. Extending this with more probes is possible, but cost becomes a significant factor.

It is likely that an alternative test concept will be needed for mmWave OTA. One possibility comprises an anechoic chamber with a small number of mmWave remote radio heads (RRH) coupled to an L1/MAC baseband transceiver with channel emulation capability (see ***Figure 15***). Such a system would not be able to arbitrarily generate any spatial channel, although it could create a diversity of potential use cases: shadow fading and in-channel impairments like frequency-selective ground bound and Doppler shift. This would test the capability of the device to both acquire and track multiple signals during a test sequence. The downside of not being able to generate spatial signals with arbitrary angles of arrival — needed for SCME at RF — is less significant. At mmWave frequencies, most signals will already have narrow beamwidths of 10 to 15 degrees, which can be generated by a single antenna.

CONCLUSION

The author hopes this article has set the scene for what lies ahead to test 5G at mmWave frequencies, almost all OTA without cables. The challenges compared to today's RF OTA testing are formidable, since existing test methods have limited scalability and timescales are extremely short. This should motivate the industry to focus and, indeed, 5G testability is already getting attention in the early NR discussions at 3GPP.■

ACKNOWLEDGMENTS

Keysight would like to thank Tom Barratt, Alberto Loaiza Freire, Wenfang Yuan, Evangelos Mellios and Mark Beach from the University of Bristol for their work presented here, part of the ICT H2020 project mm-MAGIC (Millimetre-Wave Based Mobile Radio Access Network for Fifth Generation Integrated Communications) and the EPSRC Centre for Doctoral Training (CDT) in Communications, grant number EP/I028153/1.

References

1. 3GPP TR 37.842 v2.0.0, "Radio Frequency (RF) Requirement Background for Active Antenna System (AAS) Base Station (BS)."
2. 3GPP TR 25.996 v13.0.0, "Spatial Channel Model for Multiple Input Multiple Output (MIMO) Simulations."
3. 3GPP TR 38.900 v14.0.0, "Study on Channel Model for Frequency Spectrum Above 6 GHz."
4. 3GPP R1-162872 Keysight Technologies, "Initial 60 GHz Channel Sounding Results from the mmMAGIC Project for Corner Diffraction and Surface Scattering."
5. 3GPP R4-161069 Keysight Technologies, "Root Cause Analysis of AC Method Differences," Figure 1.
6. 3GPP TR 37.977 v14.0.0, "Verification of Radiated Multi-Antenna Reception Performance of User Equipment (UE)."
7. M. Rumney, Y. Jing and H. Kong, "Practical Active Antenna Evaluation Using the Two-Stage MIMO OTA Measurement Method," EuCAP 2014.

Fingertip Gesture,
Continued from page 8

and duty cycles are user-controlled to provide maximum flexibility; a wearable might be designed to trigger a radar wake-up based on arm motion detected by a positional sensor. Other wake-up scenarios are likely for in-wall or tabletop devices.

PROJECT STATUS

Google's demonstrations of Project Soli at the Google I/O Conference in May 2016, included a smartwatch prototype that was operated with precise, close range finger gestures and a wireless speaker prototype controlled from several meters distance using hand gestures. These are expected to be the first in a wave of consumer products that can be precisely operated using hand movements only. Home appliances, smart home systems, and VR headsets controlled by hand motion are other systems that benefit from gesture control. And these are just a starting point, as developers working with the early development version of the system have demonstrated applications in object recognition, 3D imaging, security, advanced visualization and music. Google will release developer kits based on this radar-on-a-chip IC, with chip production to follow.

Effortless, intuitive gesture control frees product designers from the constraints imposed by buttons, switches and small screen display technologies. It truly represents a new paradigm in user interface design. Whether used to control IoT devices or as a way to navigate in augmented reality applications, like the scenario illustrated in ***Figure 9***, radar-based gesture control clearly is a defining technology for man-machine interaction in the 21st century.■

ACKNOWLEDGMENT

The authors would like to thank the Soli team at Google ATAP and Soli team at Infineon for the continued collaboration.

References

1. FCC, Report and Order and Further Notice of Rulemaking, July 14, 2016, http://transition.fcc.gov/Daily_Releases/Daily_Business/2016/db0728/FCC-16-89A1.pdf.
2. *Microwave Journal*, "Single-Chip 24 GHz Radar Front-End," February 13, 2014, www.microwavejournal.comarticles/21553-single-chip-24-ghz-radar-front-end.

INVITED PAPER

NB-IoT and eMTC Make 4G Networks Ready for the Internet of Things

Jörg Köpp
Rohde & Schwarz, Munich, Germany

The majority of devices that constitute the Internet of Things (IoT) will use wireless machine-to-machine communications technologies to communicate with each other and with IoT applications typically running in the cloud. Some applications that require global coverage and/or mobility will focus on cellular technologies. Currently, mainly 2G and 3G technologies are used but the future will belong to new technologies like enhanced Machine Type Communications (eMTC) and Narrow Band IoT (NB-IoT). With these technologies mobile operators will be able to address a much wider share of the overall wireless IoT market.

Features like power saving mode (PSM), extended DRX cycles (eDRX) and extended coverage (CE) will be used to tune the wireless interface to the different needs of the IoT applications. In order to meet all performance and availability requirements, all communication layers — the physical layer, the signaling layer, the IP layer and the application layer — have to work smoothly together. Consequently, there is a need for improved end-to-end application testing in order to optimize, for example, power consumption and reaction times.

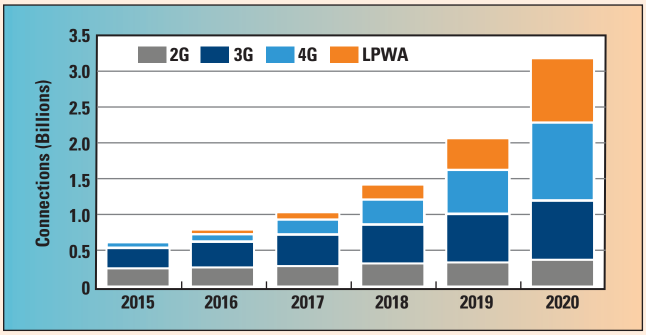

▲ *Fig. 1 Growth of cellular M2M connections. Source: Cisco.[1]*

IoT applications that depend on mobility or global accessibility make use of satellite technologies or cellular mobile radio technologies. About 86 percent of today's cellular IoT devices use second or third generation mobile communications technologies[1]. Typical applications include fleet management, container tracking, coffee vending machines, ATM banking services and personal health monitoring. For the most part, these applications generate little data traffic, often needing only an SMS service for transmission. ***Figure 1*** shows the expected increase of cellular M2M connections by year.

The fourth generation of mobile communications has played a smaller role to date. Because LTE is primarily optimized for the mobile broadband market, the IoT has generated little demand for 4G technology. Moreover, the costs for a typical LTE modem are still relatively high in comparison to a GSM modem and the global coverage of 2G/3G networks is still unbeatable. Some aspects of LTE, however, make it increasingly attractive. One of these is global accessibility: According to GSMA, 4G LTE networks covered more than a third of the global population by year-end 2015, and by the end of the decade developed countries are expected to reach ‘full’ coverage.

LTE offers additional technological advantages with respect to spectral efficiency, latency and data throughput. The long-term availability of LTE is another consideration. Second generation networks are in operation for more than 25 years and even though some future evolution provisions have been introduced in the specification, it may be possible that operators will discontinue the service on these networks in the long term. Therefore, the industry is looking for LTE solutions being competitive to today’s 2G solutions in terms of cost, power consumption and performance.

3GPP STANDARDIZATION FOR IoT

The need for optimized solutions for the IoT market was also recognized by the 3GPP standardization, and specific enhancements for machine type communication have been developed. For example, the committee has defined features in Rel. 10/11 intended to protect the mobile network against overload. Network operators need to be armed against the possibility of several thousand devices trying to connect to the network at the same time. This could happen after a sudden event such as the power grid coming back online after a power failure. Overload mechanisms and options for reducing the signaling traffic have been introduced to handle these types of occurrences. Many IoT applications — sensor networks as an example — only rarely send data and do not need to operate precisely to the second. These devices can report to the network that they are prepared to accept longer delays during the connection setup (delay tolerant access).

Rel. 10 includes a process that permits the network to initially reject the connection requests from these devices and delay them until a later time (extended wait time). With Rel. 11, access to the cellular network can be controlled by means of access classes. In this case, a device may set up a connection only if it is assigned a class that is currently permitted by the network. The network transmits a bitmap called an extended access barring (eab) bitmap that identifies which classes are permitted access. These processes introduced in Rel. 10 and 11 ensure reliable and stable operation of the IoT applications and devices of today and tomorrow within cellular networks without endangering the mobile broadband service.

LOW COST, LOW POWER DEVICES

Still missing were optimized solutions for IoT devices addressing requirements like low data traffic, low power consumption and low costs. The committee started on those in Rel. 12. It quickly became clear, however, that there will be no single, simple solution for all applications. The requirements for applications such as container tracking, waste bin management, smart meters, agricultural sensors and sports and personal health trackers are too varied. Rel. 12 therefore concentrates on the areas of reduced power consumption and cost-effective modems. The results are a power-saving mode (PSM), which is especially important for battery-operated devices, and a new LTE device category 0, which should have only 50 percent of the complexity of a LTE category 1 modem. Baseline is the sacrifice of features for the sake of less complex hardware enabling a lower cost design and a more energy efficient operation.

The PSM process starts after a data link is terminated or after the periodic Tracking Area Update (TAU) procedure completes (see ***Figure 2***). The device first goes into the idle mode in which it periodically switches to receive mode in order to receive messages (discontinuous reception). As a result, it remains reachable via paging. After timer T3324 expires, the power saving mode is entered. In this mode, the device is always ready to send messages because it remains registered in the network.

However, the receiver is literally switched off so the device is not accessible via paging. PSM is thus suited for sensor networks that only rarely need to send data to the device. This mode is not suitable for applications

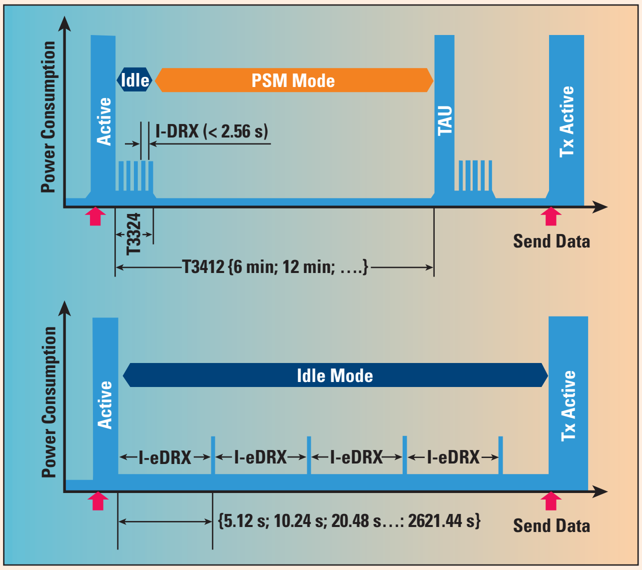

Fig. 2 PSM and extended DRX.

that require a quick response from the sensor or expect a time-critical reaction. Applications that use PSM must tolerate this behavior and the design process must include the specification of optimal timer values for idle mode and power-saving mode.

The introduction of LTE category 0 was a first attempt at permitting significantly less expensive LTE modems for the IoT market. To achieve this, the complexity of the modem was reduced by bringing the supported data rate down to 1 Mbps. This minimizes the requirements for processing power and memory. Manufacturers can also eliminate full duplex mode, i.e., the simultaneous transmission and reception and multiple antennas. As a result, the device does not require duplex filters that otherwise would be necessary to prevent interference between the transmitter and receiver. LTE category 0 was the immediate step towards LTE category M1 introduced in Rel. 13. With category M1, additional cost-reduction measures, especially lower bandwidths in the uplink and downlink, lower data rates and reduced transmit power were implemented.

A new standard called NB-IoT was developed in parallel with LTE category M1. The requirements profile for this standard includes extremely low power consumption, very low costs, improved reception in buildings and support for an enormous number of devices with very little data traffic. NB-IoT has a bandwidth of just 180 kHz and can be deployed by using unused LTE resource blocks, free

TABLE 1

LTE CATEGORIES FOR DIVERSE IoT APPLICATION REQUIREMENTS

	LTE Cat 1	*LTE Cat 0*	*LTE Cat M1*	*LTE Cat NB1*
Deployment	In-Band LTE	In-Band LTE	In-Band LTE	In-Band LTE Guard-Band LTE Stand-alone
Downlink (DL)	OFDMA (15 kHz)	OFDMA (15 kHz)	OFDMA (15 kHz)	OFDMA (15 kHz)
Uplink (UL)	SC-FDMA (15 kHz)	SC-FDMA (15 kHz)	SC-FDMA (15 kHz)	Single Tone (15/3.75 kHz) SC-FDMA (15 kHz)
Peak Rate	DL: 10 Mbps UL: 5 Mbps	DL: 1 Mbps UL: 1 Mbps	DL: 1 Mbps UL: 1 Mbps	DL: 250 kbps UL: 20 kbps (Single Tone)
UE Receiver BW	20 MHz	20 MHz	1.4 MHz	200 kHz
Duplex Mode	Full-Duplex FDD/TDD	Full/Half-Duplex FDD/TDD	Full/Half-Duplex FDD/TDD	Half-Duplex FDD
UE Transmit Power	23 dBm	23 dBm	23 or 20 dBm	23 or 20 dBm
Power Saving	PSM, eDRX	PSM, eDRX	PSM, eDRX	PSM, eDRX

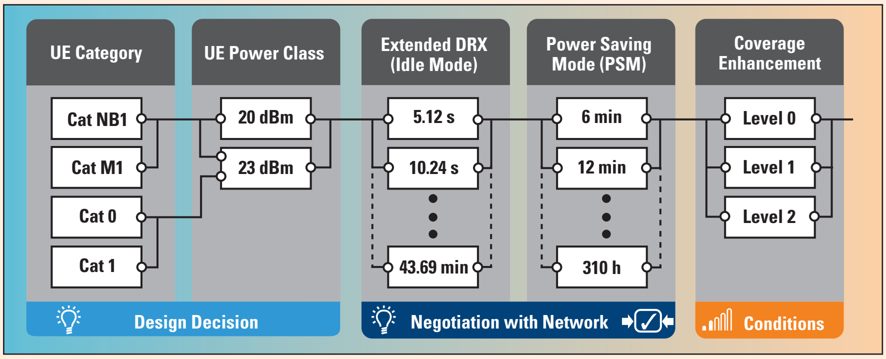

▲ *Fig. 3 Parameters influencing the battery lifetime of a device.*

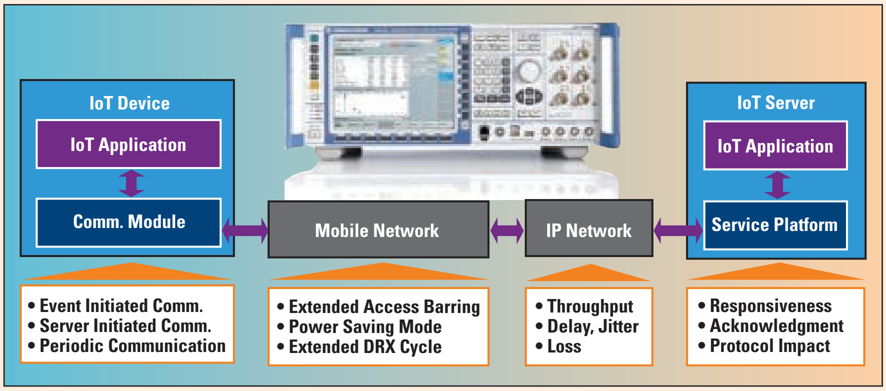

▲ *Fig. 4 End-to-end aspects to be considered.*

spectrum between neighboring LTE carriers (guard band) or stand-alone, for example, in unused GSM carriers. With the NB-IoT, 3GPP has created a new cellular air interface that is fully adapted to the requirements of typical machine type communications. ***Table 1*** gives an overview of the different LTE categories which meet diverse IoT application requirements.

An additional feature for reduction of the power consumption was implemented too. With eDRX on connected or idle mode, the time interval is extended, and the modem goes into receive mode to receive paging messages and system status information. The DRX timer determines how often this occurs. Currently, the shortest interval for the Idle DRX timer is 2.56 seconds. That is fairly frequent for a device that expects data only every 15 minutes and has relaxed delay requirements, for example.

The main differences between PSM and eDRX are the time permitted for the device to stay in a kind of power off mode and the procedure to switch into receive mode. A device using PSM mode needs to go first in the active mode to become reachable and afterwards it stays for a certain time in idle mode. A device using eDRX can stay in the idle mode and go just quickly into the receiver mode, without any additional signaling.

For example, a device may be expecting very infrequent spontaneous messages from the server (e.g., once per day) but the application requires an answer in less than 10 minutes. If the device is using the PSM, it has to leave the PSM mode at least every 10 minutes and make a TAU, followed by a short time in idle mode. If using eDRX, on the other hand, the device just goes into reception mode every 10 minutes, which consumes much less power and generates reduced signaling load. Otherwise, in the case of a sensor device that sends data once per day, and during which there is essentially no need to communicate with the sensor in the time between, PSM is probably the most appropriate power saving feature. In some cases, it would be meaningful to combine several power saving features like eDRX in connected mode, in idle mode and the power saving mode.

Moreover, in eMTC and NB-IoT some coverage enhancement features were introduced to cover use cases like smart meters installed in the basement of a house. One principle is the redundant transmission, e.g., repeatedly sending the same data over a period of time dependent on the actual coverage conditions. But transmitting the same data several times obviously takes more time and consequently has an impact on overall power consumption. As depicted in ***Figure 3***, a couple of parameters defined by the design, but sometimes dependent on the network configuration or actual network condition, influence the battery lifetime of the device.

END-TO-END APPLICATION TESTING

Theoretical calculations about battery lifetime based on assumptions

(**4G Networks,** *Continued on page 32*)

INVITED PAPER

Advantages of Near-Field Measurement When Verifying 5G Antenna Designs

Anritsu Co.
Morgan Hill, Calif.

Over the air (OTA) measurements will play a vital role in 5G designs, in part because of the introduction of massive MIMO at microwave and millimeter wave (mmWave) frequencies and mobile terminal requirements for multiband and smaller size. The conventional far-field measurement (FFM) method requires large-scale measurement infrastructure and long measurement time. In addition, using FFM in the mmWave band suffers from low measurement accuracy caused by path loss due to the long transmission distance. A proposed near-field measurement (NFM) method solves these problems and helps reduce measurement cost, making it a viable alternative in many applications, including antenna testing.

5G will affect antenna design and characterization in a few, yet significant ways. Current user equipment (UE) designs have several built-in antennas that support various wireless services, and the 5G rollout will most likely result in the antenna count increasing further. OTA testing of the UE will be necessary because implementing a measurement connector for each antenna will increase the size of the UE and raise device cost to impractical levels. Another issue is that 5G base stations will use microwave and mmWave massive MIMO technologies, which will also increase antenna count. The exploding number of antennas makes provision of a measurement connector for each antenna virtually impossible, making OTA testing a requirement.

OTA measurements can be made on the total radiated power (TRP) and total isotropic sensitivity (TIS) of the UE. For massive MIMO, measuring the antenna radiation patterns is a key evaluation item. The basic OTA measurement technique is the 3D integration method using an anechoic chamber. With this approach, the equipment under test (EUT) surroundings are measured as a spheroid form. The problem is that this method requires an anechoic chamber and large-scale measurement equipment. Because FFM is used, the electromagnetic wave loss due to the free-space path

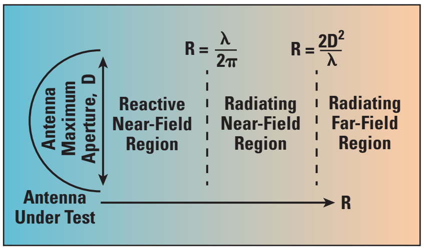

▲ *Fig. 1 Antenna field regions.*

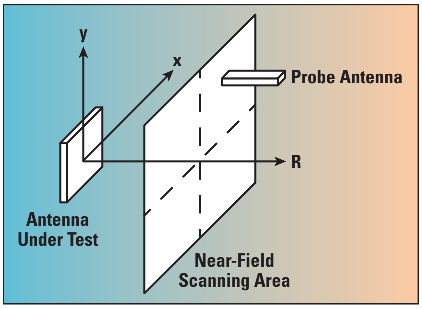

▲ *Fig. 2 Planar NFM, showing the relationship between the AUT and scanning area.*

loss (FSPL) in the mmWave band is considerable. The result is that there are measurement problems with large error and small dynamic range.

NEAR VS. FAR-FIELD MEASUREMENT

The electromagnetic field radiated from an antenna aperture is divided into regions (see ***Figure 1***). The area near the antenna aperture is called the reactive near-field region, where most of the electromagnetic field components do not contribute to emission. The space where the radiation pattern does not change with distance from the antenna aperture is the radiating far-field region. Generally, this is where the antenna radiation pattern is measured.

The far-field is defined as the distance, R, satisfying the following equation for the maximum diameter, D, of the antenna, where λ is the free space wavelength.

$$R \geq \frac{2D^2}{\lambda} \qquad (1)$$

Additionally, the maximum power W_a received by the receive (Rx) antenna in free space is defined by the following equation, where the transmit (Tx) antenna gain is G_t, the Rx antenna gain is G_r, and the Tx power is W_t.

$$W_a = \left(\frac{\lambda}{4\pi R}\right)^2 G_t G_r W_t \qquad (2)$$

Since R increases for a high gain antenna with a larger aperture, the free-space attenuation increases. The attenuation also increases in the mmWave band because λ is smaller, making measurement of low side lobes difficult.

The radiating near-field region between the near and far-field areas is where the radiation pattern changes with distance. NFM measures the electromagnetic wave in the near field and calculates the radiation pattern in the far field. The following explains the procedure for finding the radiation pattern.

First, the region near the antenna is examined with a probe antenna connected to a vector network analyzer (VNA) to determine the distribution of the electromagnetic field. Next, the radiation pattern at infinity is found by data processing the amplitude and phase of the captured electromagnetic field. The free-space attenuation is small, because measurements are made close to the antenna.

Compared to FFM, NFM can measure at higher accuracy. There are several types of NFM, depending on the scanning area near the antenna under test (AUT); planar is preferred for antenna measurements because it is suitable for high-gain antennas and has simplified data processing (see ***Figure 2***). With planar NFM, a probe antenna is used to scan and measure the amplitude and phase of the electromagnetic field at a distance of 3λ from the AUT. The distribution of the amplitude and phase at this measurement plane is the Fourier transformation of a function defined by the AUT radiation pattern and the probe antenna radiation pattern. Consequently, this function can be found by reverse Fourier transformation, and the AUT radiation pattern can be found by filtering (i.e., probe correction) the probe antenna radiation pattern from the found function. The radiation pattern is quickly calculated by a computer, because data processing uses the fast Fourier transform (FFT).

TABLE 1

COMPARISON OF NFM AND FFM

Parameter	NFM	FFM
Measurement Location	Simple Radio Anechoic Box	Radio Anechoic Chamber
Measurement Range	Near-Field About 3λ (15 to 25 mm @ 60 GHz)	Far-Field (3 m or 10 m)
Radiation Pattern Measurement	3D	2D (3D Radiation Pattern Measurement Requires Time and Facilities)
Antenna Diagnostics and Analysis	Yes	Difficult

The advantages of NFM are shown in ***Table 1***. Since NFM is a close-range measurement method, it does not require use of an anechoic chamber or other large-scale facilities. The mmWave measuring instruments are compact and the radiation pattern can be measured using a simple anechoic box in a room, which eliminates the high cost and extra time necessary to configure a measurement system using a large anechoic chamber. Accurate measurement results are obtained because the method measures a region where the free space loss is small. In addition, NFM captures the entire 3D radiation pattern immediately in front of the AUT, whereas FFM requires many measurements to capture the 2D radiation pattern, i.e., the horizontal (H) and vertical (E) planes. Using FFM to capture the 3D radiation pattern requires a complex measurement setup and a longer measurement time. NFM captures the amplitude and phase distribution near the antenna. If the radiation pattern cannot be acquired, due to the antenna design, the captured amplitude and phase distribution can be used to diagnose the cause. This is a benefit when measuring a phased array antenna, including massive MIMO.

The NFM scanning area is determined by the size of the AUT, the measurement frequency, and the required radiation pattern angular range. The scanning plane, L_x, when the measurement range of the required radiation pattern is θ_c (see ***Fig-***

ure 3) is expressed by the following equation:

$$L_x = D + 2R\tan\theta_c \quad (3)$$

NFM SUCCESS

The probe antenna used for NFM requires three characteristics. First, it must achieve the widest possible beamwidth. Ideally, an isotropic antenna should be used; however, an actual antenna has directivity. Consequently, the probe must be corrected. Probe correction removes the probe antenna radiation pattern from the AUT radiation pattern found by NFM. If a narrow beam antenna is used as the probe antenna, the dynamic range of the radiation pattern is small and causes problems with accurate measurement of low side lobes. Second, the cross-polarization ratio (XPR) must be small, as the AUT radiation pattern is measured for each polarization. Linear polarization antennas are measured by splitting into their vertical and horizontal polarizations, while circular polarization antennas are measured by splitting into the right-hand and left-hand circular polarizations. As the polarization precision of NFM depends on the probe antenna polarization, it is necessary to use a probe antenna with the smallest possible XPR to achieve precision measurements. Lastly, multiple reflections between the probe antenna and AUT must be minimized. This issue can be resolved by using a small probe antenna covered by a radio wave absorber. To minimize the impact of multiple reflections on the measurement, research was done on a measurement method using an optical probe and optoelectronic field conversion.

An open-ended waveguide used as a probe antenna meets the above requirements at mmWave frequencies. Since the aperture plane of this probe antenna is small, the beam is wide, the XPR is about -20 dB and multiple reflections are suppressed by covering the probe antenna with radio wave absorber.

The insertion loss and phase stability of the coaxial cables in an antenna measurement setup deteriorate with frequency, reducing measurement accuracy and making antenna measurements in the mmWave band and higher frequencies difficult. To deal with these challenges, miniature commercial NLTL-based reflectometers have been developed to increase the frequency range of a microwave VNA to 145 GHz (see ***Figure 4***). Essential ingredients in this approach are monolithic NLTL samplers, used so the VNA receivers can cover from 30 to 145 GHz; NLTL harmonic generators, which extend the CW source from 54 to 145 GHz; high directivity directional couplers and a 0.8 mm coaxial port connector. In addition to their miniature size, these reflectometers provide short- and long-term thermal stability (because of the low thermal gradient across the modules), high amplitude and phase stability and raw directivity. Most importantly, placing the sampling directional bridge closer to the AUT measurement signal provides long-term amplitude and phase stability. These features, in particular, lend themselves well to antenna measurements, whether they are performed in a near-field, far-field or compact range scenario. The conduits used to reduce cable complexity provide a framework

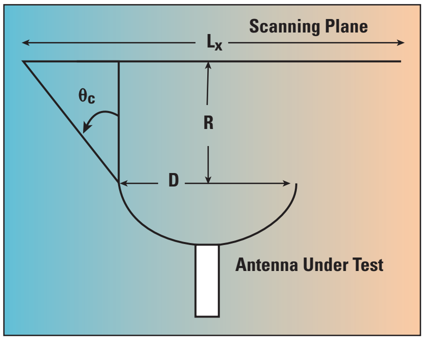

Fig. 3 NFM measurement geometry.

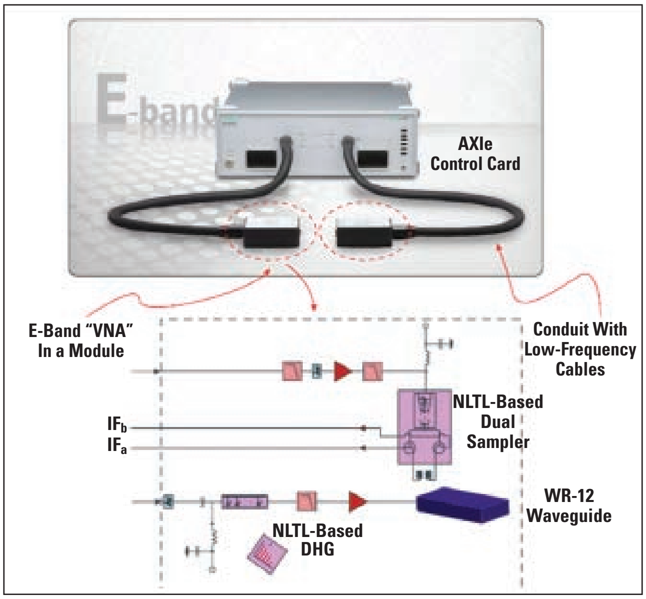

Fig. 4 E-Band VNA setup for NFM measurement. Not shown in the figure is a 0.8 mm coaxial 145 GHz VNA.

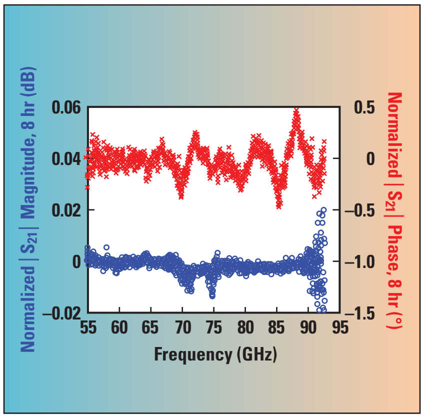

Fig. 5 Normalized S_{21} amplitude and phase measured over 8 hr.

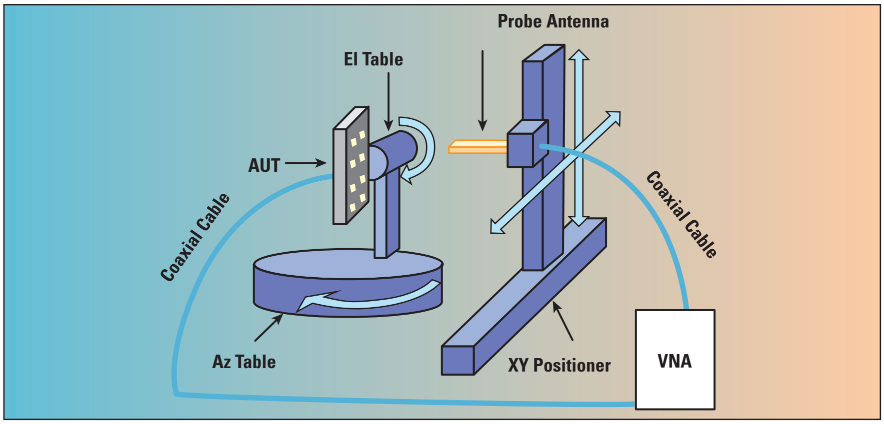

Fig. 6 NFM system for massive MIMO antennas.

for extending the length of the cables for far field antenna measurements, when required. By bringing the reflectometers closer to the waveguide probe on one hand and the AUT on the other, mmWave coaxial cable losses are eliminated compared with a traditional measurement setup. Phase and magnitude stability are also improved (see ***Figure 5***).

MASSIVE MIMO ANTENNA MEASUREMENT

A general-purpose antenna commonly has a main beam direction at right angles to the antenna front. Proposed massive MIMO antennas for 5G change the radiation direction by altering the phase of the antenna elements. There are two potential problems when performing NFM using an antenna with such a radiation pattern. First, the near field scanning area is enlarged. When the AUT beam is tilted, locating the radiation pattern of the wide angle matching this tilt requires a wide scanning area. Second, measurement accuracy decreases. FFT calculates the radiation pattern from the near-field distribution. The calculated AUT radiation pattern interval is narrowest near the center (E-plane = 0°, H-plane = 0°), based on a feature of this calculation. Conversely, the interval of the radiation pattern calculation point becomes wider as the angle becomes larger. As a result, the beam is not near the center, so the measurement accuracy may become worse when the beam width is narrow.

To solve these problems when using NFM to measure a massive MIMO antenna, a measurement system as shown in ***Figure 6*** can be used. The system is composed of an XY positioner, for scanning the near field, and azimuth and elevation tables attached to the AUT. The measurement system can perform measurements even when the AUT beam direction changes. In the case of AUT arrangement, single line scans in the horizontal and vertical planes are performed to obtain the beam direction. From this result, the AUT direction is controlled by the azimuth and elevation tables, and the AUT beam center is matched with the center of the near-field scanning area. With this arrangement, the AUT beam is always at the center of the calculated radiation pattern (E-plane = 0°, H-plane = 0°), which minimizes the measurement area and suppresses any degraded accuracy. If the AUT phase shifter can be operated from the same system, the radiation pattern can be measured automatically while the beam direction changes.

CONCLUSION

NFM is an effective method for measuring massive MIMO antennas as it reduces free-space losses, yielding measurements with good sensitivity. An NFM system is suitable for OTA measurements in the microwave and mmWave bands — including E-Band — and solves the challenge of measuring massive MIMO antennas. Continual advancement of these systems will help speed development of 5G and mmWave communications systems. ■

INVITED PAPER

LoRa: A Radio Approach Towards IoT Geo Localization

Norbert Schmidt
IMST GmbH, Kamp-Lintfort, Germany

In 2013, Semtech announced a new Long Range (LoRa®) radio technology to be operated in the public ISM radio frequency band. LoRa is able to enlarge the possible radio link distances up to more than 15 km while maintaining the radiation limits of the ISM bands. The novelty of the air interface is mainly a spread spectrum transmission technique in the RF front-end characterized by the introduction of a spreading factor, which denotes the relationship of transmission time to bit rate. The RF front-end provides 125 kHz, 250 kHz or 500 kHz signal bandwidth to enable such spreading. LoRa technology has already been successfully deployed with the Internet of Things (IoT) and machine-to-machine (M2M) applications by providing cheap and robust communication services.

Cellular systems with a coverage area of many square kilometers per infrastructure node are possible. According to the envisaged applications, tens to hundreds of end nodes can be handled within one communication cell. The central communication point in the middle of the cell — a gateway with LoRa technology inside — is capable of massive parallel receive operations on many channels, each of them individually configured for certain distances and bit rates. A typical example of the RF front-end is shown in ***Figure 1***.

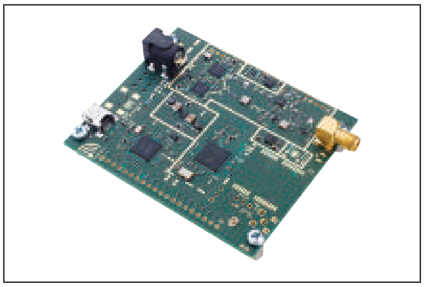

▲ ***Fig. 1** LoRa concentrator module from IMST GmbH.*

Until now IoT applications have largely been driven by the communication requirements to set up an ecosystem with small sensors or actuators, in several different application domains like agriculture, industrial, logistics, smart environment, smart metering, smart grid, smart city and smart home. So far, the deployment of LoRa communication technology has been structured and organized by the LoRa Alliance™, whereby semiconductor companies, radio equipment manufacturers, firmware and software providers, mobile operators, IT companies and test houses worked together to set up a complete LoRa ecosystem, including the required quality procedures and system certifications. The specification of a first generation LoRaWAN™ standard has been completed, resulting in complete Low Power Wide Area Network (LPWAN) implementation including physical layer and medium access specifications as well as higher layer application features such as authentication, node identification, network security, application security and packet forwarding.

LoRa LOCALIZATION

It is apparent that some of the applications will benefit from the capability to detect the position of the sensor nodes in addition to setting up a communication link only. This is especially true for permanently or frequently moving objects which are tagged with a LoRa end node. Examples for such localization applications are the tracking of animals, especially

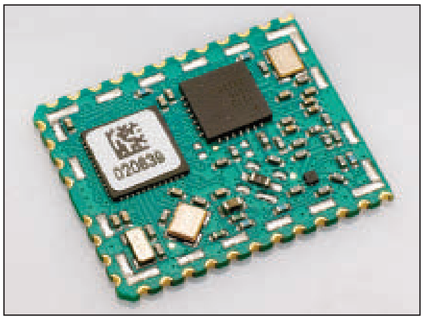

Fig. 2 *LoRa end node module from IMST GmbH.*

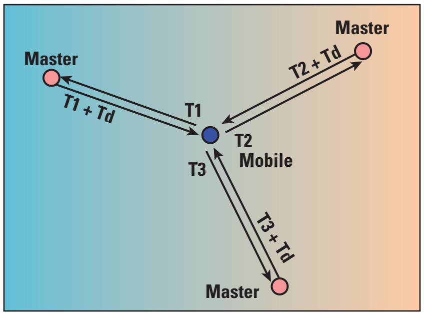

Fig. 3 *Localization based on round trip time.*

livestock and pets, private fleet management of industrial vehicles, tracking of vulnerable people, the repair of robots in tunnels, anti-theft alarms and many more. All of these applications need sporadic communication.

As the production costs of LoRa based sensors (a typical example is shown in ***Figure 2***) are often well below $10, it would be advantageous if, in addition to the communication capability, localization of the sensor would be possible without additional hardware costs as far as the sensor is concerned. Moderate cost increase in the infrastructure, however, would be acceptable because of the large coverage area of infrastructure nodes and the relatively low price of the LoRa gateways. So what is the underlying physics for the raw measurements and possible architectures built on the LoRa physical layer to enable localization?

MEASUREMENT PRINCIPLES

Several different measurement principles for the raw data required to localize an object are known. First, they can be sorted into the two different categories of exploiting time-of-flight or propagation angle of the transmitted radio signals. Most of the existing systems are based on time measurement.

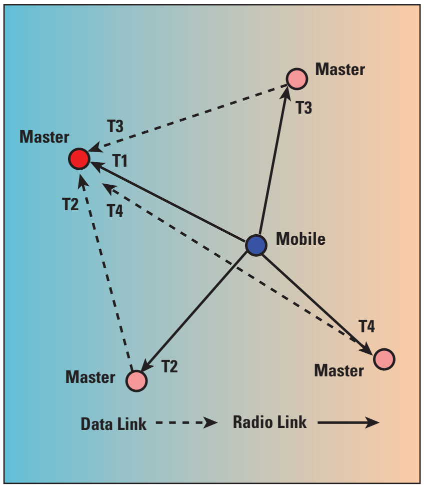

Fig. 4 *Localization based on time difference of arrival.*

All architectures with time measurements need an infrastructure with several measurement counterparts to the mobile node. One popular method is the measurement of round trip time (RTT). The architecture is shown in ***Figure 3***. Here, a radio signal is exchanged between infrastructure node and mobile node and is echoed back. The total round trip time is measured and the delay in the echoing node is transmitted and subtracted from the result. No synchronization between nodes is needed in this case, but the communication is bidirectional and must be done sequentially one after another to all infrastructure nodes. The user has a choice as to whether the position information is present in the mobile node or in the infrastructure node since both can be the first sender, although it is easier if the mobile node initiates the echoing scheme.

A unidirectional principle is based on synchronized time-of-arrival (ToA) measurements at the infrastructure node. The mobile node adds an absolute time stamp to the radio packet being sent to the infrastructure nodes. The infrastructure nodes measure the absolute arrival time of the packet and calculate the time-of-flight from the difference between the sent time and the arrival time. This principle needs only one transmission for all infrastructure nodes, but the clocks of all nodes, including the mobile node, must be precisely synchronized. However, having a precise clock in the mobile node is not feasible for most IoT applications.

A further improvement can be made when only the time differences at the infrastructure nodes are needed. This leads to a measurement principle which is called Time Difference of Arrival (TDoA), shown in ***Figure 4***. In this instance, the mobile station sends a packet without time information included. The arrival time of any packet at the infrastructure node is measured and the time tag as well as the infrastructure node ID is added to the radio packet information. The packets are collected at a central infrastructure server. To compensate for the unknown absolute time at the mobile node, there needs to be extra information for the infrastructure — this means one more infrastructure node is needed in accordance with the ToA principle.

Then, the server will be able to calculate the position of the mobile node from the relative time information and the coordinates of the receiving stations. This is the principle which is applied to the LoRa localization service. The big advantage is that the radio packets sent by the mobile nodes don't have to be changed. All that is needed is an identification number for the node, and this ID is already present in currently existing LoRaWAN implementations.

The more infrastructure nodes present, the better measurement results yielded. However, it is up to the central infrastructure server to deal with an arbitrary number of radio links, noisy measurement results, missing data, averaging in time as well as the detection of measurement errors. But these tasks are similar for the different measurement approaches, including already established systems, and thus quite well-known in research and engineering.

Localization systems are already widespread, so why should a further localization system be introduced and would it be competitive compared to existing systems that are already very refined? The answer is that requirements for IoT driven localization applications are so different that a new, additional localization technology would be a key enabler for a new application domain with disjunctive requirements and complementing architectures.

ARCHITECTURES

Geo localization applications greatly differ in their demands and

TABLE 1

ASSESSMENT OF IoT LOCALIZATION SERVICES

	GPS	LoRa	RFID	Mobile Cellular
Mobile Node Device Cost	High	Small	Very Small	High
Infrastructure Cost	High	Small	High	High
Air Time Costs	No	No	No	Yes
Size	Medium	Small	Very Small	Big
Mobile Node Battery Lifetime	Short	Long	Very Long	Short
Communication Capability	No	Fair	Very Limited	Good
Indoor Usage	No	Yes	Yes	Yes
Optimized for Small Data Packets	No	Yes	Yes	No
Range / Distance	Global	High	Very Small	High
Precision	High	Low	High	Low
Update Rate	High	Low	High	Medium
Position Known to Infrastructure	No	Yes	Yes	Yes
Dependency on Third Parties	High	Medium	Low	High
Usage	Global	Regional	Local	Regional

architectures. The most popular system, the classic GPS, has no communication features at all. The position of the mobile node is known to the node itself, but without the help of another communication system it is not known to anybody else. Many IoT applications need a different approach: The position has to be known in the infrastructure, not in the mobile node itself. Moreover, the mobile node is small, lightweight and battery-operated. The update period of the location is often minutes or hours, not seconds.

The LoRa Geo localization feature will offer the capability for localization of people or items within an area of up to 700 km^2 utilizing a cheap tag in addition to the communication capability. A key enabler will be the deployment of the infrastructure, since this will account for the main additional costs compared to the pure communication features. Infrastructure may be deployed e.g., by the big telecom operators (typically where their mobile cellular infrastructure is located since cell sizes are very similar). Other markets are driven by private installations in industry, agriculture, and other segments with large private areas. A big advantage here is that the communication technology is already established, so that the introduction of the localization feature offers an add-on. However, it is an add-on with complex system architecture and a high implementation challenge as it is a completely new approach.

Advantages compared to existing solutions can be seen in ***Table 1***. Compared to GPS, the indoor capability, device cost and communication ability are major advantages. Compared to RFID, the range is much higher and the infrastructure density and cost is much lower. Related to mobile cellular services, no air time costs, cheap infrastructure and low device cost are the main advantages. Further advantages are the long battery life compared to GPS and mobile cellular services.

Application potential and a unique selling point is offered by the merging of communication and localization, but also in the special overall combination of the features listed in Table 1, which distinguishes the application domain from the other candidate systems. These features are a unique combination of capabilities satisfying a variety of requirements required by typical IoT applications that other localization services are not able to cope with. Investments would only be needed for the evolution of the technology, since 'generation one' LoRa communication technology has already been developed and standardized. This lowers the hurdle for implementation compared to a completely new development and makes an attractive business case. Customers already using 'generation one' equipment are familiar with the technology and migration on the end node side is easy to handle and bears no additional hardware costs.

Implementation challenges are present mostly in the setup of the infrastructure. Due to the chosen TDoA measurement principle, the clocks in the infrastructure nodes have to be synchronized precisely. In outdoor solutions an additional GPS module can be used to provide the position of the infrastructure node (which is needed to calculate positions of the mobile nodes) and accurate time base with a resolution of about 1 ns (although that is not possible in indoor installations). In this case, accurate timings may be achieved with the Precision Time Protocol (PTP) of the Ethernet specification when the device can be connected to another source of time information and the coordinates of the infrastructure must be found with additional help, such as diagrams of the building.

Not only do technical challenges have to be solved, but the infrastructure has to be changed — at least on the gateway side. LoRa infrastructure gateways which are capable of localization will need different hardware architecture compared to existing communication infrastructure of the first generation and their complexity will be significantly higher.

The implementation of estimation algorithms and position solvers is already going on and might not be such a problem. Some companies already offer libraries exploiting the raw localization information to yield the positions of mobile nodes.

EXPECTED PERFORMANCE

The precision of radio localization systems measuring round trip times or time of arrival depends mainly on the bandwidth of the radio waves used. The reason is that not only the signal traveling the direct path from sender to receiver is present at the receiver input, but so too can be one or more echoes, which are caused by reflections from items or obstacles between senders and receivers. When the signal bandwidth is limited, these echoes merge with each other and cannot

be separated. The achievable performance depends on the statistics of the echoes, the signal-to-noise ratio of the received signal, the overall integration time, and the bandwidth and spectral characteristics of the transmit signal.

When B is the bandwidth of the radio transmit signal, the achievable temporal resolution is in the order of 1/B with an estimator using a correlation approach, which is the basic mechanism for TDoA estimations. For a LoRa system with 500 kHz bandwidth, this results in precision of about 600 m. This number can be interpreted as a worst case threshold. When the signal of the direct path is significantly stronger than the signal of the echoes, the results will be better. With other estimators, which exploit the radio channel information (the channel delay spread or, better, an estimate of the channel impulse response) in addition to the pure signal correlation characteristics, better results can also be achieved. However, LoRa based localization will never directly compete with the precision of GPS, which is several meters down to centimeters when applying differential GPS. This will have to be reflected in the application domain.

CONCLUSION

LoRa based localization will complement the traditional localization systems adequately while satisfying the new set of application requirements of IoT implementations that have not been matched by traditional localization techniques so far. No additional costs for air time or end nodes will occur, the devices are cheap, and battery time is much better than with traditional localization systems. However, users with diverse applications should be aware of the physical limits that will allow for only moderate precision and update rate. Whenever applications only need limited performance of a narrowband localization system, LoRa based localization will be a good choice.■

Note: The LoRa® name and associated logo are registered trademarks of Semtech Corporation. LoRaWAN™ is a trademark of the LoRa Alliance.

(**4G Networks,** *Continued from page 22*)

about the communication behavior of the applications and parameters is a good starting point. But applications may behave quite differently in reality, and this behavior can also change over time depending on the actual situation. For example, a sensor reports the actual value only if a certain threshold is reached, but as long as the sensor value is above this threshold it will be reported periodically. In general, the overall communication behavior of the end-to-end application including communication triggers (client initiated, server initiated, periodic), delay requirements, network configuration, data throughput, or mobility needs to be considered (see ***Figure 4***).

PSM and eDRX are just tools with slightly different characteristics that can be helpful to meet the battery lifetime requirements. The challenge for the device and application developer is to use these tools in the most efficient way. This requires an understanding and analysis of all aspects influencing the power consumption. It starts with the applications running on the device and on the server side, and includes also the mobile network's behavior as well as the IP network characteristics.

The situation provides a motivation to evaluate parameters like RF performance, battery consumption, protocol behavior and application performance. Overall, it will start with detailed analysis based on communication models selecting different features and varying different parameters on paper, but in the end, it would be very useful to verify the results under well controlled, simulated, yet realistic network conditions. This will not only verify the model assumption but will also reveal the impact of non-perfect network conditions. Also scenarios in which the network does not support a feature or use different timers can be verified. And after all, a better understanding of the overall application behavior can be gained.

A UNIQUE TEST SOLUTION

There is a growing demand for test, verification and optimization of end-to-end applications, which is going far beyond pure RF and protocol testing. Manufacturers of test and measurement equipment are addressing this demand. Rohde & Schwarz, for example, offers a solution based on the R&S CMW500/290 multi-radio communication test platform and the R&S CMWrun sequencer tool. It allows a detailed view on different parameters like mobile signaling traffic, IP data traffic or power consumption on one platform. In real networks, it is not possible to reliably reproduce and test end-to-end application requirements. But the test platform simultaneously emulates, parameterizes and analyzes wireless communication systems and their IP data throughput.

The sequencer tool allows straightforward configuration of test sequences without requiring specific programming knowledge of how to remotely control the instrument. It also provides full flexibility when configuring parameters and limits for the test items. One of the key differentiators of this solution is the intuitive way the user can combine and run applications in parallel with common event markers out of signaling or IP activities.

For example, in end-to-end application tests, synchronized traces show the current drain and IP data throughput. During analysis time, synchronized event markers indicating signaling events or IP status updates are displayed in both graphs. This ensures a deeper testing level where the user can see the impact of a signaling or IP event on the current drain and IP throughput. This helps to understand the dependencies and to optimize the application parameters.

The starting point could be to just look at the overall communication behavior, e.g., number of IP connections, transmitted messages, or communication and signaling events. Moreover, it could be interesting to see the power consumption in different activity states, or in eDRX or PSM status. Later it would be useful to tune the related parameters for eDRX or PSM and probably the application behavior. Finally, it could be helpful to analyze different scenarios reflecting possible real-world situations. Thus, end-to-end application testing becomes more and more important in order to meet such challenging application requirements as a 10-year battery lifetime.■

Reference

1. Cisco Visual Network Index 2016 Global Mobile Data Traffic Forecast Update, 2015–2020 White Paper.

INVITED PAPER

5G Opens Up mmWave Spectrum: Which Frequencies Will Be Adopted?

James Kimery
National Instruments, Austin, Texas

As the world's standardization bodies move to define the next generation of wireless networks, the goals and objectives for 5G are forcing researchers to change the way they think. Increasing the spectral efficiency of a 4G-based network is not enough to deliver the step function in data rates, latency and capacity necessary for the three high level 5G use cases defined by 3GPP (see ***Figure 1***) to provide ubiquitous, instantaneous mobile broadband data.

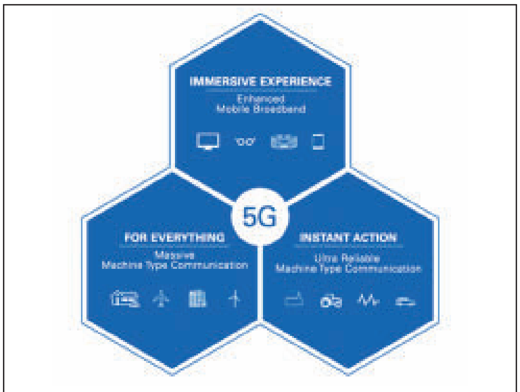

▲ ***Fig. 1** Three 5G use cases defined by 3GPP and IMT 2020.*

The enhanced mobile broadband (eMBB) use case, as defined by the IMT 2020, envisions peak data rates exceeding 10 Gbps, which is 100× faster than 4G. Data rates are empirically linked to available spectrum, according to the Shannon-Hartley theorem, which states that capacity is a function of bandwidth (i.e., spectrum) and channel noise. With spectrum below 6 GHz fully allocated, spectrum above 6 GHz — specifically in the millimeter (mmWave) range — presents an attractive alternative to address the eMBB use case. But at what mmWave frequency?

SPECTRUM OPTIONS

The International Telecommunication Union (ITU) and 3GPP have aligned on a plan for two phases of research for 5G standards. The first defines research for frequencies under 40 GHz, to address the urgent subset of commercial needs by September 2018. The second phase, slated to begin in 2018 and end in December 2019, addresses the key performance indicators outlined by the IMT 2020. This second phase focuses on frequencies over 40 GHz.

To globally align the standardization of mmWave frequencies, ITU released a list of

TABLE 1 mmWAVE FREQUENCIES (GHz) PROPOSED AT WRC-15
24.25 to 27.5
31.8 to 33.4
37 to 40.5
40.5 to 42.5
45.5 to 50.2
50.4 to 52.6
66 to 76
81 to 86

proposed globally viable frequencies between 24 and 86 GHz at the World Radiocommunications Conference last November (WRC-15), shown in ***Table 1***. Shortly after the ITU proposal, on October 21, 2015, the Federal Communications Commission (FCC) in the United States issued a Notice of Proposed Rule Making (NPRM) that recommended new flexible service rules among the 28, 37, 39 and the 64 to 71 GHz bands (see ***Figure 2***).

While the ITU, 3GPP and other standards bodies decided on 2020 as the deadline for the 5G standard to be defined, cellular providers are working on an accelerated schedule for delivering 5G service. In the U.S., Verizon and AT&T plan to test an early version of 5G in 2017. Korea will conduct 5G trials at the 2018 Olympics, and Japan wants to demonstrate 5G technologies at the 2020 Tokyo Olympics. Through these varying groups and motivations, the following frequencies are emerging as the initial candidates for 5G: 28, 39 and 73 GHz.

These three frequency bands have emerged for several reasons. First, unlike 60 GHz, which has approximately 20 dB/km loss due to oxygen absorption, they have much lower oxygen absorption rates. This makes them more viable for long distance communications. These frequencies also function well in multipath environments and can be used for non-line-of-sight (NLoS) communications. By combining highly directional antennas with beam forming and beam tracking, mmWaves can provide a reliable and very secure link. Ted Rappaport and his students at NYU Polytechnic School of Engineering have already begun research on the channel properties and potential performance for 28, 39 and 73 GHz. They have published several papers with propagation measurements and studies on potential service outages at these frequencies. This data and research, combined with the availability of spectrum worldwide, make these three bands the starting point for mmWave prototyping.

Service providers, eager to access the extensive unallocated mmWave spectrum, are the key influencers for the frequencies to be used. In Japan, NTT DOCOMO partnered with Nokia, Samsung, Ericsson, Huawei and Fujitsu to do its own field trials at 28 GHz as well as with other frequencies. In February 2015, Samsung performed its own channel measurements and showed that 28 GHz is viable for cellular communications. These measurements validated the expected path loss for urban environments: The path loss exponent is 3.53 in NLoS links. Samsung claims this data suggests a mmWave communications link can be supported for greater than 200 m. Researching phased array antennas, Samsung has begun characterizing designs that could fit phased arrays inside cell phones.

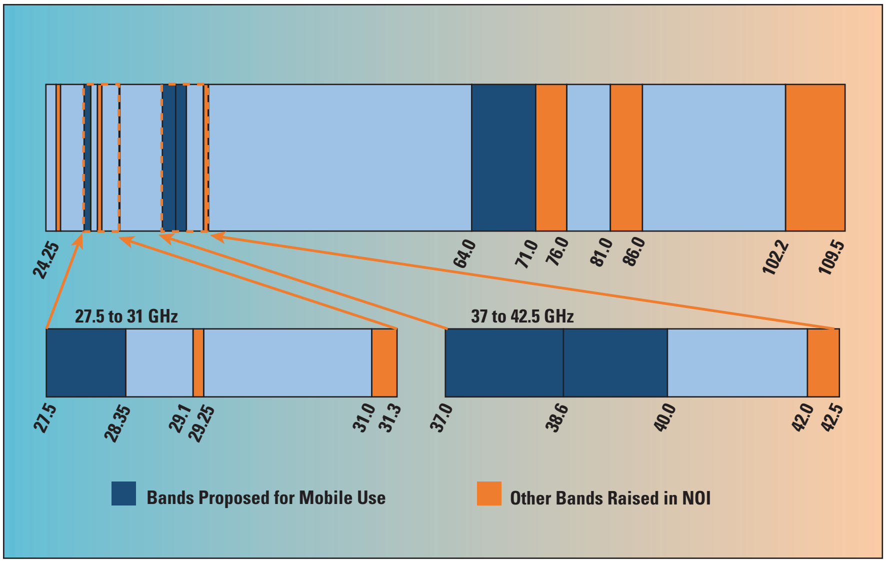

▲ *Fig. 2 mmWave bands proposed by the FCC for mobile use.*

In September 2015, Verizon announced that it will conduct field trials in the U.S. with key partners, including Samsung, in 2016. In November 2015, Qualcomm conducted experiments at 28 GHz with 128 antennas to demonstrate mmWave technology in a dense urban environment. It showed how directional beam forming can be used for NLoS communications. With the FCC announcement that the 28 GHz spectrum can be used for mobile communications, further experiments and field trials in the U.S. are expected. Verizon has also completed an agreement with XO Communications to lease 28 GHz spectrum, with the option to purchase it by the end of 2018.

Note, however, that the 28 GHz band is not included in the ITU's list of globally viable frequencies. Whether it will be the long-term frequency option for 5G mmWave applications still must be determined. The spectrum availability in the U.S., Korea and Japan, along with U.S. service provider commitments to early field trials, could push 28 GHz into U.S. mobile technology regardless of the global standards. Korea's desire to show 5G technology at the 2018 Olympics might also push 28 GHz into consumer products before the standards bodies finalize the 5G standards. The fact that this frequency was not on the International Mobile Telecommunications (IMT) spectrum list did not go unnoticed and has drawn attention from the FCC.

On July 14, 2016, the FCC voted unanimously to adopt new rules to free nearly 11 GHz of high frequency spectrum for flexible, mobile and fixed use wireless broadband, comprising 3.85 GHz of licensed and 7 GHz of unlicensed spectrum. The rules create a new Upper Microwave Flexible Use service in the 28 GHz (27.5 to 28.35 GHz), 37 GHz (37 to 38.6 GHz) and 39 GHz (38.6 to 40 GHz) bands and a new unlicensed band from 64 to 71 GHz. While 28 GHz may not be used globally for mobile access, the U.S. is aggressively moving in this direction.

PROTOTYPES MOVING FORWARD

Though the possible wide adoption of 28 GHz for 5G may not be seen for a while, if at all, it is clearly important right now. Mobile communications in the last several years has also focused on 73 GHz (in E-Band). Nokia used the channel measurements at 73 GHz performed by NYU to begin its research at this frequency. In 2014, at NI's annual user conference (NIWeek), Nokia used NI prototyping hardware to demonstrate the first over-the-air link operating at 73 GHz. The company continued to evolve the prototype with public demonstrations to display new achievements. By Mobile World Congress (MWC) 2015, the prototyping system was capable of over 2 Gbps data throughput using a lens antenna and beam tracking. Nokia showcased a MIMO version of this system operating at over 10 Gbps at the Brooklyn 5G Summit in 2015; less than a year later, at MWC 2016, the company demonstrated a two-way over-the-air link achieving over 14 Gbps. Nokia was not the only company with a 73 GHz demo at MWC 2016. Huawei presented a prototype with Deutsche Telekom operating at 73 GHz. This demo, using multi-user MIMO, displayed high spectrum efficiency and the potential for more than 20 Gbps throughput for individual users.

More 73 GHz research is anticipated in the coming years. One of the defining characteristics of this frequency, that sets it apart from 28 GHz and 39 GHz, is greater than 2 GHz contiguous bandwidth, which is the widest of the proposed frequency spectra. By comparison, 28 GHz has 850 MHz of bandwidth, and the two bands around 39 GHz have 1.6 GHz and 1.4 GHz in the U.S. As previously mentioned, more bandwidth equates to more data throughput, which gives 73 GHz a big advantage over 28 and 39 GHz.

The 39 GHz bands are under investigation, but significant public support and research have not materialized. Nonetheless, this band features some characteristics that may make it a compromise for wider adoption. The FCC has proposed 39 GHz for potential mobile use. Verizon, while focusing on 28 GHz for its initial field trials in 2017, has access to 39 GHz via its business relationship with XO Communications, which owns substantial 39 GHz licenses. Still, public support and acknowledgment of 28 GHz and 73 GHz research are more visible than that for other frequencies.

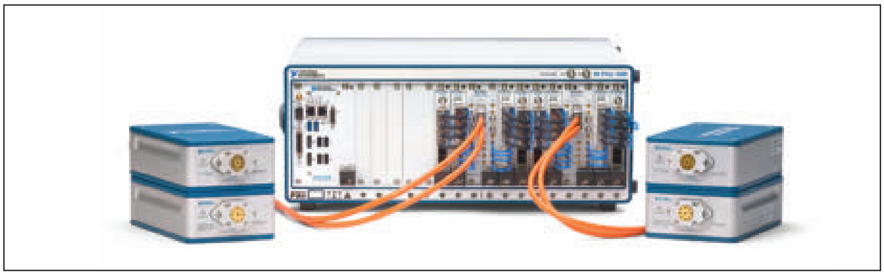

▲ ***Fig. 3*** *NI's mmWave transceiver system provides a configurable set of mmWave hardware with a physical layer in source code, enabling rapid prototyping.*

To capitalize on the promise of mmWave for 5G, researchers must develop new technologies, algorithms and communications protocols. The fundamental properties of the mmWave channel are different from current cellular models and are relatively unknown. The importance of building mmWave prototypes cannot be overstated, especially in this early timeframe. Building system prototypes demonstrates the viability and feasibility of a technology or concept in a way that simulation alone cannot (see ***Figure 3***). mmWave prototypes communicating in real time, over the air, in a variety of scenarios will unlock the secrets of the mmWave channel and enable innovation, technology adoption and proliferation.

CHALLENGES

mmWave for mobile access faces challenges, including the availability of commercial off-the-shelf silicon and analog components, as well as other elemental building blocks for developing systems. This hinders commercialization. Consider a baseband subsystem capable of processing a multi-gigahertz signal. Today's LTE implementations typically use 10 MHz channels (20 MHz maximum), and the computation load increases linearly with bandwidth. So the computational capacity must increase by 100× or more to address 5G data rate requirements. To conduct mmWave system physical layer computations for infrastructure, FPGAs are an essential technology to develop real-time prototypes. After all, the motivation for moving to mmWave is the large contiguous bandwidth.

In addition to FPGA boards, a mmWave prototyping system needs state-of-the-art DACs and ADCs to capture up to 2 GHz of contiguous bandwidth. Some RFICs on the market today include chips that convert between baseband and mmWave frequencies, but these options are limited and mostly cover the unlicensed 60 GHz band. Engineers can use IF and RF stages as alternatives to RFICs. Once they develop baseband and IF solutions, engineers have a few more vendor-provided options for mmWave radio heads than they do for baseband RFICs, but not many. Developing a mmWave radio head requires RF and microwave design expertise. This is an entirely different skill than developing FPGA boards, so pulling together all of the necessary hardware requires a team with diverse experience. FPGAs must be considered core components in a mmWave baseband prototyping system, and programming a multi-FPGA system capable of processing multi-gigahertz channels increases system complexity.

mmWAVE IS INEVITABLE

Though the future of 5G is not yet clear, mmWave will surely be one of the technologies used to define it. The large amount of contiguous bandwidth available above 24 GHz is needed to meet data throughput requirements, and researchers have already used prototypes to show that mmWave technology can deliver data rates above 14 Gbps. While questions remain around the global spectrum allocation, the U.S. is moving directly and decisively toward 28, 37 and 39 GHz.■

Laminate for Active Antennas

Antennas for next-generation wireless systems (e.g., LTE-Advanced and 5G) are becoming more complex. With demand for mobile data projected to grow at a ~53 percent compound annual growth rate (CAGR) through 2020, active antennas and small cells will be deployed to increase data throughput. These trends and the associated growth are expanding the use of printed circuit board (PCB) materials in antenna designs.

With the use of additional frequency bands and consumer demand for better performance and lower latency, PCBs have advantages compared to competing technologies such as bent metal and cable. Antenna OEMs find that PCB-based designs shorten the design iteration cycle and enable the development of complex, multi-layer board (MLB) designs. However, PCB-based designs have challenges:

- Integration of the power amplifier (PA) and antenna into one structure for active antennas
- High fabrication and assembly costs of PTFE MLBs
- Limited thermoset materials that are low loss, low PIM and meet UL 94 V-0.

Addressing these challenges, Rogers launched the RO4730G3™ UL 94 V-0 antenna grade laminates, which combine a flame retardant, low loss thermoset dielectric with low profile copper foil and incorporate a proprietary filler system. The material has a Dk of 3.0 and a Df of 0.0023, measured at 2.5 GHz. RO4730G3 laminates offer a practical, cost-effective circuit material for active antenna arrays and PCB antennas, whether for current wireless systems or those on the horizon. With the right combination of materials, these laminates provide the optimum blend of price, performance and durability.

VENDORVIEW

Rogers Corp.
Chandler, Ariz.
www.rogerscorp.com/acs

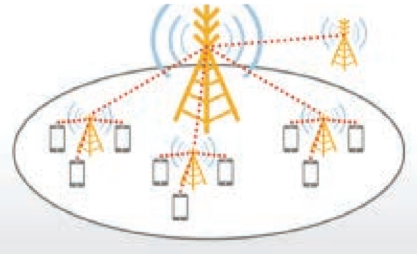

Dual-Channel BTS PA Linearizer

Maxim Integrated's SC2200 dual-path RF power amplifier linearizer (RFPAL) significantly improves base station efficiency and reduces the size and cost of the RF transmitter. The fourth-generation linearizer enables power amplifiers to consume up to 70 percent less power compared to operation in back-off. The RFPAL consumes less than 1.5 W when both paths are operating. Packaged in an 11 mm × 11 mm QFN, the SC2200 solution occupies less than 1 sq. in. of board area, which is up to 8× smaller than other digital predistortion (DPD) solutions. Further, it reduces the bill of materials (BOM) cost by up to 50 percent.

With cellular data traffic increasing exponentially, the communications industry is migrating from macro networks to heterogeneous networks to improve coverage and capacity. The SC2200 is a superior alternative to the inefficient approach of operating power amplifiers in back-off, preferred over DPD since it requires no software or complex algorithm development. The device uses the PA output and input to adaptively generate an optimized correction signal to minimize the PA's distortion. Using analog signal processing in the RF domain enables the RFPAL to operate over wide bandwidths and with very low power consumption.

The SC2200 works with a wide range of PA architectures, technologies and power levels. It is ideal for cellular applications including macro and small cells, distributed antenna systems (DAS), active antenna systems (AAS) and other multiple-input-multiple-output (MIMO) systems. The SC2200 operates in the cellular bands from 698 to 2700 MHz, with signal bandwidths from 1.2 to 60 MHz, and meets the stringent spectral emission and error vector magnitude (EVM) regulatory requirements for 2G, 3G and 4G, including both TD-LTE and FD-LTE.

Maxim Integrated
San Jose, Calif.
www.maximintegrated.com


Millimeter Wave
Measurement
110 GHz
SPINNER EasyLaunch
Coaxial PCB Adaptor
SPINNER EasyLaunch
Waveguide PCB Adaptor
SPINNER EasySnake
Flexible Dielectric Waveguide

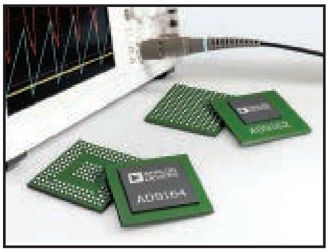

D/A Converters

VENDORVIEW

ADI's new AD9162 D/A converter provides broadband and wireless service operators with the industry's highest bandwidth and dynamic range to satisfy rising consumer demand for higher quality, always-on data and video streaming without requiring expensive, large-scale architecture or design changes. Also, the new AD9164 D/A converter brings high resolution images for military and commercial radar designers while significantly reducing solution component count. The new device ensures improved accuracy as well as speed of test, contributing to faster market-ready time while significantly decreasing tester complexity and size.

Analog Devices Inc.
www.analog.com

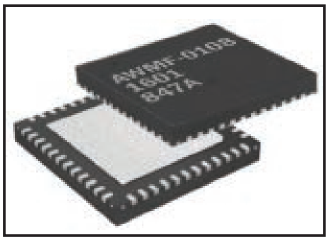

Silicon Core ICs

VENDORVIEW

Anokiwave offers a family of Active Antenna ICs at X and K/Ka-Bands for 5G, commercial radar and satcom markets. Supported with expert systems engineering and optimal technology solutions, the company's highly integrated core ICs and system-in-package solutions provide its customers the fastest-time-to-market. Anokiwave's patent-pending IP blocks implemented in silicon technology enable low-cost hybrid beam forming for 5G multi-antenna arrays with high energy efficiency and low latency beam steering™.

Anokiwave
www.anokiwave.com

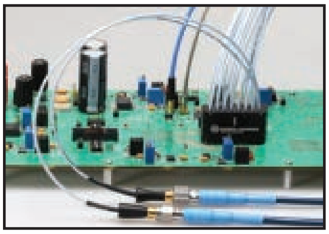

MXP-Multicoax Test Solution

VENDORVIEW

In a world where performance, speed and density matter, the MXP multicoax solution is the perfect fit. The small form factor and outstanding electrical characteristics combined with reliable mating and ease of use makes the MXP an excellent solution for benchtop and system testing with a large selection of bandwidths. MXP50 (50 GHz), MXP40 (40 GHz) and MXP18 (18 GHz) cover current data rate requirements. The entire MXP family comes with the highly flexible and ultra-stable MULTIFLEX cable as a standard.

Huber + Suhner AG
www.hubersuhner.com

Mote II for LoRa®

Mote II, the successor of LoRaMote, impresses with a new design and new features, including the new LoRa® module iM881A-M, a display and three buttons. Just like the LoRaMote, the Mote II includes a GPS module, sensors for temperature, pressure and acceleration. With its waterproof IP65 housing the Mote II is also suitable for outdoor use. Display and buttons make the handling more comfortable. The Mote II is certified by the LoRa® Alliance according to the LoRaWAN® standard.

IMST GmbH
www.wireless-solutions.de

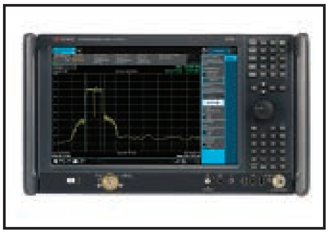

Continuous Frequency Coverage

VENDORVIEW

The Keysight N9041B UXA X-Series signal analyzer is the first to provide continuous frequency coverage to 110 GHz with a maximum analysis bandwidth of 5 GHz. Advanced front-end circuitry achieves low loss and efficient mixing, providing a displayed average noise level (DANL) as low as –150 dBm/Hz when characterizing wideband modulated signals in the millimeter-wave band. This adds new level of insight to applications including 5G, 802.11ad/ay and automotive radar.

Keysight Technologies Inc.
www.keysight.com

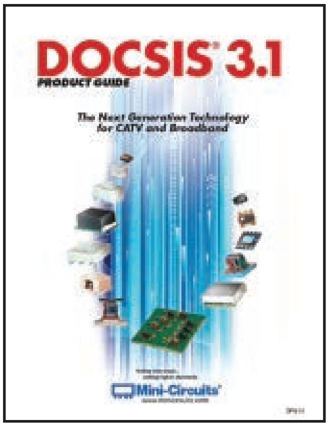

DOCSIS 3.1 Product Guide

VENDORVIEW

Mini-Circuits' DOCSIS® 3.1 Product Guide, a 116-page full-color catalog, showcases the company's line of next-generation products for CATV and broadband markets. The guide provides detailed information on Mini-Circuits' wide range of RF components, all carefully specified to meet DOCSIS 3.1 standards. This includes everything from passive devices such as its transformers, couplers and splitter/combiners, to active elements such as amplifiers, equalizers and more. With over 70 different DOCSIS®-compliant models, chances are Mini-Circuits has your application covered.

Mini-Circuits
www.minicircuits.com

5G/LTE Envelope Tracking PAs

VENDORVIEW

Next-generation communication systems will rely on system architectures that will challenge component level design. This NI AWR software white paper examines the use of envelope tracking (ET), digital pre-distortion and impedance matching via load pull to improve the efficiency and linearity performance of RF PAs targeting 4G and 5G applications. National Instruments has equipped engineers and scientists with tools that accelerate productivity, innovation and discovery since 1976.

National Instruments

www.ni.com

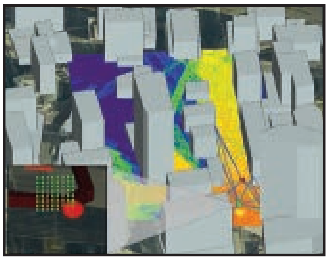

Simulating Massive MIMO Beamforming

This presentation demonstrates a new predictive capability for simulating massive MIMO antennas and beamforming in dense urban propagation environments. Remcom's unique approach allows the prediction of the signal-to-interference-plus-noise ratio (SINR) at specific device locations and the actual physical beams formed using these techniques, including unintentional distortions caused by pilot contamination. Learn more at www.remcom.com/massive-mimo-beamforming.

Remcom

www.remcom.com

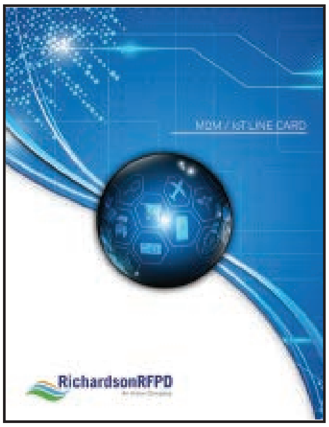

M2M/IoT Line Card

VENDORVIEW

Richardson RFPD offers a full line of IoT products and services from market-leading suppliers for your wireless products and applications. The company's broad range of wireless connectivity products range from low-cost embedded modules to full-function gateway solutions, designed to address diverse applications in public safety, oil and gas, utility, mobile data, transportation, medical and transaction processing markets. Richardson RFPD's strong and diverse alliance partner network offers extensive expertise to provide assistance with cellular data plans, cloud services, certifications and design services.

Richardson RFPD

www.richardsonrfpd.com

5G Test & Measurement Solutions

VENDORVIEW

Rohde & Schwarz is supporting researchers around the globe seeking concepts and technologies for 5G wireless networks. The R&S SMW200A vector signal generator and the R&S FSW85 signal and spectrum analyzer both provide outstanding T&M capabilities for the generation and analysis of 5G signals based on the characteristics as specified in the Verizon open trial specifications. Equipped with a 5G waveform candidate software option and using an OFDM vector signal analysis software the devices make it easy to test waveform candidates and new frequency bands for commercial wireless communications.

Rohde & Schwarz GmbH & Co. KG

www.rohde-schwarz.com

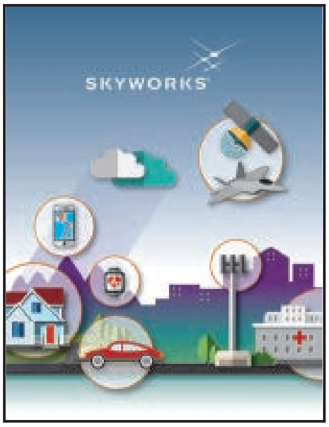

Solutions For a Connected World

VENDORVIEW

Skyworks invites you to browse their innovative Internet of Things (IoT) featured products for a broad array of markets and applications. The company's transformative solutions connect people, places and things — from automotive to the connected home, industrial, machine-to-machine, medical, mobile devices and wearables. Skyworks connectivity solutions help you develop and launch your great new ideas. To learn more, visit www.skyworksinc.com/iot to review products and download a brochure.

Skyworks Solutions Inc.

www.skyworksinc.com

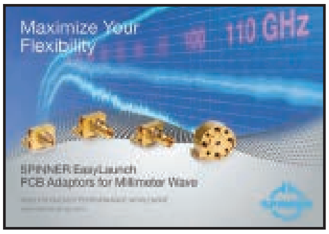

SPINNER EasyLaunch

VENDORVIEW

The flexible, soft-launch PCB adapter SPINNER EasyLaunch is mounted flush with the printed circuit board (PCB) surface and ensures excellent RF performance, even with multiple launches. This technology permits variable positioning of the connectors everywhere at the board, maximizes flexibility for placing RF contacts and enable a more compact board design. Conventional solutions either limit the range of possible PCB layouts or reduce RF performance.

SPINNER GmbH

www.spinner-group.com

Sales Representatives

Microwave Journal
Frequency Matters.

Eastern and Central Time Zones
Chuck Boyd
Northeast Reg. Sales Mgr.
(New England, New York, Eastern Canada)
685 Canton Street
Norwood, MA 02062
Tel: (781) 619-1942
FAX: (781) 769-5037
cboyd@mwjournal.com

Michael Hallman
Eastern Reg. Sales Mgr.
(NJ, Mid-Atlantic, Southeast, Midwest, TX)
4 Valley View Court
Middletown, MD 21769
Tel: (301) 371-8830
FAX: (301) 371-8832
mhallman@mwjournal.com

Pacific and Mountain Time Zones
Brian Landy
Western Reg. Sales Mgr.
(CA, AZ, OR, WA, ID, NV, UT, NM, CO, WY, MT, ND, SD, NE & Western Canada)
144 Segre Place
Santa Cruz, CA 95060
Tel: (831) 426-4143
FAX: (831) 515-5444
blandy@mwjournal.com

International Sales
Richard Vaughan
International Sales Manager
16 Sussex Street
London SW1V 4RW, England
Tel: +44 207 596 8742
FAX: +44 207 596 8749
rvaughan@horizonhouse.co.uk

Germany, Austria, and Switzerland (German-speaking)
WMS.Werbe- und Media Service
Brigitte Beranek
Gerhart-Hauptmann-Street 33,
D-72574 Bad Urach
Germany
Tel: +49 7125 407 31 18
FAX: +49 7125 407 31 08
bberanek@horizonhouse.com

Korea
Young-Seoh Chinn
JES Media International
2nd Floor, ANA Bldg.
257-1, Myungil-Dong
Kangdong-Gu
Seoul, 134-070 Korea
Tel: +82 2 481-3411
FAX: +82 2 481-3414
yschinn@horizonhouse.com

China
Shenzhen
Michael Tsui
ACT International
Tel: 86-755-25988571
FAX: 86-10-58607751
michaelt@actintl.com.hk

Shanghai
Linda Li
ACT International
Tel: 86-21-62511200
lindal@actintl.com.hk

Beijing
Cecily Bian
ACT International
Tel: +86 135 5262 1310
cecilyb@actintl.com.hk

Hong Kong, Taiwan, Singapore
Mark Mak
ACT International
Tel: 852-28386298
markm@actintl.com.hk

Japan
Katsuhiro Ishii
Ace Media Service Inc.
12-6, 4-Chome,
Nishiiko, Adachi-Ku
Tokyo 121-0824, Japan
Tel: +81 3 5691 3335
FAX: +81 3 5691 3336
amskatsu@dream.com

Ed Kiessling Traffic Manager/Inside Sales • 685 Canton Street Norwood, MA 02062 • Tel: (781) 619-1963 FAX: (781) 769-6178 • ekiessling@mwjournal.com